Acoustic Monitoring During Scotian Basin Exploration Project

Summer 2018

Cash Fay

BP Canada Energy Group ULC
Contract: *WR-CEG-20180121//BP01508737*

Authors:

Bruce Martin
Katie Kowarski
Emily Maxner
Colleen Wilson

6 March 2019

P001410-001
Document 01687
Version 2.0

JASCO Applied Sciences (Canada) Ltd
Suite 202, 32 Troop Ave.
Dartmouth, NS B3B 1Z1 Canada
Tel: +1-902-405-3336
Fax: +1-902-405-3337
www.jasco.com

Suggested citation:

Martin, S.B., K.A., Kowarski, E.E. Maxner, and C.C. Wilson. 2019. *Acoustic Monitoring During Scotian Basin Exploration Project: Summer 2018*. Document 01687, Version 2.0. Technical report by JASCO Applied Sciences for BP Canada Energy Group ULC.

Disclaimer:

The results presented herein are relevant within the specific context described in this report. They could be misinterpreted if not considered in the light of all the information contained in this report. Accordingly, if information from this report is used in documents released to the public or to regulatory bodies, such documents must clearly cite the original report, which shall be made readily available to the recipients in integral and unedited form.

Contents

EXECUTIVE SUMMARY 1
1. INTRODUCTION 2
1.1. Background: Ambient Sound Levels 3
1.2. Anthropogenic Contributors to the Soundscape 4
1.2.1. Vessel traffic 4
1.2.2. Drilling activities 5
2. METHODS 6
2.1. Data Collection 6
2.1.1. Acoustic recorders 6
2.1.2. Deployment locations 6
2.1.3. CTD data 8
2.2. Automated Data Analysis 8
2.2.1. Total Ocean sound and time series analysis 8
2.2.2. Vessel sound detection 9
2.2.3. Marine mammal occurrence 10
3. RESULTS 12
3.1. Ambient Sound Measurements 12
3.1.1. Total sound levels 12
3.2. Marine Mammals 18
3.2.1. Mysticetes 18
3.2.2. Odontocetes 22
4. DISCUSSION 31
4.1. Ambient Sound and Drilling Measurements 31
4.1.1. Correlations of Sound Levels with Wind Speed and Wave Height 31
4.1.2. Effects of MODU West Aquarius on the Soundscape 33
4.1.3. West Aquarius Radiated Sound Level 34
4.1.4. Expected versus Measured Sound Levels 37
5. CONCLUSION AND RECOMMENDATIONS 43
GLOSSARY 44
LITERATURE CITED 50
APPENDIX A. CALIBRATION AND MOORING DESIGNS A-1
APPENDIX B. CTD RESULTS B-1
APPENDIX C. ACOUSTIC DATA ANALYSIS METHODS C-1

Figures

Figure 1. Wenz curves 3
Figure 2. Vessel traffic off the US and Canadian east coast for 2017 4
Figure 3. BP's Scotian Basin MODU (left) and a close-up of the drill bit (right). 5

Figure 4. Deployment locations of AMAR recorders 7
Figure 5. Deployment locations of the recorders at 2 km and 20 km from the source, and in the Gully. 7
Figure 6. Minos Plus X used for CTD casts 8
Figure 7. Marine mammal auditory weighting functions from NMFS (2018). 9
Figure 8. Example of broadband and 40–315 Hz band SPL, as well as the number of tonals detected per minute as a ship approached a recorder, stopped, and then departed. 10
Figure 9. Recorders at (A) 2 km and (B) 20 km: (Bottom) Spectrogram and (top) in-band SPL for underwater sound. 13
Figure 10. 2 km: The operational activities associated with the MODU, sound exposure levels, and sound pressure levels recorded at 2 km. 14
Figure 11. 20 km: The operational activities associated with the MODU, sound exposure levels, and sound pressure levels recorded at 20 km. 14
Figure 12. Water pump hydraulics contributing to the soundscape at 2 km on 12 May 2018. 15
Figure 13. Drilling sounds occurring at 2 km on 16 May 2018. 15
Figure 14. Median in-band SPL across tidal cycles at the Gully recording site. 16
Figure 15. Gully recorder data before 3–8Hz data removal (A) and after 3–8Hz data removal (B): Spectrogram (bottom) and in-band SPL (top) for underwater sound. 16
Figure 16. Power spectral density (PSD; bottom panels) and 1/3-octave-band analysis (top panels) 17
Figure 17. Power spectral density (PSD) restricted to the range of 100–1000 Hz 17
Figure 18. Locator beacon signals at the 2 km location that were detected throughout the recording period. 17
Figure 19. Blue whales: Spectrogram of audible call at 20 km on 3 Jun 2018 18
Figure 20. Blue whales: Daily and hourly occurrence (black) and possible occurrence (blue) at 2 km, 20 km, and the Gully. 19
Figure 21. Fin whales: Spectrogram of calls at the Gully on 4 Sep 2018 19
Figure 22. Fin whales: Daily and hourly occurrence at 2 km, 20 km, and the Gully. 20
Figure 23. Humpback whales: Daily and hourly occurrence at 20 km and the Gully. 20
Figure 24. Humpback whales: Spectrogram of moans at the Gully on 4 Sep 2018 21
Figure 25. Sei whales: Spectrogram of downsweeping moans at 20 km on 9 May 2018 21
Figure 26. Sei whales: Daily and hourly occurrence at 2 km, 20 km, and the Gully. 22
Figure 27. Sperm whales: Spectrogram of clicks at 20 km on 21 Jul 2018 23
Figure 28. Sperm whales: Daily and hourly occurrence at 2 km, 20 km, and the Gully. 23
Figure 29. Pilot whales: Spectrogram of whistles at the Gully on 30 Aug 2018 24
Figure 30. Killer whales: Spectrogram of whistles at 20 km on 12 Aug 2018 24
Figure 31. Pilot whales: Daily and hourly occurrence at 2 km, 20 km, and the Gully. 25
Figure 32. Dolphin clicks: Daily and hourly occurrence at 2 km, 20 km, and the Gully. 25
Figure 33. Dolphin whistles: Daily and hourly occurrence at 2 km, 20 km, and the Gully. 26
Figure 34. Dolphins: Spectrogram of whistles at 20 km on 5 Aug 2018 26
Figure 35. Dolphins: Spectrogram of click trains at the Gully on 1 Aug 2018 27
Figure 36. Dolphins: Spectrogram of click at the Gully on 1 Aug 2018 27
Figure 37. Cuvier's beaked whales: Spectrogram of a click train recorded at 20 km on 16 Aug 2018 28
Figure 38. Cuvier's beaked whales: Spectrogram of click recorded at 20 km on 16 Aug 2018 28
Figure 39. Cuvier's beaked whales: Daily and hourly occurrence at 2 km and 20 km. 29
Figure 40. True's or Gervais' beaked whales: Daily and hourly occurrence at 2 km and 20 km 29
Figure 41. True's or Gervais' beaked whales: Spectrogram of click recorded at 20 km on 14 Aug 2018 30

Figure 42. True's or Gervais' beaked whales: Spectrogram of a click train recorded at 20 km on 22 Jun 2018 30
Figure 43. Correlogram for the 20 km location, ... 32
Figure 44. Correlogram for the 2 km location 33
Figure 45. 1-minute average SPL broadband and band levels for 2 km, 20 km, and Stn 4. 34
Figure 46. Received sound pressure levels at the 2 km site attributed to the West Aquarius and the computed radiated sound levels. 35
Figure 47. Comparison of the West Aquarius radiated sound levels with the spectrum used for pre-operations modeling (Zykov 2015) and the Stena IceMAX (MacDonnell 2017). 36
Figure 48. Sound speed profiles for the project site. (a) winter (February) and (b) summer (August) profiles from GDEM that were used in the pre-operations propagation modeling; (c) GIOPS data 38
Figure 49. Received sound levels as a function of range, depth, and frequency for a winter sound speed profile (Figure 48a) at the drill site. 39
Figure 50. Received sound levels as a function of range, depth, and frequency for the top 500 m of the water column for a winter sound speed profile (Figure 48a) at the drill site. 40
Figure 51. Received sound levels as a function of range, depth, and frequency for the top 500 m of the water column for the summer sound speed profile (Figure 48a) at the drill site 41
Figure 52. Received sound levels as a function of range, depth, and frequency for the top 500 m of the water column for the GIOPS sound speed profile with the strongest subsurface duct (Figure 48c) at the drill site. 42

Figure A-1. Split view of a G.R.A.S. 42AC pistonphone calibrator with an M36 hydrophone. A-1
Figure A-2. JASCO mooring design 197 used at the 2 km and 20 km locations. A-2
Figure A-3. JASCO mooring design 151 used at the Gully location. A-3
Figure B-1. 2 km: Sound velocity versus depth measured on 14 Apr 2018 (black) and estimated (blue). B-1
Figure B-2. 20 km: Sound velocity versus depth measured on 15 Apr 2018 (black) and estimated (blue). B-2
Figure B-3. The Gully: Sound velocity versus depth measured on 16 Apr 2018. ..... B-3
Figure C-1. Major stages of the automated acoustic analysis process performed with JASCO's custom software suite. C-1
Figure C-2. One-third-octave-bands shown on a linear frequency scale and on a logarithmic scale. C-4
Figure C-3. A power spectrum and the corresponding 1/3-octave-band sound pressure levels of example ambient noise shown on a logarithmic frequency scale. C-5
Figure C-4. The click detector/classifier and a 1-ms time-series of four click types. C-8
Figure C-5. Illustration of the search area used to connect spectrogram bins. C-9

Tables

Table 1. Description of measurement locations. 6
Table 2. Analysis bands and sources. 31
Table 3. West Aquarius MODU radiated sound levels. 36

Table C-1. Third-octave-band frequencies (Hz). C-6
Table C-2. Decade-band frequencies (Hz). C-7
Table C-3. Fast Fourier Transform (FFT) and detection window settings used to detect tonal vocalizations of marine mammal species expected in the data. C-9

Table C-4. A sample of vocalization sorter definitions for the tonal vocalizations of cetacean species expected in the area. C-9

Executive Summary

In 2018, BP Canada Energy Group ULC (herein “BP”) conducted an exploratory drilling campaign in an area with water depths of ~2775 m on the Scotian Shelf using the West Aquarius Mobile Offshore Drilling Unit (MODU). BP contracted JASCO Applied Sciences to undertake an acoustic monitoring study and data analysis during the drilling operations. The objectives of the study were: to characterize how underwater sound levels vary with distance from the drilling activity; to identify natural and anthropogenic sounds present during this monitoring period; and to compare the received sound levels with pre-operations modelling predictions (Zykov 2015).

Acoustic recorders were deployed in mid-April 2018 and retrieved in late September 2018. The recordings were made at the seabed, at radial distances of 2 and 20 km from the drill site. A third recorder was deployed at the edge of the Gully marine protected area (145 km from the drill site). The 2 and 20 km recorders worked as planned; however, the Gully recorder malfunctioned and did not start recording until 25 Jul 2018.

The data collected during the drilling program were compared with two years of measurements made 45 km away from the drill site by JASCO under an Environmental Studies Research Fund (ESRF) Contribution Agreement (ESRF Stn 4). Further comparisons were made to measurements of the Stena IceMAX used by Shell Canada to drill an exploratory well in 2016. That drill site was 13 km from the ESRF Stn 4.

Analysis of the recordings focused on understanding the ambient soundscape, measuring the contributions of the drilling operations, and studying the presence of vocalizing marine mammals in the project area. Marine mammal presence was summarized by the percentage of days in which calls from species or groups (e.g., dolphins) were manually or automatically identified in the acoustic data.

The average daily sound exposure level at the 2 km location was ~8 dB higher than at the 20 km station. The largest differences between the sites was in the 100–1000 Hz frequency band. The stage of operations (e.g., drilling, pulling out, moving) did not correlate with the generated sound levels. The sound levels did correlate with the wind speed. At the 20 km station, 60% of the changes in the sound pressure levels above 200 Hz correlated with changes in wind speed. At the 2 km station, the 200 Hz octave-band was the only band where at least 33% of the change in sound pressure levels correlated with change in wind speed. The results at 20 km were expected for an environment dominated by wind and wave generated sound levels. The results indicate that the MODU generated a broad spectrum of sounds that did not depend on the wind speed, except in the 200 Hz band where additional thruster power was required to compensate for increased wind forcing.

The peak frequency generated by the West Aquarius is 190 Hz, unlike the Stena IceMAX, which had a 100 Hz peak. For all frequencies except 200 Hz, the sound pressure levels generated by the West Aquarius were lower than those of the Stena IceMAX. The West Aquarius sound levels were also below the theoretical model for a dynamic positioning thruster used during the pre-season modeling of the radiated sound field. These differences in spectral signature are likely due to the thruster technologies. The Stena IceMAX is equipped with the Rolls Royce UUC-355 geared thruster, whereas the West Aquarius has ABB’s gearless Azipod CX 3300 thrusters. The 90th percentile of the broadband radiated sound levels was 186.3 dB re 1 µPa, which is significantly less than the 196 dB re 1 µPa that was modelled as the full power output of 8 thrusters. No thrust power logs for the drilling operations were available.

The 190 Hz signal from the West Aquarius was not detected at the Gully location 145 km from the MODU.

Collecting a long-term data set at multiple ranges from the drill site during a ‘real-world’ industrial operation has identified differences in the sounds produced by different DP thruster systems. Interpretation of the measurements was greatly enhanced by the two-year baseline data set previously collected under an ESRF Contribution Agreement.

1. Introduction

The Canadian Atlantic seaboard is home to a wealth of marine life and is the site of diverse human activities including fishing, maritime shipping, and oil and gas exploration and production activities. To varying degrees, these anthropogenic activities contribute to the soundscape of the surrounding waters. The Canadian Atlantic Exclusive Economic Zone (EEZ) has seen relatively few dedicated acoustic monitoring efforts, except for a two year program (2015–2017) funded by the Environmental Studies Research Fund (ESRF) that spanned from Newfoundland and Labrador to the Scotian Shelf (Delarue et al. 2018) and ongoing acoustic monitoring in and around Marine Protected Areas such as the Gully Canyon (Whitehead 2013, Kowarski et al. 2015). Monitoring efforts are particularly important when additional anthropogenic activities are introduced to the environment, in this case the Scotian Basin Exploration Project undertaken by BP Canada Energy Group ULC (BP).

For the BP Project, JASCO Applied Sciences (JASCO) deployed three bottom-mounted acoustic recorders that collected data while the mobile offshore drilling unit (MODU) West Aquarius was installed and actively drilling during summer 2018. Recorder locations were selected to meet the following program objectives:

- To characterize how underwater sound levels vary with distance from the drilling activity,
- To identify natural and other anthropogenic sound events that may have been present during this monitoring period, and
- To compare the received sound levels with pre-operations predictions (Zykov 2015)

These findings were compared to data collected in previous years in the region during the ESRF monitoring program and to previous modelling completed on sound propagation in the area.

1.1. Background: Ambient Sound Levels

The ambient, or background, sound levels that create the ocean soundscape are comprised of many natural and anthropogenic sources (Figure 1). The main environmental sources of sound are wind, precipitation, and sea ice. Wind-generated sound in the ocean is well-described (e.g., Wenz 1962, Ross 1976), and sea state is known to be an important contributor to near-shore soundscapes (Deane 2000). In polar regions, sea ice can produce loud sounds that are often the main contributor of acoustic energy in the local soundscape, particularly during ice formation and break up. Precipitation is a frequent sound source, with contributions typically concentrated at frequencies above 500 Hz. At low frequencies (<100 Hz), earthquakes and other geological events contribute to the soundscape (Figure 1).

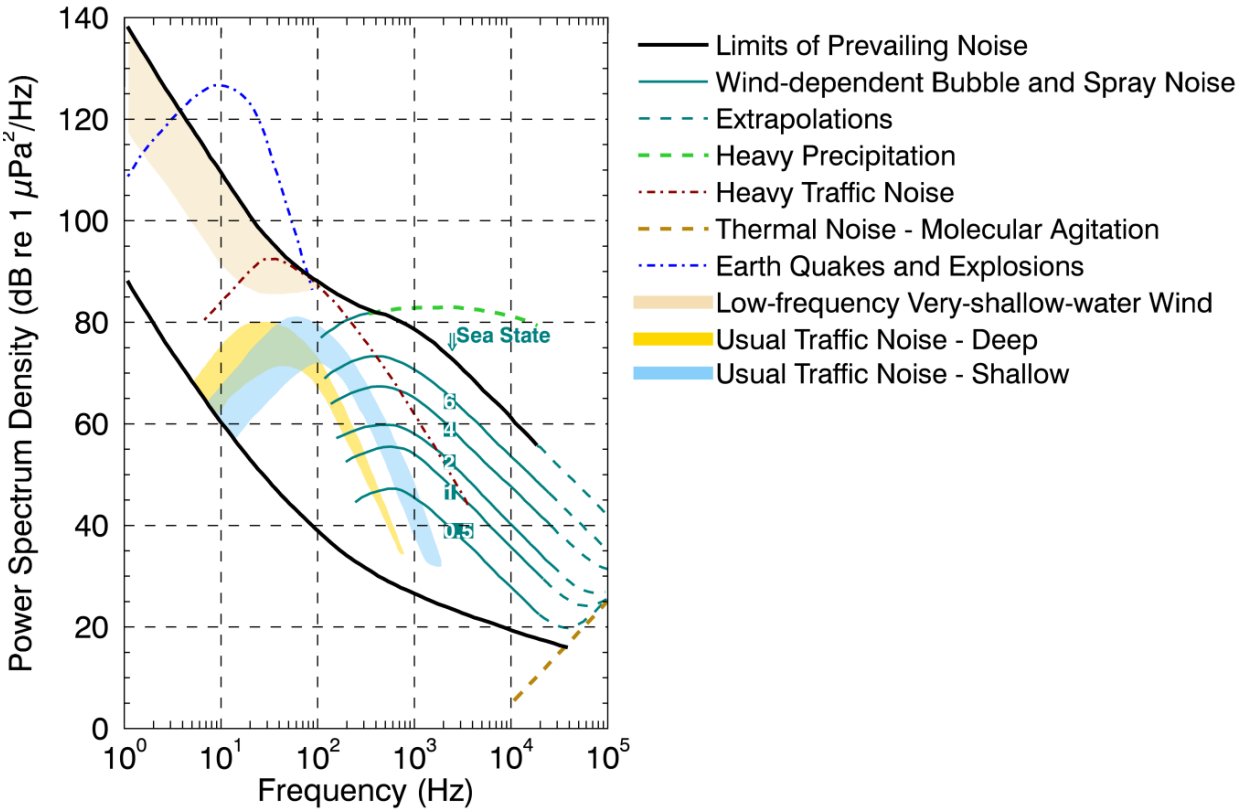

Figure 1. Wenz curves (NRC 2003), adapted from (Wenz 1962), describing pressure spectral density levels of marine ambient noise from weather, wind, geologic activity, and commercial shipping.

Marine mammals are the main biological contributors to the underwater soundscape. For instance, fin whale songs can raise sound levels in the 18–25 Hz frequency band by 15 dB for extended durations (Simon et al. 2010). Marine mammals, cetaceans in particular, rely almost exclusively on sound for navigating, foraging, breeding, and communicating (Clark 1990, Edds-Walton 1997, Tyack and Clark 2000). Although species differ widely in their vocal behaviour, most can be reasonably expected to produce sounds on a regular basis. Passive acoustic monitoring is therefore increasingly considered a useful tool to provide a cost-effective and efficient survey method for detecting marine mammals, and more specifically vocalising cetacean species. Seasonal and sex- or age-biased differences in sound production, as well as signal frequency, source level, and directionality, all influence the applicability and success rate of acoustic monitoring, and its effectiveness must be considered separately for each species.

1.2. Anthropogenic Contributors to the Soundscape

Anthropogenic (human-generated) sound can be a by-product of vessel operations, such as use of engines, with sound radiating through vessel hulls and cavitating propulsion systems, or it can be a product of active acoustic data collection, with seismic surveys, military sonar, and depth sounding as the main contributors. The contribution of anthropogenic sources to the ocean soundscape has increased steadily over the past several decades. This increase is largely driven by greater maritime shipping and seismic survey explorations for oil and gas (Hildebrand 2009). Both shipping and seismic survey sounds are from moving sources; therefore, they contribute to the soundscape in their vicinity, generally for tens of kilometers for shipping and for 100 km or more for seismic surveys. Both sources can contribute at very long ranges when the sounds enter the deep sound channel and cross ocean basins (Nieukirk et al. 2004). The main anthropogenic contributors to the ambient soundscape in the present study area were vessel traffic and those associated with the drilling operations.

1.2.1. Vessel traffic

Vessel traffic, both from shipping and from vessels associated with the MODU, will contribute to the soundscape. There are several major shipping lanes in or near the study area. Vessels fan out after leaving the Gulf of St. Lawrence and Halifax harbour, resulting in consistent traffic on the Scotian shelf (Figure 2). Support vessels for safety, transport of goods, waste, and/or passengers to and from the MODU will be regular contributors to the soundscape.

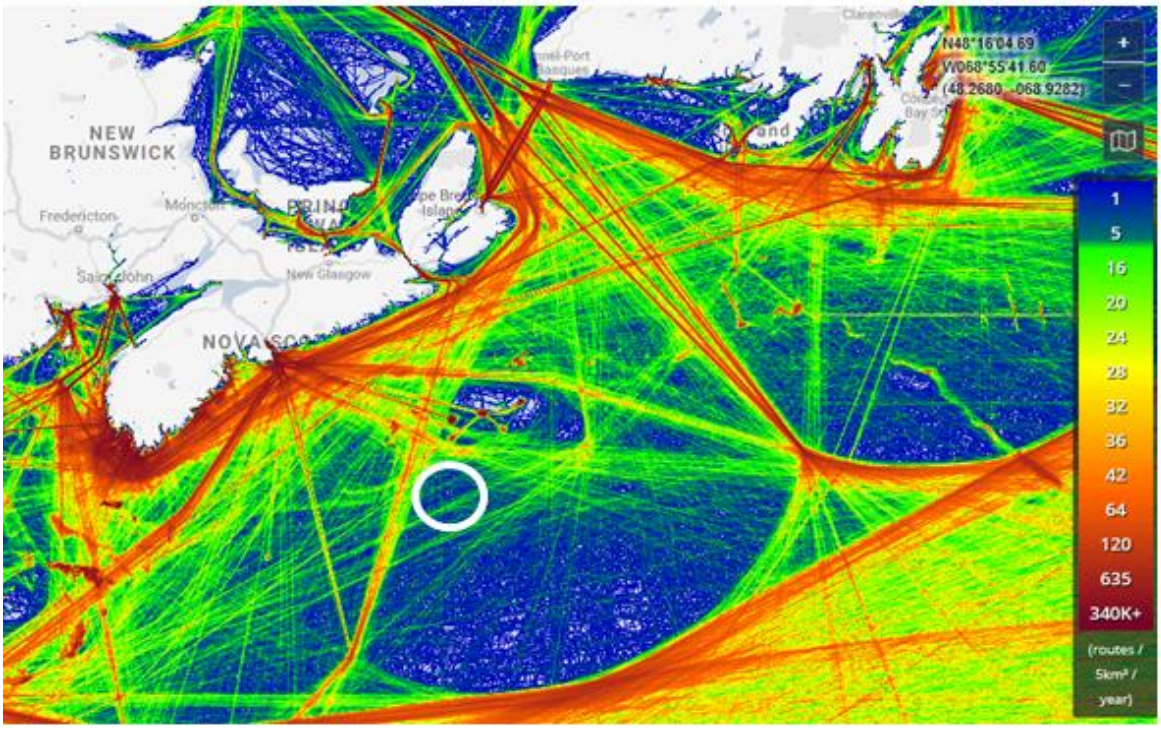

Figure 2. Vessel traffic off the US and Canadian east coast for 2017 (source: marinetraffic.com; accessed 13 Nov 2018). The study area is within the white circle.

1.2.2. Drilling activities

The MODU itself will produce a range of sounds. Some will be constant, such as mechanical vibration and thruster cavitation from the MODU's dynamic positioning (DP) system. Other sounds will be limited in time, such as emissions from pumps and direct drilling sounds from the drill string and the drill bit (Figure 3).

Figure 3. BP's Scotian Basin MODU (left) and a close-up of the drill bit (right).

2. Methods

2.1. Data Collection

2.1.1. Acoustic recorders

Underwater sound was recorded with Autonomous Multichannel Acoustic Recorders (AMAR G3s; JASCO). Each AMAR was fitted with an M36-V35dB omnidirectional hydrophone (GeoSpectrum Technologies Inc., −165 ± 3 dB re 1 V/µPa sensitivity) that was protected by a hydrophone cage. The cage was covered with a shroud to minimize noise artifacts due to water flow.

The AMARs operated on a duty cycle alternating between 10 min at 16,000 Hz and for 60 s at 375,000 Hz. The recorders were calibrated to verify the sensitivity of each recording apparatus (i.e., the hydrophone, pre-amplifier, and AMAR) in JASCO's warehouse, prior to deployment, and after retrieval in the field. The post-retrieval calibration allows us to ensure no loss of sensitivity occurred during the deployment. Details about the mooring designs and calibration procedure can be found in Appendix A.

2.1.2. Deployment locations

AMARs were deployed at three stations along a transect heading toward the Gully canyon (Figure 4). The recorders were deployed at 2 and 20km from the drilling site and on the shelf beside the Gully submarine canyon, approximately 145 km from the drilling location (Table 1, Figure 5). The recorders deployed at 2 and 20 km allowed us to characterize the soundscape and valid sound propagation models near the bottom in relative proximity of the drilling site. The Gully recorder was deployed along the first 100 m isobath encountered on the transect and took advantage of the local bathymetry to record sound in the upper part of the water column.

The Gully AMAR malfunctioned at the start-up phase and did not start recording until 25 Jul 2018. The recording that were retrieved provided valuable information for the period of 25 Jul to 5 Sep 2018. The 2 km and 20 km AMARs recorded as expected with recordings continuing until 16 and 18 Aug, respectively, when AMARs reached the expected end of battery life.

Table 1. Description of measurement locations.

Station	Deployment	Retrieval	Mooring design	Latitude	Longitude	Depth (m)	Location description
2 km	14 Apr 2018	23 Sep 2018	197*	42.8481ºN	060.2831ºW	2384	~2 km from drill site
20 km	15 Apr 2018	23 Sep 2018	197*	42.9699ºN	060.1415ºW	2060	~20 km from drill site
Gully	16 Apr 2018	23 Sep 2018	151**	43.8249ºN	059.1343ºW	93	~145 km from drill site

* See Figure A-2.
** See Figure A-3.

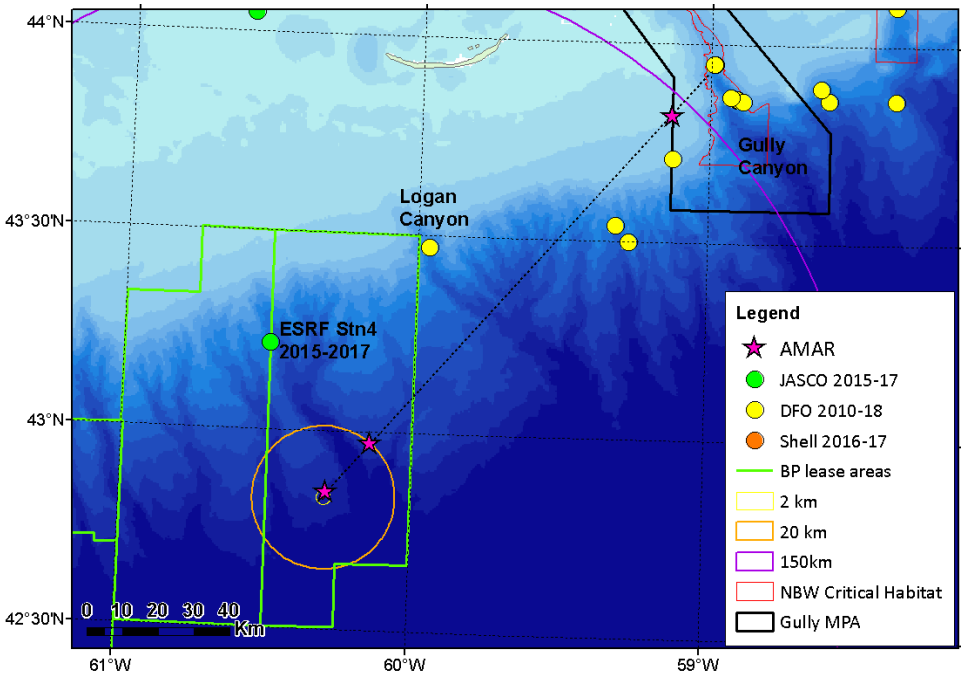

Figure 4. Deployment locations of AMAR recorders (pink stars) as well as other previous acoustic programs in the area including those carried out by the Department of Fisheries and Oceans (DFO) and JASCO's ESRF Stn 4. The drilling site is at the centre of the concentric rings. The Gully Marine Protected Area (MPA) and Northern bottlenose whale (NBW) critical habitat is also included for context.

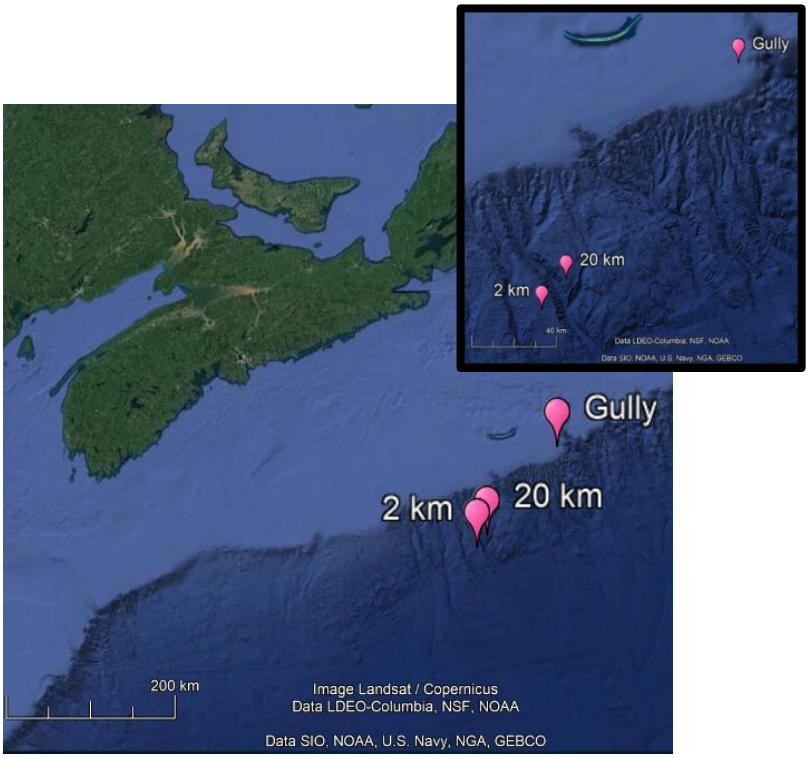

Figure 5. Deployment locations of the recorders at 2 km and 20 km from the source, and in the Gully.

2.1.3. CTD data

CTD casts were performed using a Minos Plus X (Figure 6) prior to deploying and retrieving the AMARs. The CTD instrument was rated to 5000 m, but the depth of the cast was determined by the equipment (winch, wire length) onboard the *Strait Hunter* and *Lundstrom Tide*. CTD results are included in Appendix B.

Figure 6. Minos Plus X used for CTD casts at the three AMAR sites.

2.2. Automated Data Analysis

During this study, 3.62 TB of acoustic data were collected. Automated analysis of the total ocean soundscape, including sounds from vessels and marine mammal vocalizations was performed. Appendix C outlines the stages of the analyses.

2.2.1. Total Ocean sound and time series analysis

Ambient sound levels at each location were examined to document the local baseline underwater sound conditions. In Section 3.1, ambient sound levels are presented as:

- Statistical distribution of SPL in each 1/3-octave-band. The boxes of the statistical distributions indicate the first (L_{25}), second (L_{50}), and third (L_{75}) quartiles. The whiskers indicate the maximum and minimum range of the data. The solid line indicates the mean sound pressure level (SPL), or L_{mean}, in each 1/3-octave.
- Spectral density level percentiles: Histograms of each frequency bin per 1 min of data. The L_{eq}, L_5, L_{25}, L_{50}, L_{75}, and L_{95} percentiles are plotted. The L_5 percentile curve is the frequency-dependent level exceeded by 5% of the 1 min averages. Equivalently, 95% of the 1 min spectral levels are above the 95th percentile curve.
- Broadband and approximate-1/3-octave-band sound pressure levels (SPL) over time for these frequency bands: 10 Hz to 16 kHz, 10–100 Hz, 100 Hz to 1 kHz, and 1–10 kHz.
- Spectrograms: Ambient sound at each station was analyzed by Hamming-windowed fast Fourier transforms (FFTs), with 1 Hz resolution and 50% window overlap. The 120 FFTs performed with these settings are averaged to yield 1 min average spectra.
- Daily sound exposure levels (SEL): The SEL represents the total sound energy received over a 24 hour period. SEL can be calculated over any time period, over 24 hours has been recommended as an appropriate metric to inform assessment of potential hearing impairment impacts to marine mammals such as temporary or permanent hearing threshold shift (Southall et al. 2007, NMFS 2018). Long-term exposure to sound only impacts an animal if the sounds are within its hearing frequency range. Therefore, SEL threshold criteria are typically filtered or weighted by an animal's auditory frequency weighting function before integrating to obtain SEL. For this analysis the 10 Hz and above SEL were computed as well as the SEL weighted by the marine mammal auditory filters (Figure 7, NMFS 2018). As a first approximation, the low-frequency auditory weighting function may be thought of as a 100 Hz high pass filter. Similarly, the phocid and otariid seal auditory weighted functions are ~4 kHz high pass filters, the mid-frequency function is ~10 kHz high pass filter, and the high-

frequency function is ~20 kHz high pass filter. The SEL thresholds for possible hearing impacts from sound on marine mammals are provided in Table AE-1 of NMFS (2018).

The 50th percentile (median of 1 min spectral averages) of the power spectral density can be compared to the well-known Wenz ambient noise curves (Figure 1), which show the variability of ambient spectral levels off the U.S. Pacific coast as a function of frequency of measurements for a range of weather, vessel traffic, and geologic conditions. The Wenz curve levels are generalized and are used for approximate comparisons only.

The 1 min averaged, 1 Hz spectral density levels are summed over the 1/3-octave and decade bands to calculate the 1 min averaged broadband levels (dB re 1 µPa). They are presented with the density levels. Table C-1 lists the 1/3-octave-band frequencies. Table C-2 lists the decade-band frequencies. Weather conditions throughout the deployment periods were also gathered to inform the discussion on the factors driving recorded sound levels and influencing probability of marine mammal detections. Detailed description of acoustic metrics and 1/3-octave-band analysis can be found in Appendices C.1 and C.2.

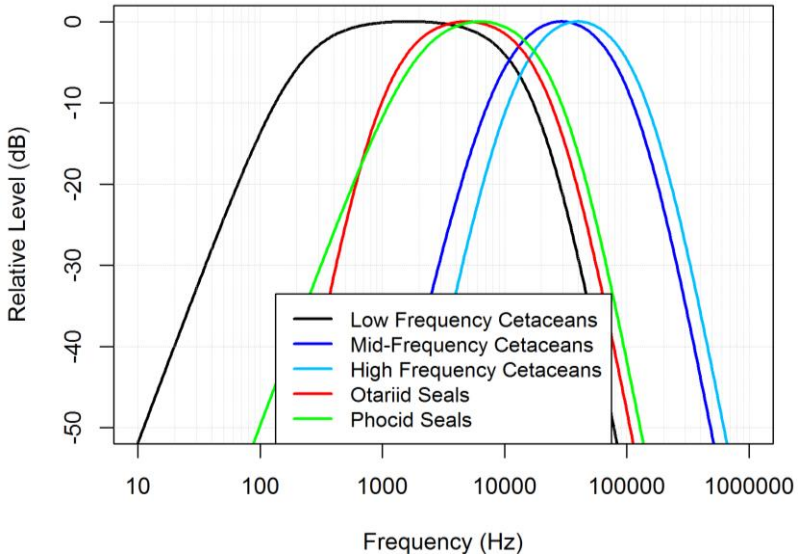

Figure 7. Marine mammal auditory weighting functions from NMFS (2018).

2.2.2. Vessel sound detection

Vessels are detected in two steps:

1. Constant, narrowband tones produced by a vessel's propulsion system and other rotating machinery (Arveson and Vendittis 2000) are detected. These sounds are also referred to as tonals. We detect the tonals as lines in a 0.125 Hz resolution spectrogram of the data.
2. The root-mean-square sound pressure levels (SPL) are assessed for each minute in the 40–315 Hz frequency band, which commonly contains most sound energy produced by mid-sized to large vessels. Background estimates of the shipping band SPL and broadband SPL are then compared to their median values over the 12 h window, centred on the current time.

Vessel detections are defined by three criteria (Martin 2013):

- The SPL in the shipping band is at least 3 dB above the median.
- At least five shipping tonals (0.125 Hz bandwidth) are present.
- The SPL in the shipping band is within 8 dB of the broadband SPL (Figure 8).

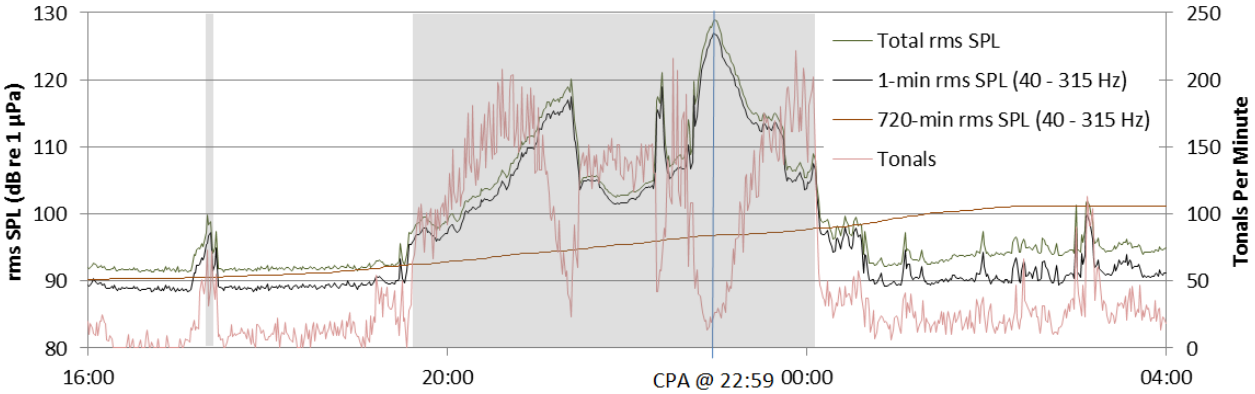

Figure 8. Example of broadband and 40–315 Hz band SPL, as well as the number of tonals detected per minute as a ship approached a recorder, stopped, and then departed. The shaded area is the period of shipping detection. Fewer tonals are detected at the ship's closest point of approach (CPA) at 22:59 because of masking by broadband sound associated with propeller cavitation and due to Doppler shift that affects the tone frequencies.

2.2.3. Marine mammal occurrence

We used a combination of automated detectors and manual review by experienced analysts to determine the presence of sounds produced by marine mammals. First, automated detectors identified acoustic signals potentially produced by odontocetes and mysticetes (Appendices C.3.1 and C.3.2). We manually reviewed (validated) detections within a sample of the data set, critically reviewed the results of each detector, and restricted the detectors' results where necessary to most accurately describe marine mammal presence (Appendix C.3.3). Where detector results were found to be unreliable, only the validated results are presented.

In this report, the term detector is used to describe automated algorithms that combine detection and classification steps. A detection refers to an acoustic signal that has been flagged as a sound of interest based on spectral features and subsequently classified based on similarities to several templates in a library.

2.2.3.1. Click detection

Odontocete clicks are high-frequency impulses ranging from 5 to over 150 kHz (Au et al. 1999, Mohl et al. 2000). We applied an automated click detector to the 375 kHz data (audio bandwidth up to 175 kHz for ~1 min of every 11 min) to identify clicks from sperm whales, beaked whales, porpoises, and delphinids. This detector is based on zero-crossings in the acoustic time series. Zero-crossings are the rapid oscillations of a click's pressure waveform above and below the signal's normal level (e.g., Figure C-4). Zero-crossing-based features of detected events are then compared templates of known clicks for classification (see Appendix C.3.1 for details).

2.2.3.2. Tonal signal detection

Tonal signals are narrowband, often frequency-modulated, signals produced by many species across a range of taxa. Examples include the moans of baleen whales and whistles of delphinids that range predominantly between 15 Hz and 4 kHz (Berchok et al. 2006, Risch et al. 2007), thus detectors for these species were applied to the 16 kHz data (audio bandwidth up to 16 kHz for ~10 min every 11 min). In contrast, the detector for small dolphin tonal acoustic signals was applied to the high-frequency data as these whistles can reach 20 kHz (Steiner 1981b). The tonal signal detector identifies continuous contours of elevated energy and classifies them against a library of marine mammal signals (see Appendix C.3.2 for details).

2.2.3.3. Validation of automated detectors

We develop and test automated detectors with example data files that contain a range of vocalization types and background sound conditions. However, test files cannot cover the full range of possible vocalization types and background sound conditions. Therefore, a selection of files was manually validated to check each detector's performance for a specific location to determine how best to refine the detector results and when to entirely rely on manually validated results to accurately represent marine mammal occurrence. Details of the file selection and validation process can be found in Appendix C.3.3.1.

To determine the performance of each detector and any necessary thresholds (minimum number of detections per file to accept detection as true), the automated and validated results (excluding files where an analyst indicated uncertainty in species occurrence) were fed to a maximum likelihood estimation algorithm that maximizes the probability of detection and minimizes the number of false alarms using the Mathew's Correlation Coefficient (MCC). It also estimates the precision (*P*) and recall (*R*) of the detector. *P* represents the proportion of files with detections that are true positives. A *P* of 0.9 means that 90% of the files with detections truly contain the targeted signal. *R* represents the proportion of files containing the signal of interest that were identified by the detector. An *R* of 0.8 means that 80% of files known to contain a target signal had automated detections. The algorithm determines a detector threshold for each species, at every station that maximizes MCC. Section 3.2 presents the resulting thresholds.

The occurrence of each species (both validated and automated, or validated only where appropriate) was plotted using JASCO's Ark software as time series showing presence/absence by hour over each day. Only detections associated with a *P* greater than or equal to 0.75 were considered sufficiently reliable to be presented. When *P* was less than 0.75, only the validated results were used to describe the acoustic occurrence of a species.

3. Results

3.1. Ambient Sound Measurements

3.1.1. Total sound levels

This section presents the total sound levels from the data sets. We present the results in four ways:

1. **Band-level plots**: These strip charts show the averaged received sound levels as a function of time within a given frequency band. We show the total sound level (10 Hz to 16 kHz) and the decade bands for 10–16000, 10–100, 100–1000, 1000–10000, and 10–16 kHz. The 10–100 Hz band is associated with fin, sei, and blue whales, large shipping vessels, seismic surveys, and mooring movement. Sounds within the 100–1000 Hz band is generally associated with physical environment such as wind and wave conditions, but can also include both biological and anthropogenic sources such as minke, right, and humpback whales, nearby vessels, dynamic positioning sound and seismic surveys. Sounds above 1000 Hz include humpback whales, pilot whales, and dolphin whistles, and wind and wave conditions and close range human sources.
2. **Long-term Spectral Averages (LTSAs)**: Color plots showing power spectral density levels as a function of time (*x* axis) and frequency (*y* axis). The LTSAs are excellent summaries of the temporal and frequency variability in the data.
3. **Distribution of 1/3-octave-band SPL**: These box-and-whisker plots show the average and extreme sound levels in each 1/3-octave-band. As discussed in Appendix C.2,1/3-octave-bands represent the hearing bands of many mammals. They are often used as the bandwidths for expressing the source level of broadband sounds from activities such as shipping and seismic surveys. The distribution of 1/3-octave sound levels can be used as the background sound levels or noise floor for modelling the detection of vessels or marine mammal vocalizations.
4. **Power Spectral Densities (PSDs)**: These plots show the statistical sound levels in 1 Hz frequency bins. These levels can be directly compared to the Wenz curves (see Figure 1). We also plot the spectral probability density (Merchant et al. 2013) to assess whether the distribution is multi-modal.

Figure 9 shows the LTSAs and Band-Level plots for the 2 and 20 km locations. As expected, sound levels were higher closer to the drilling activity, at the 2 km than the 20 km location. The 2 km recorder had a maximum and minimum broadband SPL of 125.6 and 102.8 dB re 1 µPa, respectively (Figure 9A). Engine sound from vessels and, more likely, from the MODU DP, was present throughout the recording, as indicated by the horizontal lines in the spectrograms. The maximum and minimum broadband SPL measured at 20 km were 124.6 and 95.6 dB re 1 µPa, respectively (Figure 9B). The factors contributing to the soundscape are described below and further explained in Section 4. The peak in sound pressure levels around 10–12 Jul, that is more visible at 20 km than 2 km, was due to Hurricane Chris passing over the study area (Figure 9).

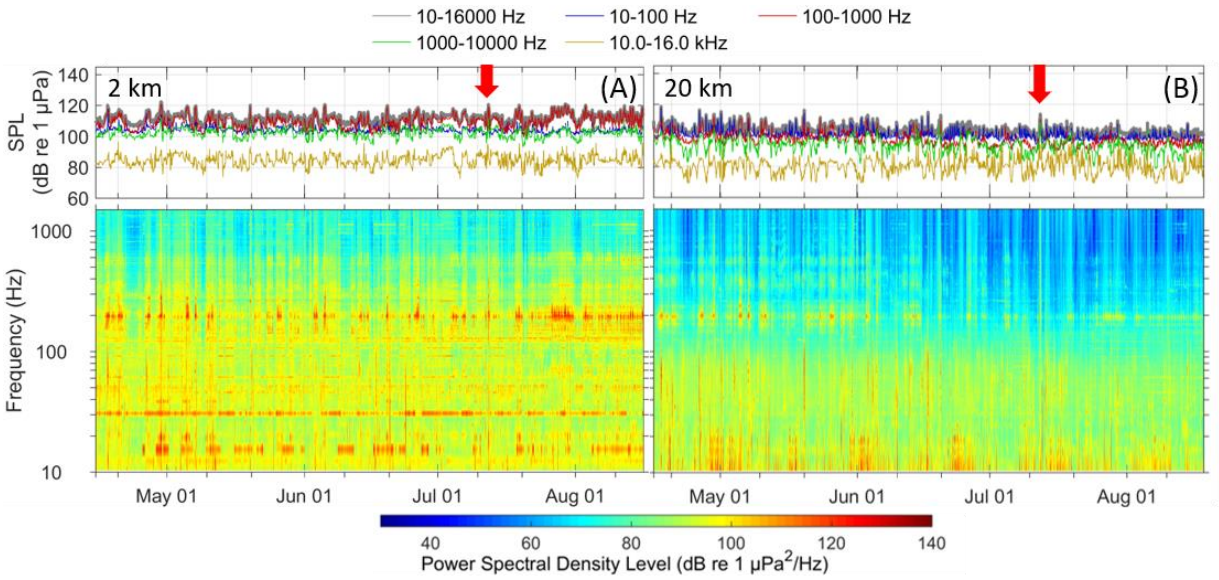

Figure 9. Recorders at (A) 2 km and (B) 20 km: (Bottom) Spectrogram and (top) in-band SPL for underwater sound. Red arrows indicate a weather event.

Drilling, pulling out of hole (POOH) and moving the MODU all acoustically contributed to the sound pressure levels recorded at 2 and 20 km (Figures 10 and 11, respectively). Sounds levels in the 100–1000 Hz band at 2 km were particularly high, driven by vessels being present at close range, DP, and weather (Figure 10). The sound pressure levels were lower in all bands at 20 km compared to 2 km. At the 20 km station, the 10–100 Hz band sound pressure levels were higher than the 100–1000 Hz band, likely due to longer propagation distances for low-frequency sounds (Figure 11). Drilling operations (Figure 12) and water pump hydraulics (Figure 13) also contributed to the overall soundscape. There is no obvious trend in overall sound levels relative to the operational activities. A Kruskal-Wallis test determined that the broadband SPL was significantly different between 2 km and 20 km ($\chi^2 = 2581.25$, $df = 1$, $P = 0$).

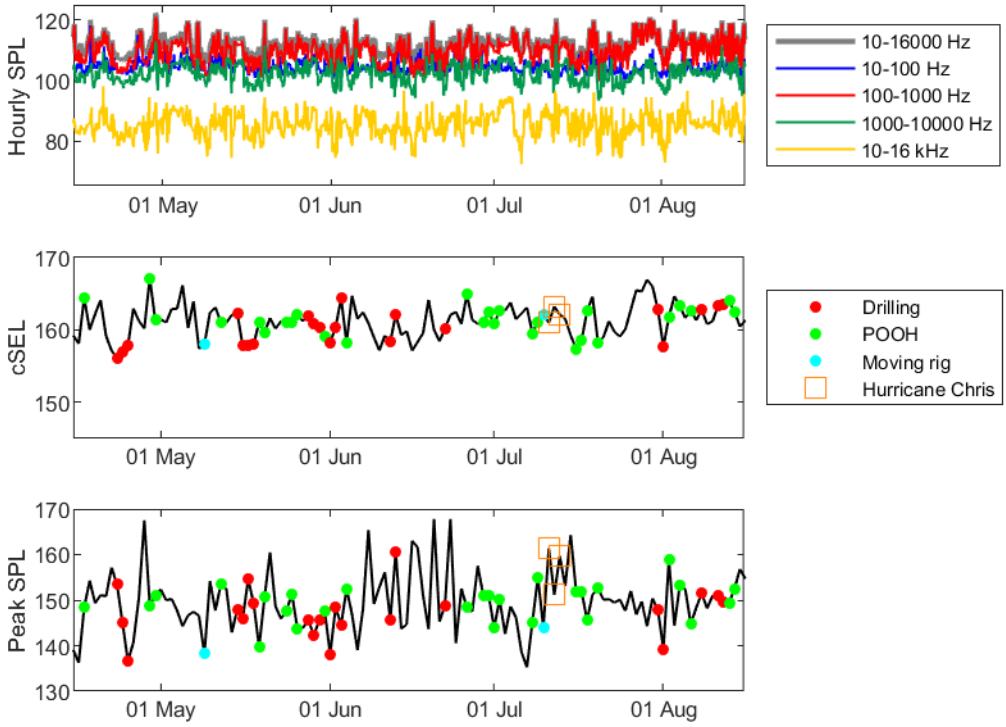

Figure 10. 2 km: The operational activities associated with the MODU, sound exposure levels, and sound pressure levels recorded at 2 km.

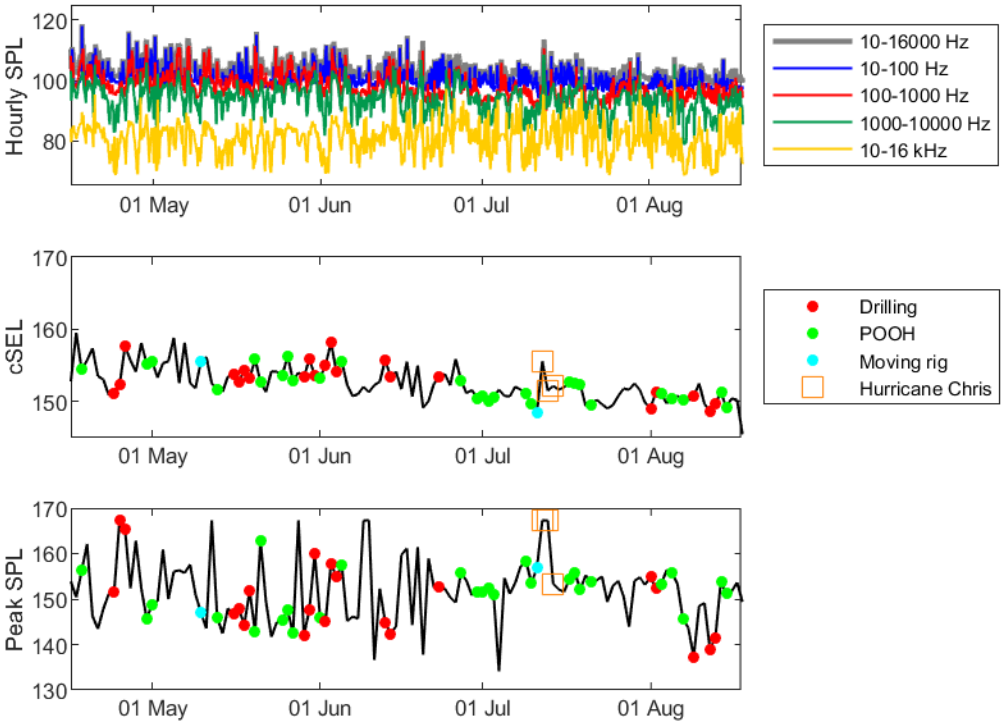

Figure 11. 20 km: The operational activities associated with the MODU, sound exposure levels, and sound pressure levels recorded at 20 km.

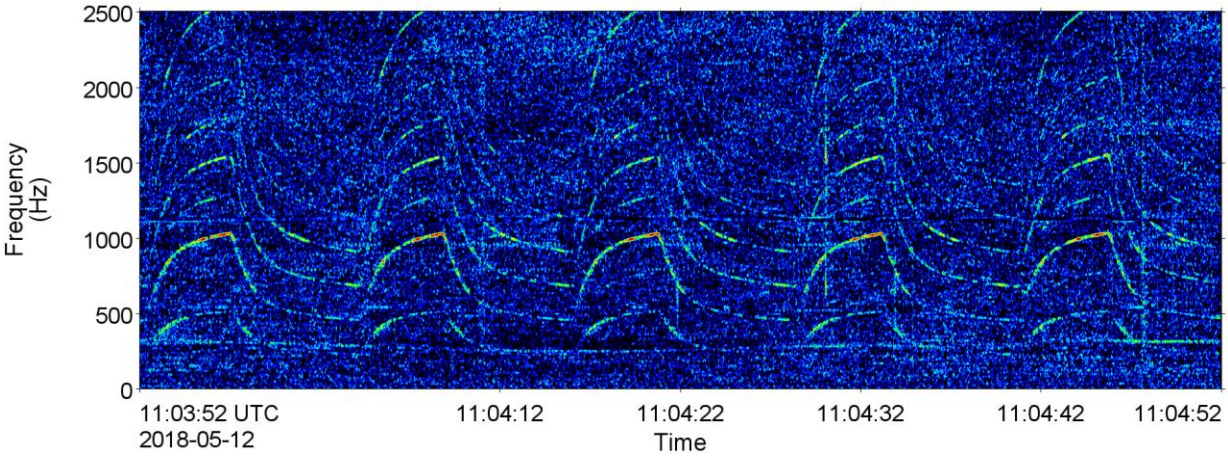

Figure 12. Water pump hydraulics contributing to the soundscape at 2 km on 12 May 2018.

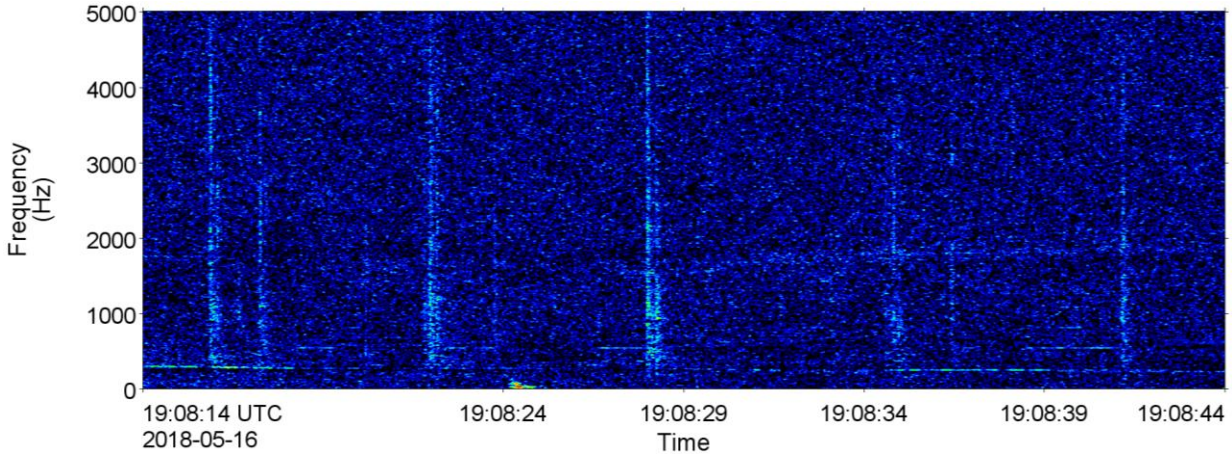

Figure 13. Drilling sounds occurring at 2 km on 16 May 2018.

The Gully recorder was farthest from the MODU, located on the shelf at 93 m water depth. A combination of bottom currents, internal waves, and tidal currents caused movements of the mooring within the water column, resulting in sounds being produced intermittently in the 10–100 Hz bands, occasionally reaching much higher in frequency (Figures 14 and 15). The median band SPL for these frequencies was lowest during the slack tide associated with high tide but highest during the slack tide associated with low tide (Figure 14), suggesting an interplay between tides and internal currents. To visualize the true ocean sound levels, rather than that of sound produced by movements of the mooring, we removed all data from 3–8 Hz that was greater than 115 dB re 1 µPa (Figure 15). The remaining data was smoothed in the resulting spectrogram. Sound levels at the Gully had a maximum and minimum 1-minute broadband SPL of 147.6 and 96.4 dB re 1 µPa, respectively. Sound levels after filtering had a maximum and minimum broadband SPL of 124.1 and 96.4 dB re 1 µPa, respectively, a 23 dB difference attributed to mooring movements. Filtered sound levels at the Gully were similar to the 20 km location (Figures 9 and 15). Sounds from vessels associated with ongoing extraction operations by Exxon were evident at the Gully data, as indicated by the horizonal lines in Figure 15. The sounds from oil and gas activities recorded at the Gully where likely from the Exxon operations near Sable Island. The Exxon platform only ~30 km away from the recorder, while the BP MODU was 145 km away.

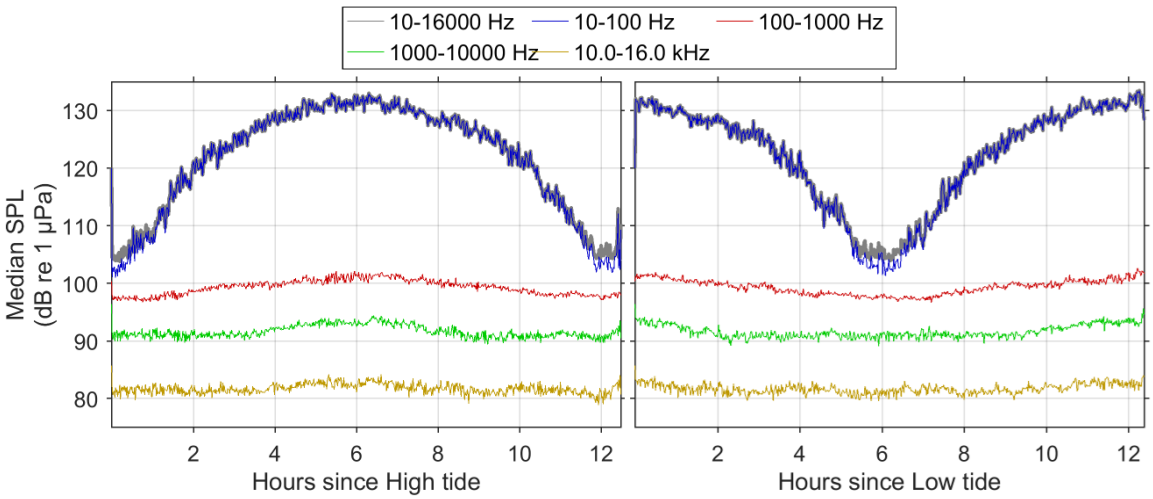

Figure 14. Median in-band SPL across tidal cycles at the Gully recording site.

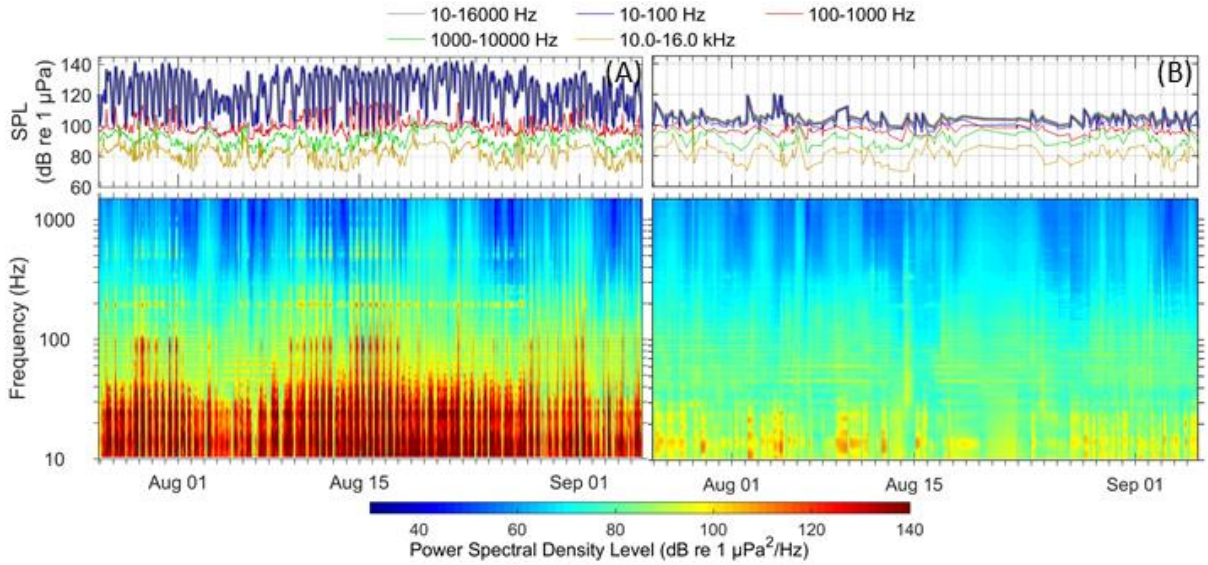

Figure 15. Gully recorder data before 3–8Hz data removal (A) and after 3–8Hz data removal (B): Spectrogram (bottom) and in-band SPL (top) for underwater sound.

There are three notable features in the power spectral density levels and 1/3-octave-band analysis (Figures 16 and 17):

1. All three stations had a spectral peak at 190 Hz. Recordings made 10 and 209 km from the West Aquarius in 2014/2015 in a similar water depth north of the Flemish Pass also had this feature. The shape of the peak was broader and smoother in the Gully recordings than at 2 and 20 km (Figure 17). The peak at the Gully was associated with periods of higher low frequency noise (Figure 15, left) and was absent after filtering (Figure 15, right). These features make it uncertain that the sound at the Gully originated with BP's MODU. This is discussed further in Section 4.1.
2. All three stations had a spectral peak in the 40–100 Hz frequency band that is associated with distant shipping (Figure 16), although it was much harder to visualize at the 2 km location). The amplitude of this peak was ~80 dB re 1 µPa²/Hz and is typical for Canada's east coast (Delarue et al. 2018).
3. There was also a 25 kHz spectral peak in the 2 km data whose source was locator beacons on the rig (Figures 16 and 18). A similar peak was noted in the recordings from the Stena IceMAX (MacDonnell 2017).

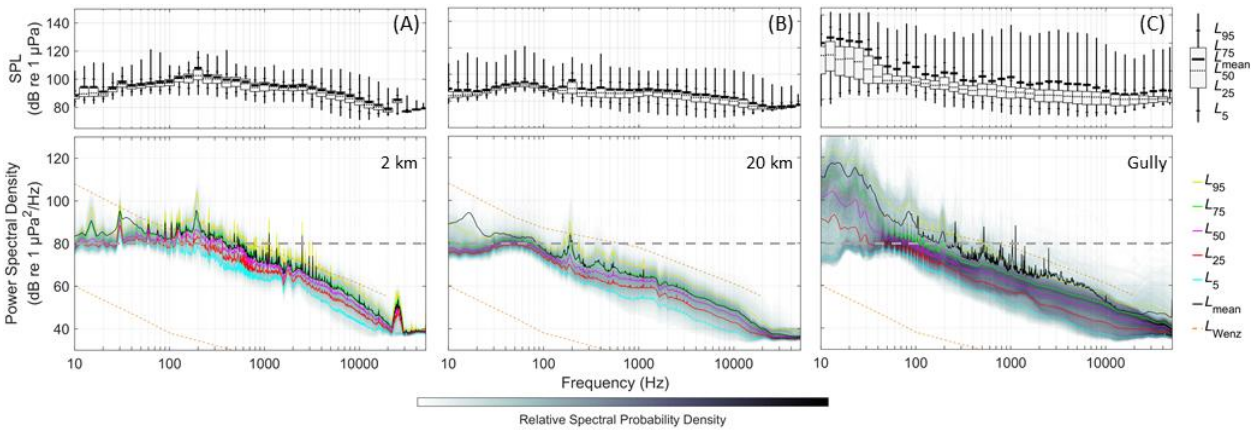

Figure 16. Power spectral density (PSD; bottom panels) and 1/3-octave-band analysis (top panels) for (A) 2 km, (B) 20 km, and (C) Gully (without 3–8Hz data removal). The PSD figures show the relative spectral density in grayscale overlaid with percentile spectra.

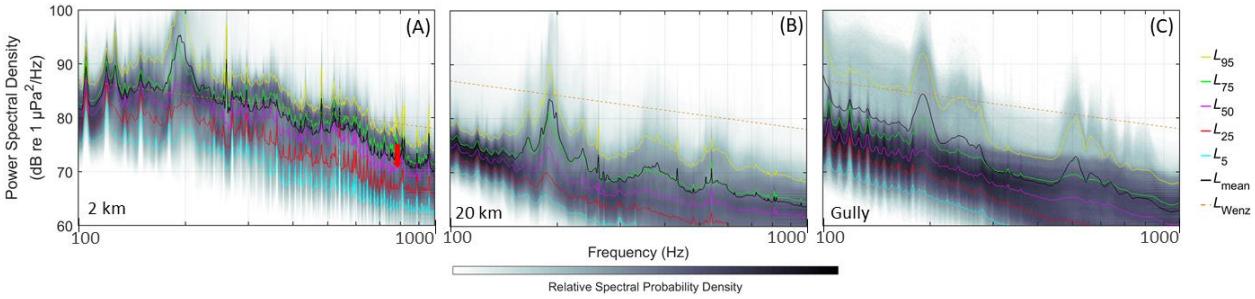

Figure 17. Power spectral density (PSD) restricted to the range of 100–1000 Hz for (A) 2 km, (B) 20 km, and (C) Gully (without 3–8Hz data removal). The PSD figures show the relative spectral density in grayscale overlaid with percentile spectra.

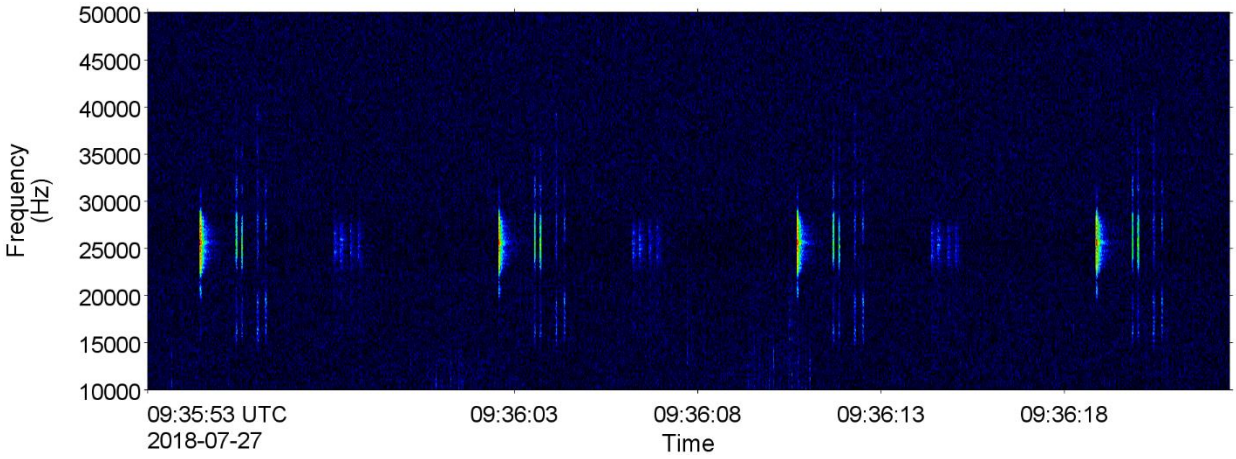

Figure 18. Locator beacon signals at the 2 km location that were detected throughout the recording period.

3.2. Marine Mammals

The acoustic presence of marine mammals was identified through automatic detection of vocalization signals and validated via a manual review of 1% of the low- and high-frequency datasets (Section 2.2.3), which represents 783 sound files, or 6.7 h of 1-min 375 kHz sound files and 63.3 h of 10-min 16 kHz sound files. In the 16 kHz data, detectors and/or analysts found acoustic signals of blue, fin, humpback, sei, long-finned pilot, and killer whales. In addition to these species, the high-frequency acoustic recordings contained signals of Cuvier's beaked whales, sperm whales, dolphins, and one unidentified species of Mesoplodon that was most likely a True's or Gervais' beaked whale.

3.2.1. Mysticetes

3.2.1.1. Blue whales

Blue whale audible downsweeps (Figure 19) (Berchok et al. 2006) occurred during the first half of the recording at 2 km and 20 km and only in late July at the Gully (Figure 20). These vocalizations had substantial overlap in spectral characteristics with sei whale vocalizations and some overlap with fin whale vocalizations, especially when the signal in question had a low signal-to-noise ratio. Therefore, the audible signals of these species were not effectively differentiated by an automated detector, and there was often uncertainty when the acoustic data were manually reviewed. We provided the occurrence of these vocalizations both when they were confirmed (validated) by an analyst and when there was a validation of a large baleen whale, but the analyst could not confidently differentiate between species (Figure 20).

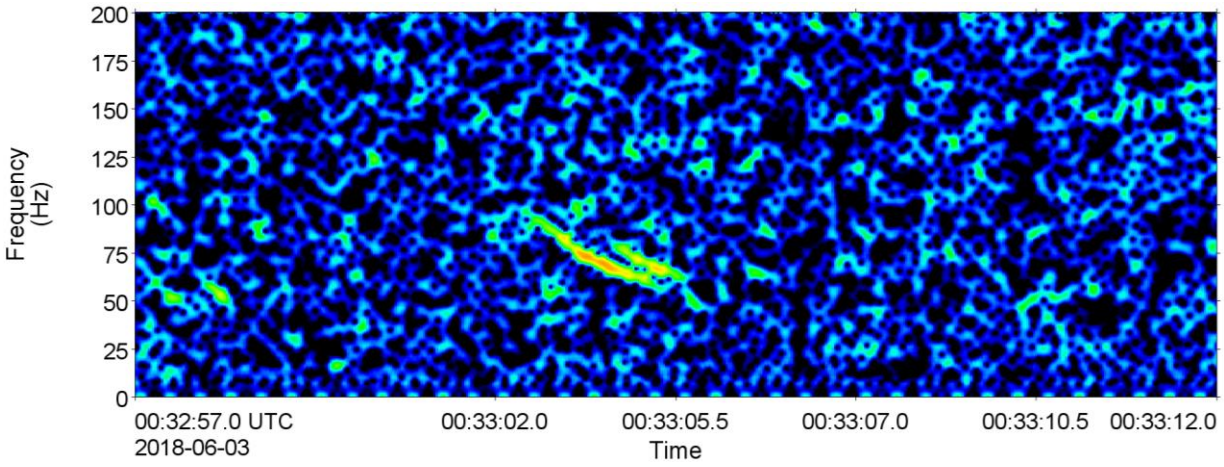

Figure 19. Blue whales: Spectrogram of audible call at 20 km on 3 Jun 2018 (0.25 Hz frequency step, 0.3 s frame length, 0.03 s time step, Hamming window).

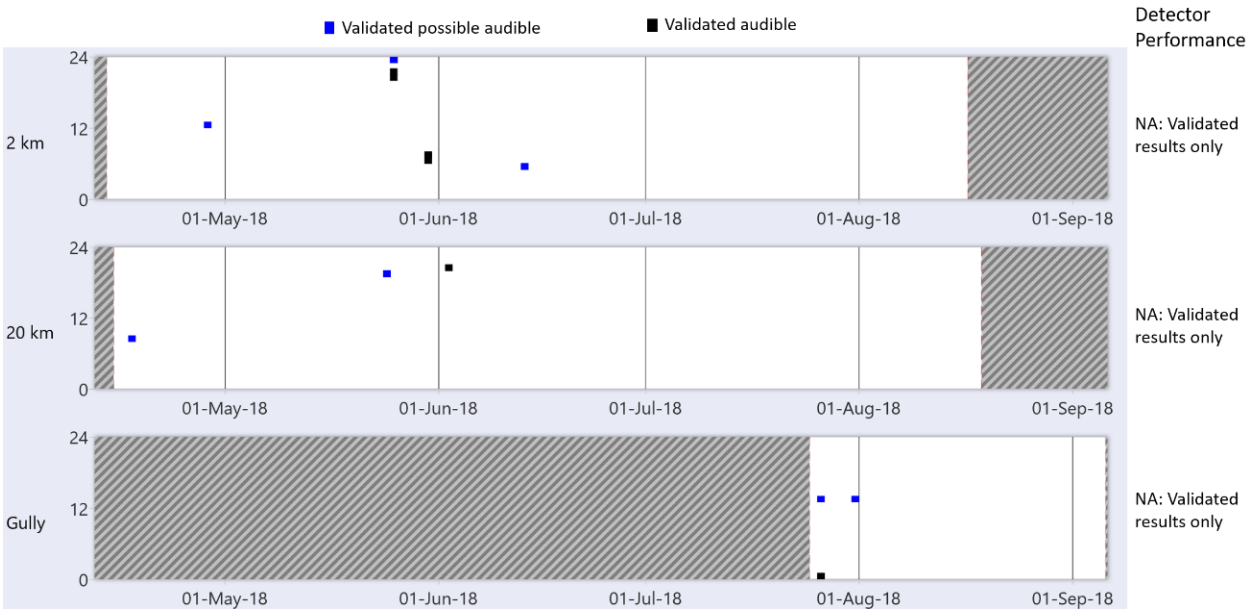

Figure 20. Blue whales: Daily and hourly occurrence (black) and possible occurrence (blue) at 2 km, 20 km, and the Gully. Dashed lines indicate periods when AMARs were not recording.

3.2.1.2. Fin whales

Fin whale infrasonic 20-Hz signals (Figure 21) (Watkins 1981) occurred sporadically in the first and last months of recordings at 2 km and 20 km (Figure 22). In contrast, fin whale infrasonic vocalizations occurred regularly throughout the Gully recording (Figure 22). The automated detector for fin whale infrasonic vocalizations performed very well, identifying 90–100% of all files with fin whale vocalizations (R = 0.90–1.00) and correctly classifying vocalizations as fin whale in 83–100% of acoustic files (P = 0.83–1.00). The lower precision of the detector at the Gully is a result of the detector being regularly falsely triggered by sounds associated with the movement of the mooring that was likely created by interactions between currents and tides (described in Section 3.1.1). Baleen whale audible moans (for which there is currently no effective automated detector) that could not be confidently differentiated between fin whales, sei whales, and/or blue whales were validated sporadically at all stations (Figure 22).

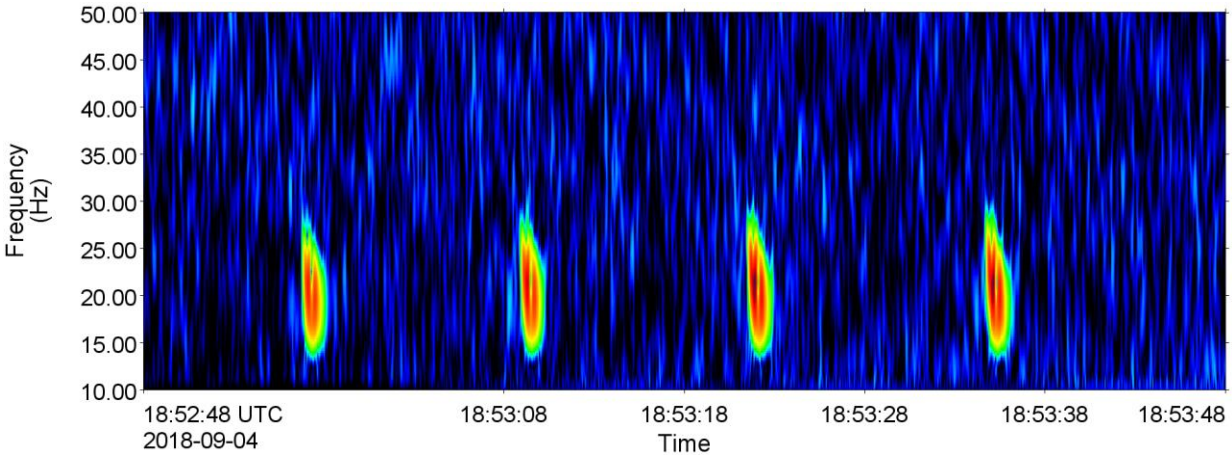

Figure 21. Fin whales: Spectrogram of calls at the Gully on 4 Sep 2018 (0.25 Hz frequency resolution, 0.3 s time window, 0.03 s time step, Hamming window).

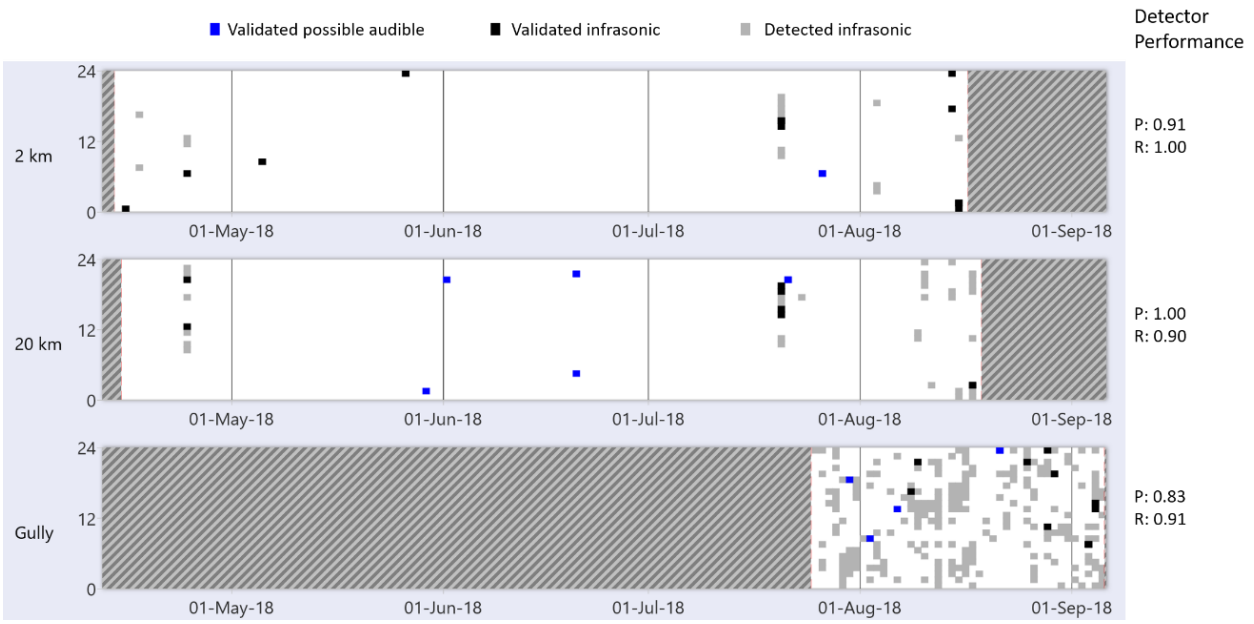

Figure 22. Fin whales: Daily and hourly occurrence at 2 km, 20 km, and the Gully. Dashed lines indicate periods when AMARs were not recording.

3.2.1.3. Humpback whales

The humpback whale automated detector was falsely trigger by MODU-related sounds at the 2 km and 20 km locations and by sounds associated with the mooring movement at the Gully location; therefore, humpback whale wops, grunts, and purrs ranging from 50–700 Hz were manually validated and presented here, representing a minimum estimate of acoustic occurrence (Figures 23 and 24). No humpback vocalizations were recorded at 2 km and if present, they were likely masked by the operational sounds spanning the 10–1000 Hz band (Figure 9). One vocalization was validated at 20 km on 24 Apr 2018, and calls were sporadically validated throughout the Gully recording from 30 Jul to 4 Sep 2018.

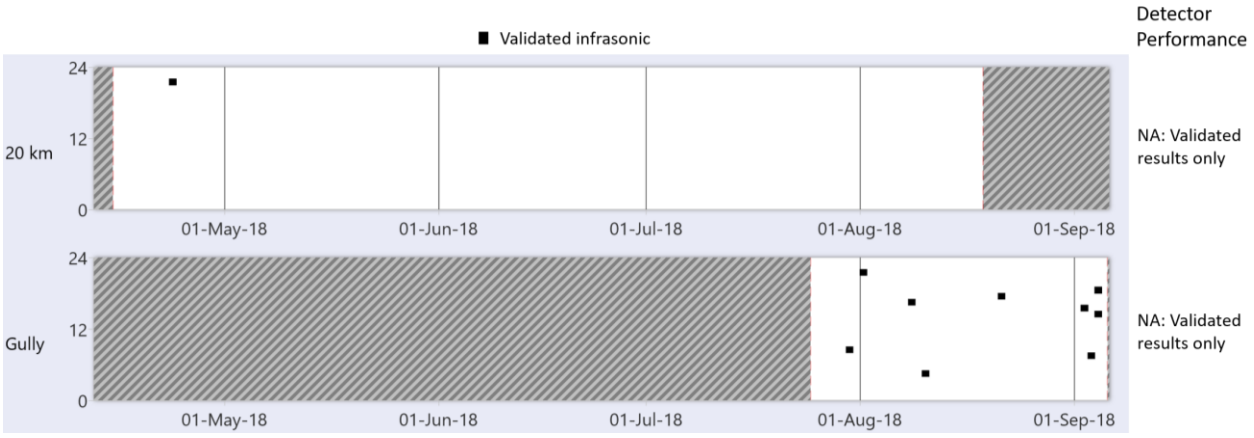

Figure 23. Humpback whales: Daily and hourly occurrence at 20 km and the Gully. Dashed lines indicate periods when AMARs were not recording.

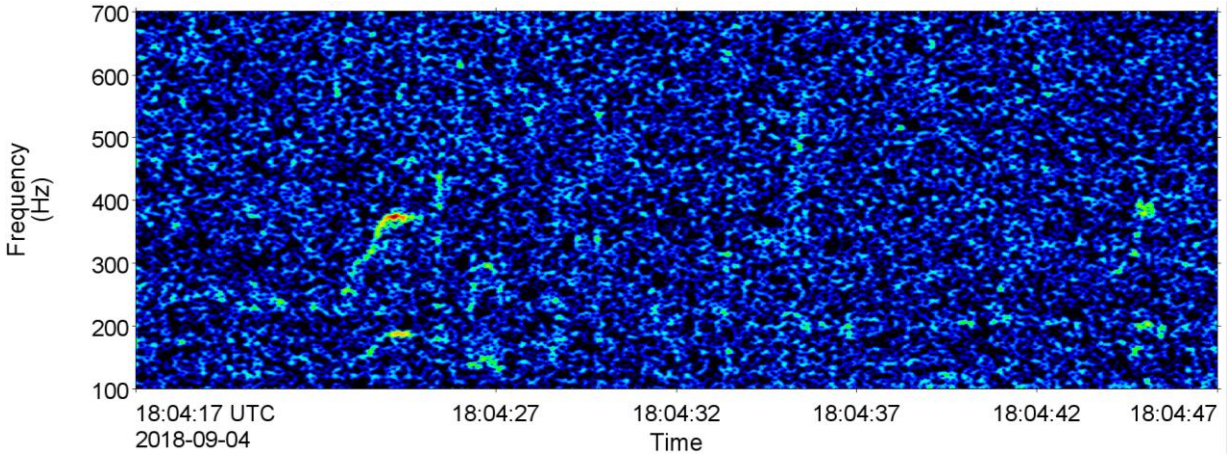

Figure 24. Humpback whales: Spectrogram of moans at the Gully on 4 Sep 2018 (0.25 Hz frequency resolution, 0.3 s time window, 0.03 s time step, Hamming window).

3.2.1.4. Sei whales

Sei whale downsweeps typically last ~1–2 s, decreasing from ~90–40 Hz (Baumgartner et al. 2008). They occur in singles, pairs, and triplets (Figure 25). The sei whale detector was systematically triggered by anthropogenic sounds, as well as audible fin and blue whale vocalizations, making the detector's results unusable. Sei whale vocalizations were validated by analysts during the manual review process. It was challenging to differentiate sei whale vocalizations during summer when blue and fin whale vocalizations occur at similar frequencies. Therefore, we present sei whale occurrence both when we were certain of the species' acoustic occurrence and when the species was possibly present (Figure 26). Sei whale presence was validated in at the 2 km station, in May and June at the 20 km station, and in August at the Gully station, though possible sei whale signals were validated sporadically throughout all recordings (Figure 26).

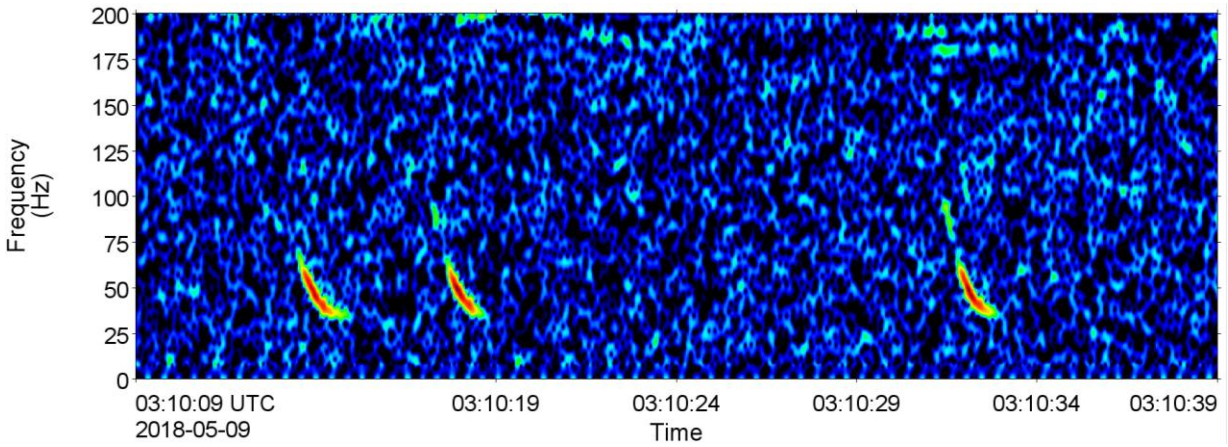

Figure 25. Sei whales: Spectrogram of downsweeping moans at 20 km on 9 May 2018 (0.25 Hz frequency resolution, 0.3 s time window, 0.03 s time step, Hamming window).

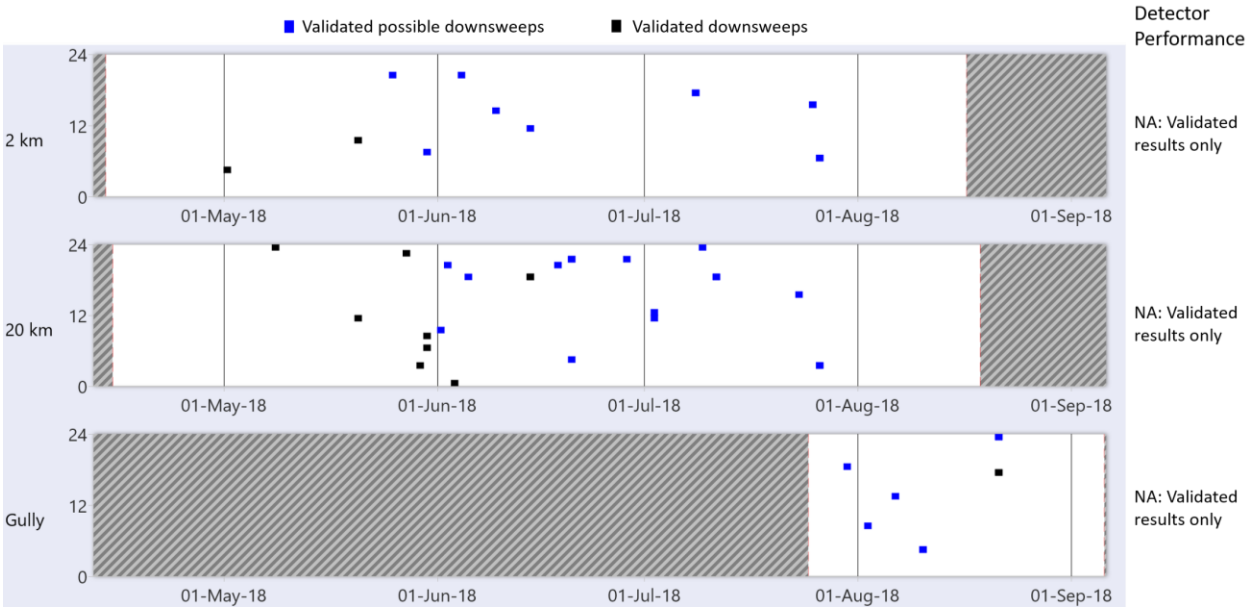

Figure 26. Sei whales: Daily and hourly occurrence at 2 km, 20 km, and the Gully. Dashed lines indicate periods when AMARs were not recording.

3.2.2. Odontocetes

Sperm and pilot whales, dolphin species, as well as Cuvier's and True's or Gervais' beaked whales were identified in the acoustic recordings, as presented here. The project location was just south of the known extent of northern bottlenose whales (a species of beaked whale); however, none were detected in the 2 km or 20 km data. The Gully recorder was located in water too shallow for beaked whales.

3.2.2.1. Sperm whales

Sperm whale clicks (Figure 28) were regularly automatically detected throughout the 2 km and 20 km recordings, with detections becoming more frequent in July and August (Figure 28). Automated detectors at these stations performed well with 97–100% of acoustic files with detections truly containing sperm whale clicks (P = 0.97–1.00). These results are an underestimate of true sperm whale acoustic occurrence, representing 78–80% of acoustic files that contained sperm whale clicks (Figure 28). The automated detector results were not reliable at the Gully, as the detector was regularly triggered by sound associated with the mooring movement (see Section 3.1.1). Validated results indicate that sperm whales were acoustically present throughout the Gully recording period (Figure 28).

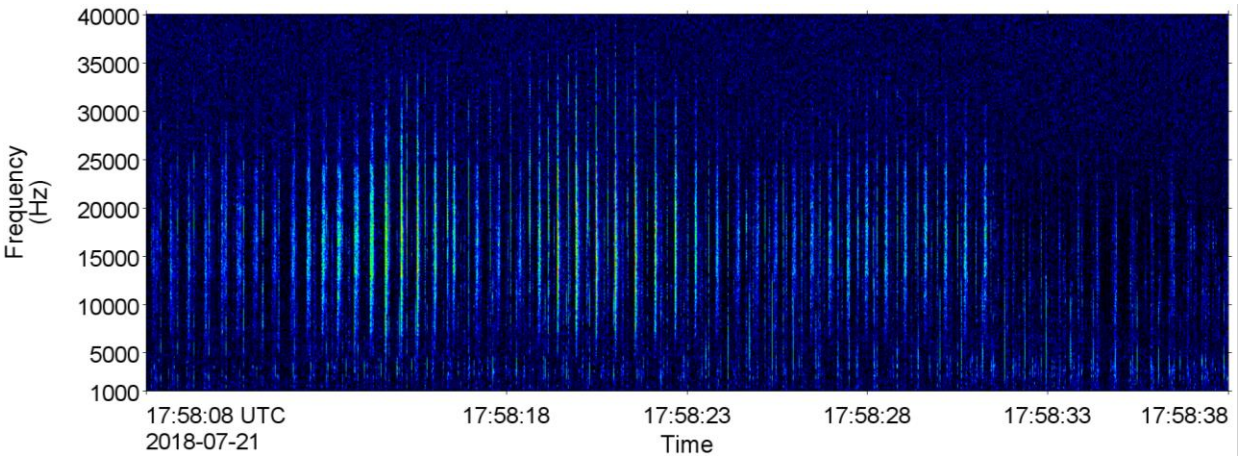

Figure 27. Sperm whales: Spectrogram of clicks at 20 km on 21 Jul 2018 (64 Hz frequency resolution, 0.01 s time window, 0.005 s time step, Hamming window).

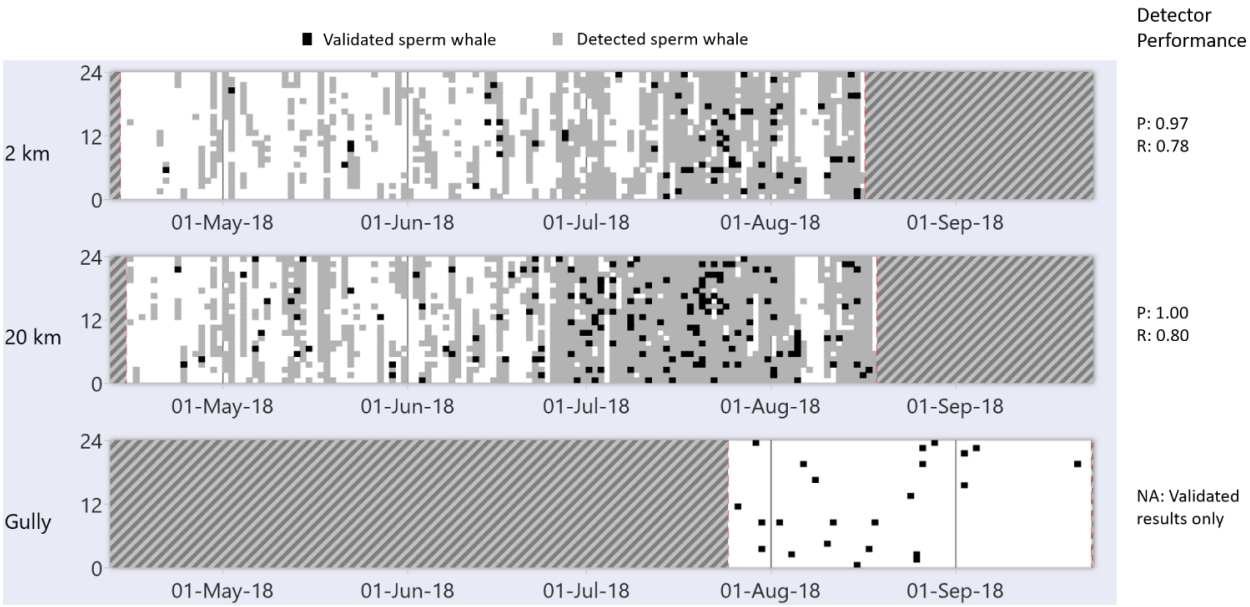

Figure 28. Sperm whales: Daily and hourly occurrence at 2 km, 20 km, and the Gully. Dashed lines indicate periods when AMARs were not recording.

3.2.2.2. Pilot whales and killer whales (large delphinids)

Pilot whale and killer whale whistles overlap in frequency characteristics (e.g., Figures 29 and 30) (Steiner 1981a, Rendell et al. 1999, Riesch and Deecke 2011), resulting in signals from both species being identified by the same automated detector. Through manual validation, we concluded that most detections were pilot whale whistles.

Pilot whale whistles occurred at 2 km and 20 km stations, though they were all but absent in June (Figure 31). The detector was ineffective at the 2 km station due to the increased anthropogenic sounds; therefore, only the manual validations are shown. The automated detector performed acceptably at station 20 km where 80% of files with detections truly contained pilot whale whistles. The detector greatly underestimated the true occurrence of the species, with the results only displaying 34% of files containing pilot whale whistles. This suggests the signal-to-noise ratio of many signals were below the threshold of the detector. Pilot whale whistles occurred almost constantly at the Gully, a finding that is still an underestimate with the detector, only identifying 52% of files containing pilot whales (Figure 31). Killer whale acoustic signals were validated at 20 km on 12 Aug 2018 (Figure 31).

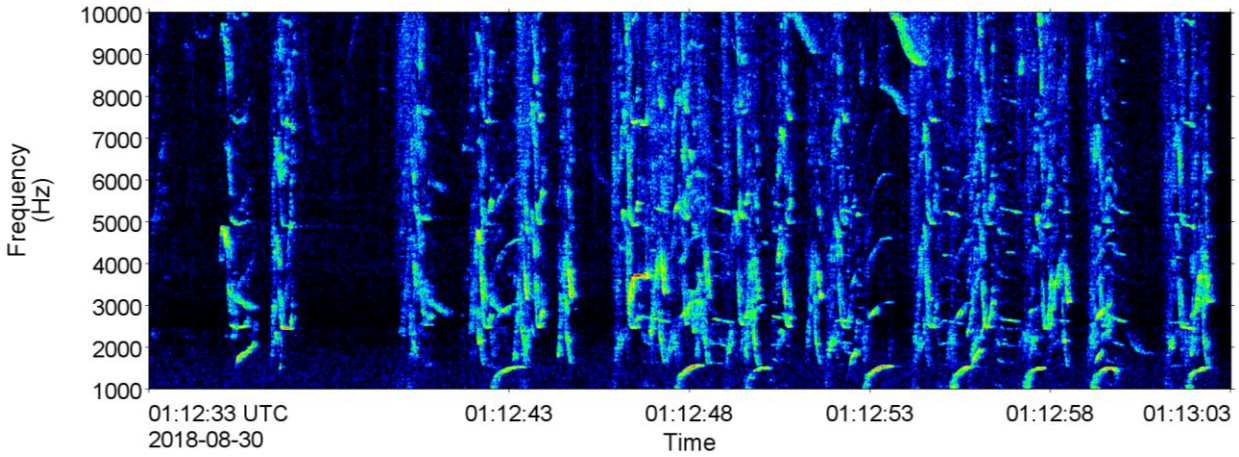

Figure 29. Pilot whales: Spectrogram of whistles at the Gully on 30 Aug 2018 (4 Hz frequency resolution, 0.05 s time window, 0.01 s time step, Hamming window).

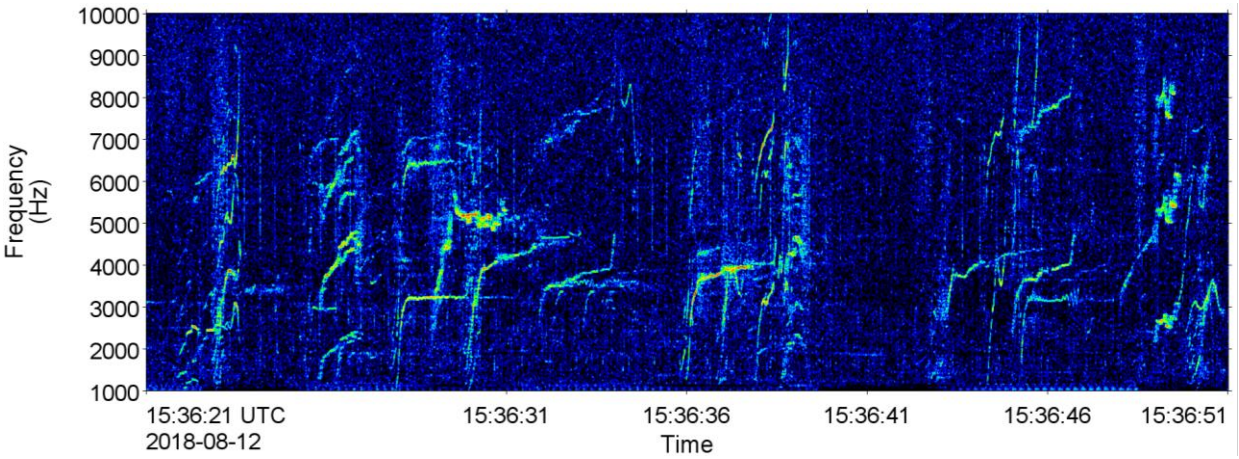

Figure 30. Killer whales: Spectrogram of whistles at 20 km on 12 Aug 2018 (4 Hz frequency resolution, 0.05 s time window, 0.01 s time step, Hamming window).

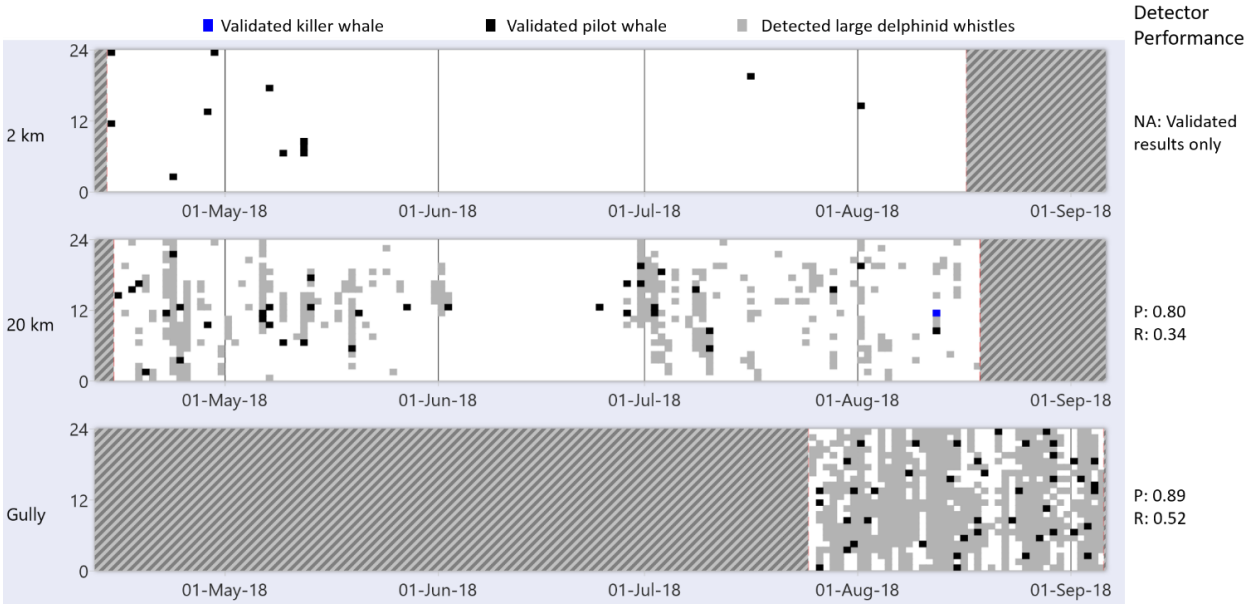

Figure 31. Pilot whales: Daily and hourly occurrence at 2 km, 20 km, and the Gully. Dashed lines indicate periods when AMARs were not recording.

3.2.2.3. Dolphins (small delphinids)

Dolphin click and whistle detections occurred throughout the recording period at all stations and were accurately identified (*P* = 90–100%; Figures 32 and 33). Because dolphin clicks are difficult to discern from pilot whale clicks, a portion of the detections in Figure 32 may have been triggered by pilot whale clicks. Clicks showed a diel pattern, occurring more often during hours of darkness than light (Figure 32). In contrast, whistles were detected nearly constantly throughout all hours of the day (Figure 33) but were sometimes faint or masked (*R* = 23–56%). Dolphin whistles occurred at 8–20 kHz (Figure 34). Clicks were predominantly broadband in nature, often seeming to span beyond the scope of the recorders, with centre frequencies spanning from 20–185 kHz (Figures 35 and 36).

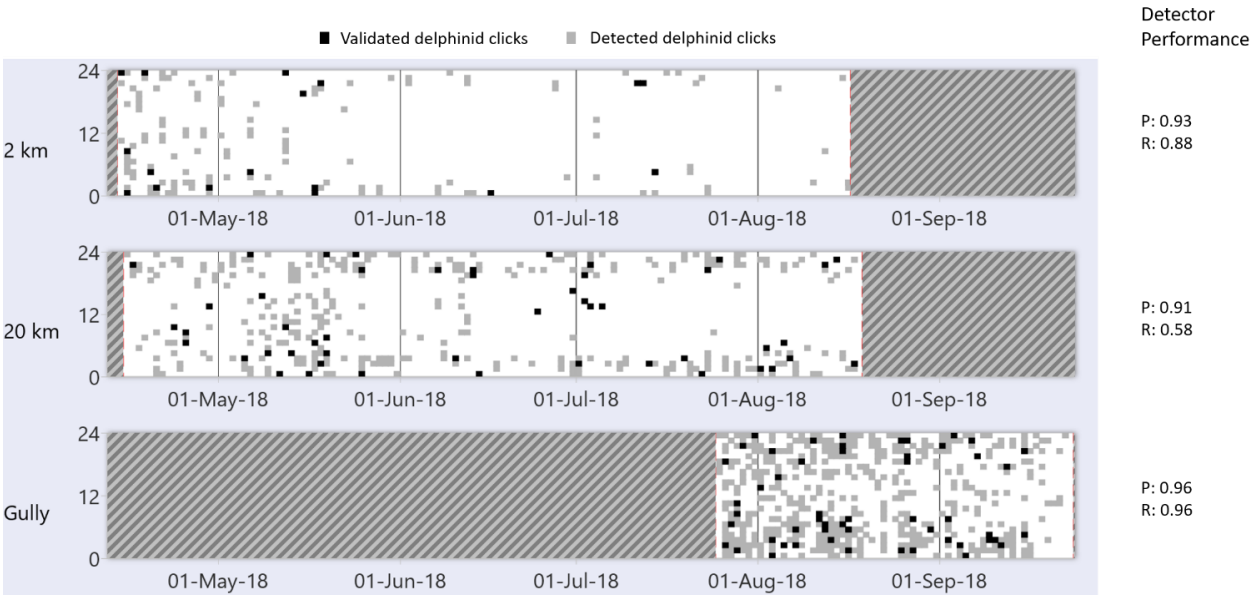

Figure 32. Dolphin clicks: Daily and hourly occurrence at 2 km, 20 km, and the Gully. Dashed lines indicate periods when AMARs were not recording.

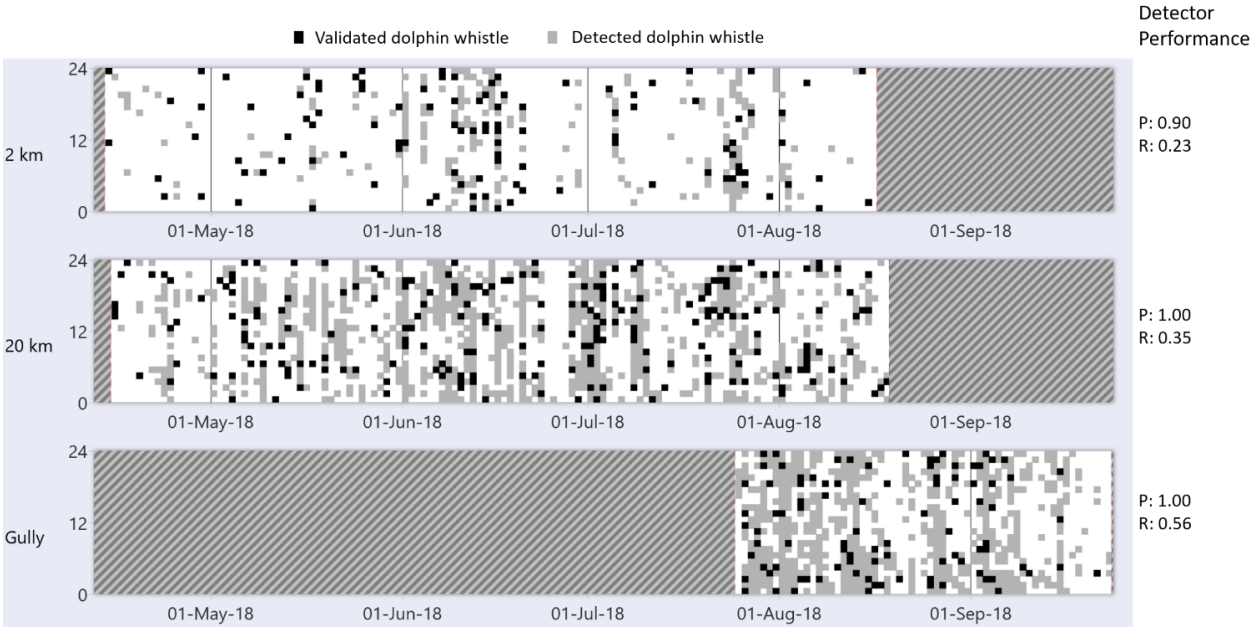

Figure 33. Dolphin whistles: Daily and hourly occurrence at 2 km, 20 km, and the Gully. Dashed lines indicate periods when AMARs were not recording.

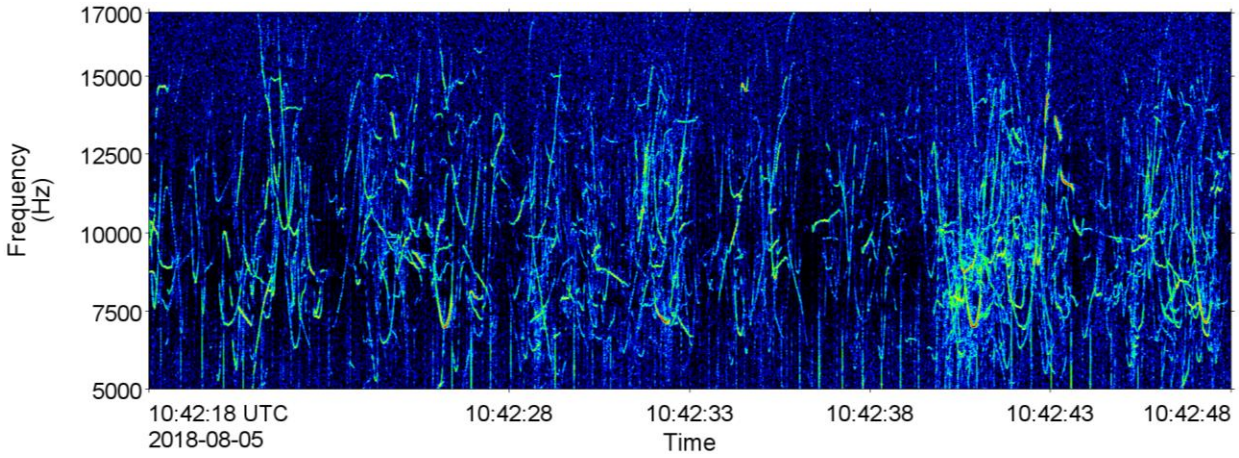

Figure 34. Dolphins: Spectrogram of whistles at 20 km on 5 Aug 2018 (64 Hz frequency resolution, 0.01 s time window, 0.005 s time step, Hamming window).

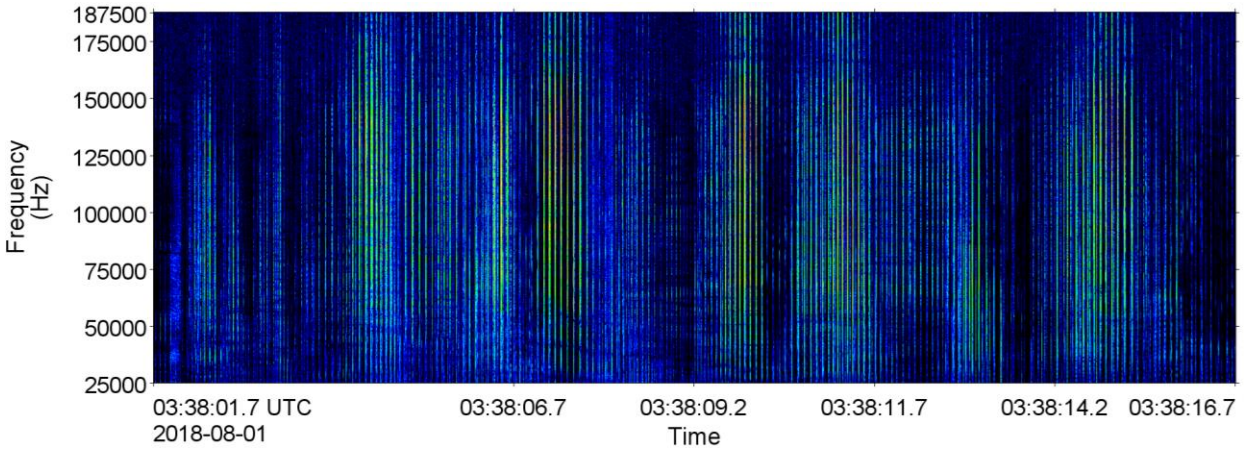

Figure 35. Dolphins: Spectrogram of click trains at the Gully on 1 Aug 2018 (64 Hz frequency resolution, 0.01 s time window, 0.005 s time step, Hamming window).

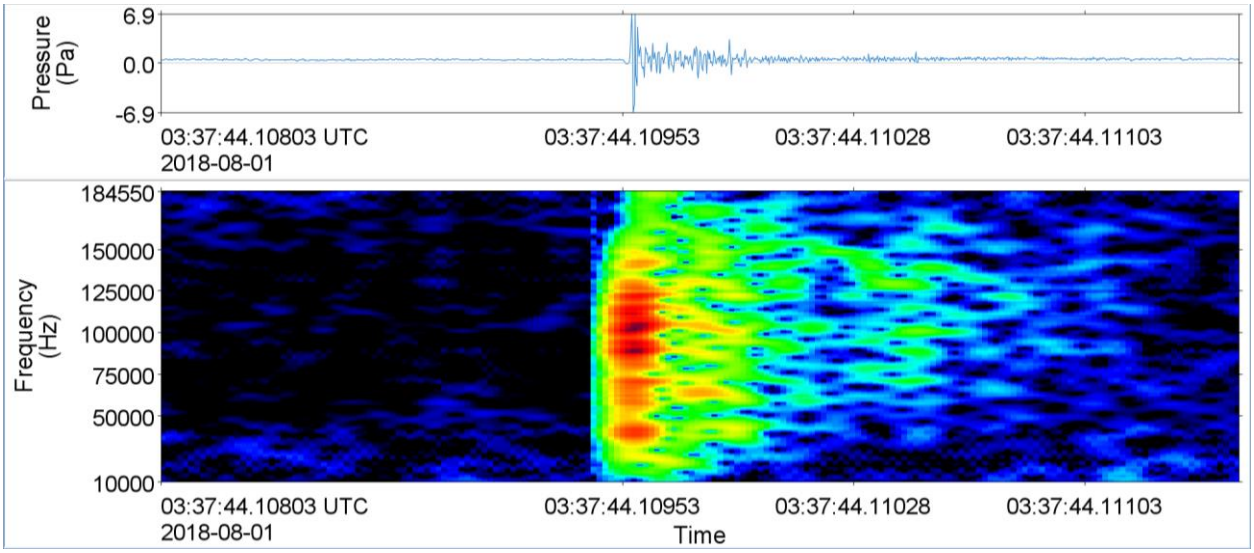

Figure 36. Dolphins: Spectrogram of click at the Gully on 1 Aug 2018 (512 Hz frequency resolution, 0.26 ms time window, 0.02 ms time step, Hamming window).

3.2.2.4. Cuvier's beaked whales

The Cuvier's beaked whale clicks recorded in this study (Figure 37) were identified on the basis of descriptions by several authors in different areas of the world (Zimmer et al. 2005, Baumann-Pickering et al. 2013). The detected clicks had a centroid frequency of ~40 kHz and often had a characteristic C-shaped contour (Figure 38). Cuvier's beaked whale clicks were dected and validated on 20–21 Apr 2018 at the 2 km station (Figure 39). In contrast, clicks were detected throughout the 20 km recording with high detector performance (Figure 39). No Cuvier's beaked whale clicks were validated at the Gully station.

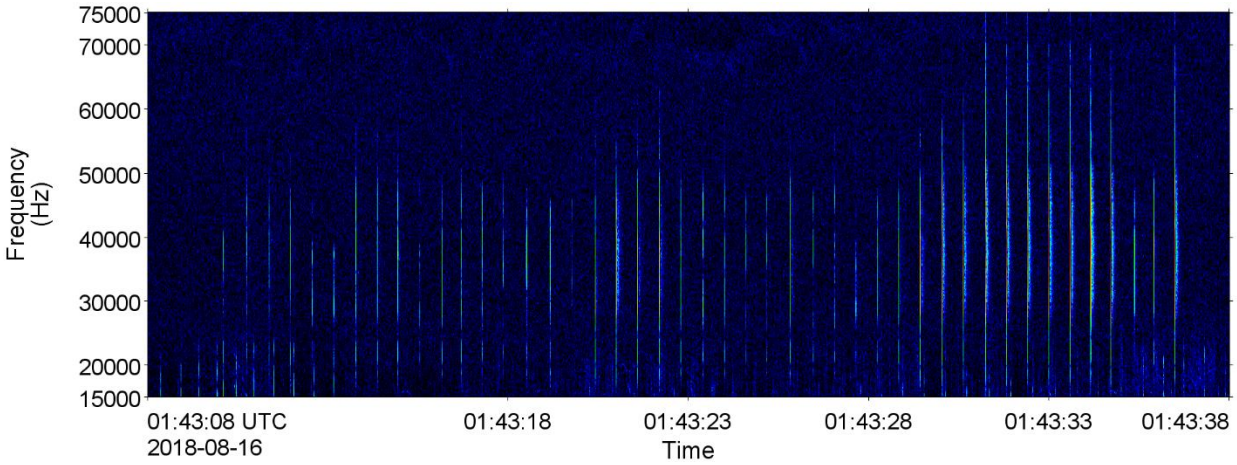

Figure 37. Cuvier's beaked whales: Spectrogram of a click train recorded at 20 km on 16 Aug 2018 (64 Hz frequency resolution, 0.01 s time window, 0.005 s time step, Hamming window).

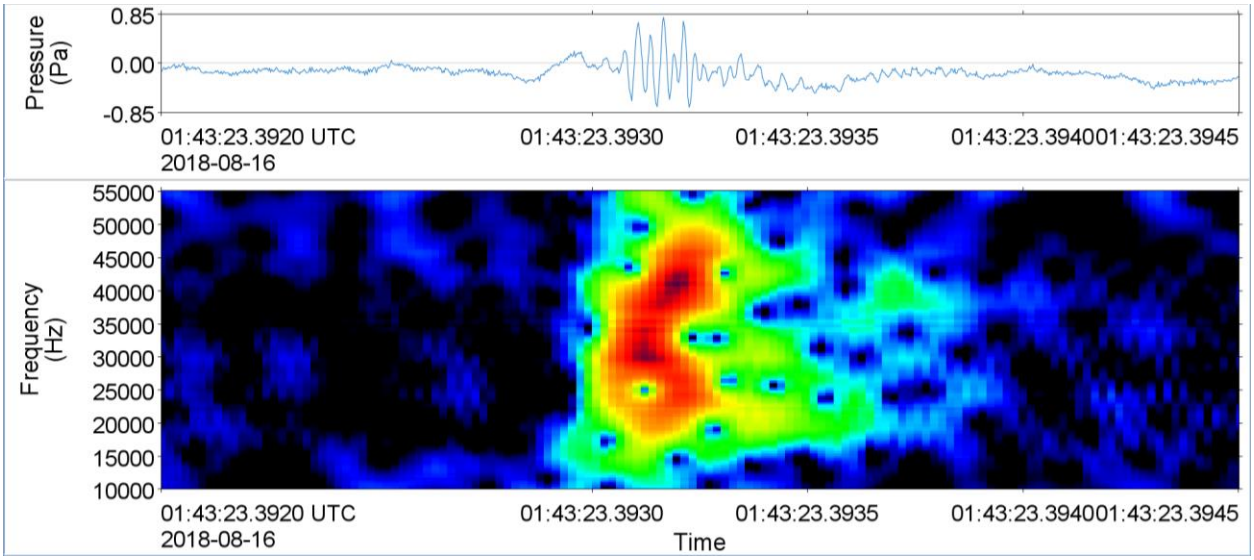

Figure 38. Cuvier's beaked whales: Spectrogram of click recorded at 20 km on 16 Aug 2018 (512 Hz frequency resolution, 0.26 ms time window, 0.02 ms time step, Hamming window).

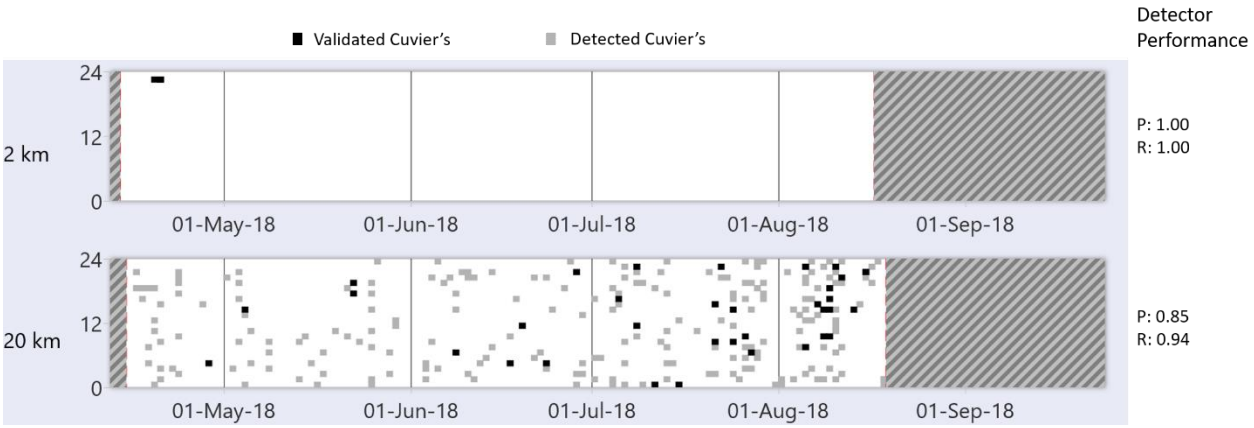

Figure 39. Cuvier's beaked whales: Daily and hourly occurrence at 2 km and 20 km. Dashed lines indicate periods when AMARs were not recording.

3.2.2.5. True's or Gervais' beaked whales

The echolocation signals of Gervais' beaked whales are relatively well described (Johnson et al. 2006, Gillespie et al. 2009), and the first description of True's beaked whale signals has recently become available (DeAngelis et al. 2018). Based on the current knowledge of these species and the great overlap in click characteristics, it is currently impossible to confidently distinguish between them, either automatically or manually. Our findings, therefore, do not distinguish between these species. Similar to Cuvier's beaked whales, True's/Gervais beaked whale clicks were detected and validated on a few occasions at the 2 km station, occurred regularly at the 20 km station, and were absent from the Gully station (Figure 40). The detector sometimes missed faint clicks (R = 0.67–0.87), but clicks were accurately classified (P = 95–100%; Figure 40). The detected clicks had a centroid frequency of ~45–48 kHz (Figure 41) and an inter-click interval (ICI) of 0.19 s (Figure 42).

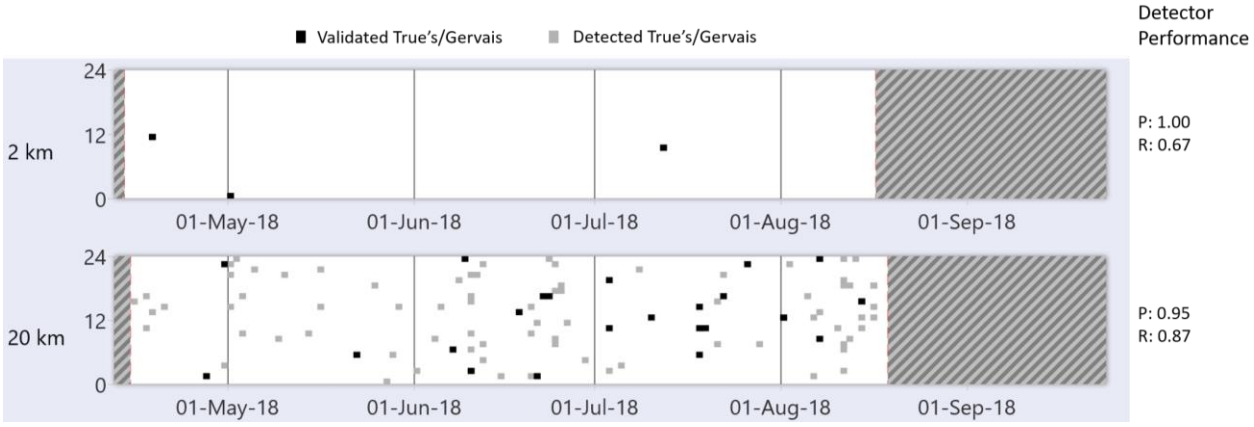

Figure 40. True's or Gervais' beaked whales: Daily and hourly occurrence at 2 km and 20 km. Dashed lines indicate periods when AMARs were not recording.

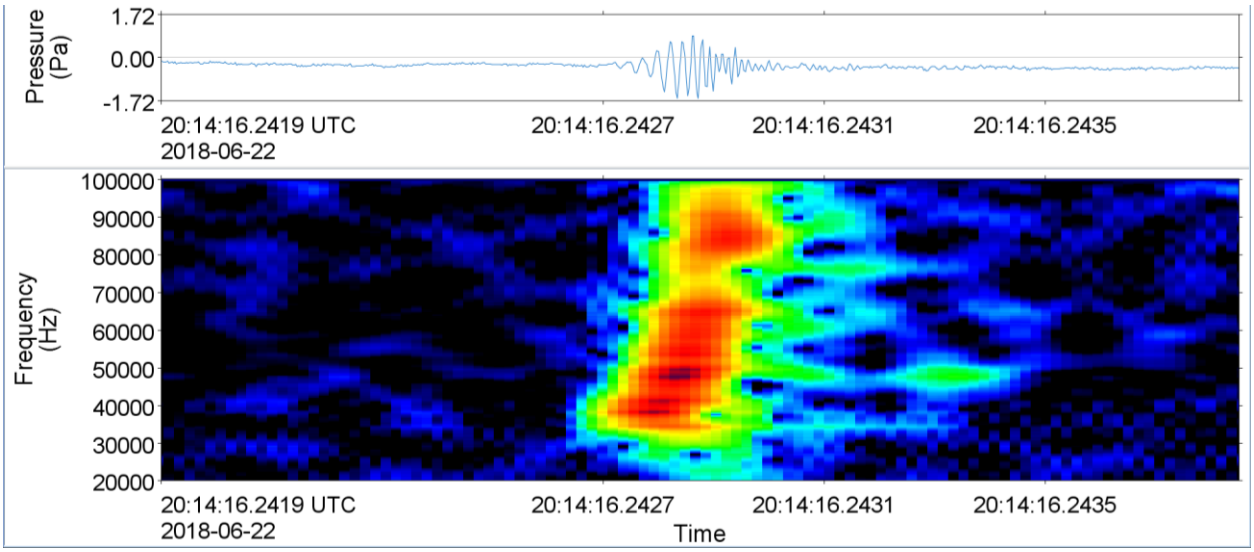

Figure 41. True's or Gervais' beaked whales: Spectrogram of click recorded at 20 km on 14 Aug 2018 (512 Hz frequency resolution, 0.26 ms time window, 0.02 ms time step, Hamming window).

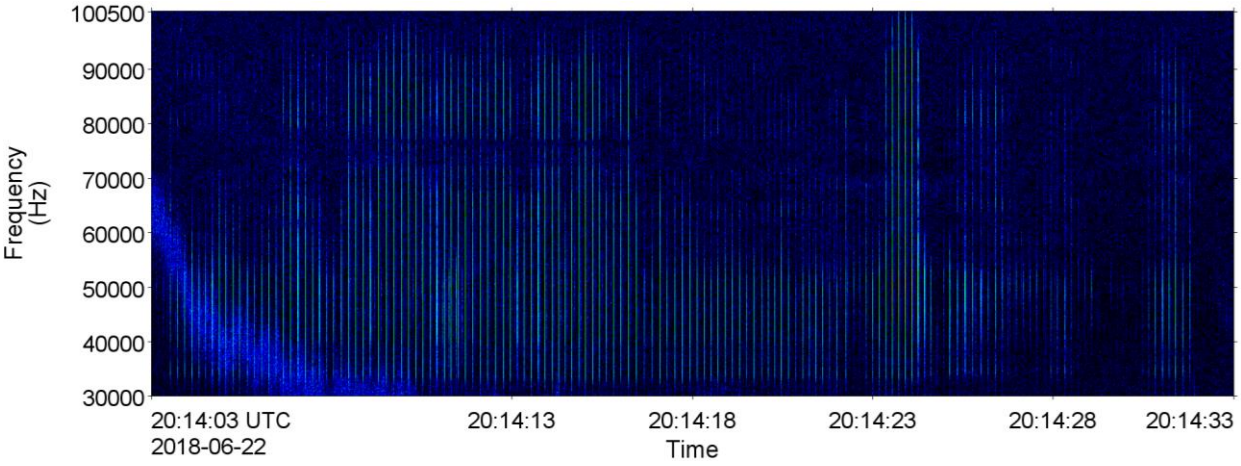

Figure 42. True's or Gervais' beaked whales: Spectrogram of a click train recorded at 20 km on 22 Jun 2018 (64 Hz frequency resolution, 0.01 s time window, 0.005 s time step, Hamming window).

4. Discussion

4.1. Ambient Sound and Drilling Measurements

Wind, waves, ice-cracking events, geological seismic events, biological sources, and human activities all contribute to sound levels in the ocean (Table 2). Sound levels were assessed at all three stations of this study. The primary anthropogenic sounds at the 2 km and 20 km stations were from the BP drilling operations. The contributions of were constant at 2 km and consistent at 20 km, influenced by the proximity of the stations to the MODU that was continuous DP mode. DP creates more cavitation than transiting vessels because the DP thruster propellers are not moving smoothly through the water, hence creating more sound.

This section discusses the contributions of wind, waves and the MODU to the measured soundscape.

Table 2. Analysis bands and sources.

Frequency band (Hz)	Biologic	Anthropogenic	Geologic	Other
10–100	Fin whales, blue whales	Seismic		Movement of mooring due to tide/current
100–1000	Fish, baleen whales	Seismic, large vessels, drilling-related operations		Movement of mooring due to tide/current
1000–10,000	Baleen whales, fish	Smaller vessels, large vessels at close range, dynamic positioning	Wind and wave action	
10,000 to +16,000	Whistles, sperm whale clicks, baleen song, shrimp	Naval sonar, cavitation bubbles, chains	Sediment movement, rain	

4.1.1. Correlations of Sound Levels with Wind Speed and Wave Height

Understanding the correlation of wind and wave action with ambient sound levels as a function of frequency helps identify the importance of these sound sources on the recorded soundscape, and by extension, sound levels of other sound sources. The 20 km location recorded much lower sound levels from the MODU, and hence better represents the existing soundscape (Figure 43). In this figure, the bottom two rows (and two right hand columns) show the correlations of wind speed and wave height with each of the octave sound pressure levels. The wind speed was measured at the MODU, and we found that a 2.5 hour lag between the wind and sound levels maximized the wind correlation. The figure shows that for frequencies of 200 Hz and above, the increase and decrease in wind speed accounts for between 60–75% of the changes in sound levels, which is an expected result. The wind speed and wave heights are correlated to a similar degree.

The results at the 2 km location (Figure 44) are much different. Here the wind speed changes only account for 25–40% of the changes in received sound pressure levels for frequencies of 200 Hz and above. Thus, at the 2 km location, most of the sound variations were not due to wind but due to MODU operations. Interestingly, the 200 Hz octave-band had the highest correlation for frequencies above 100 Hz, which suggests that the 190 Hz tone was related to the DP thrusters, whose power output and sound emission were proportional to the wind speed.

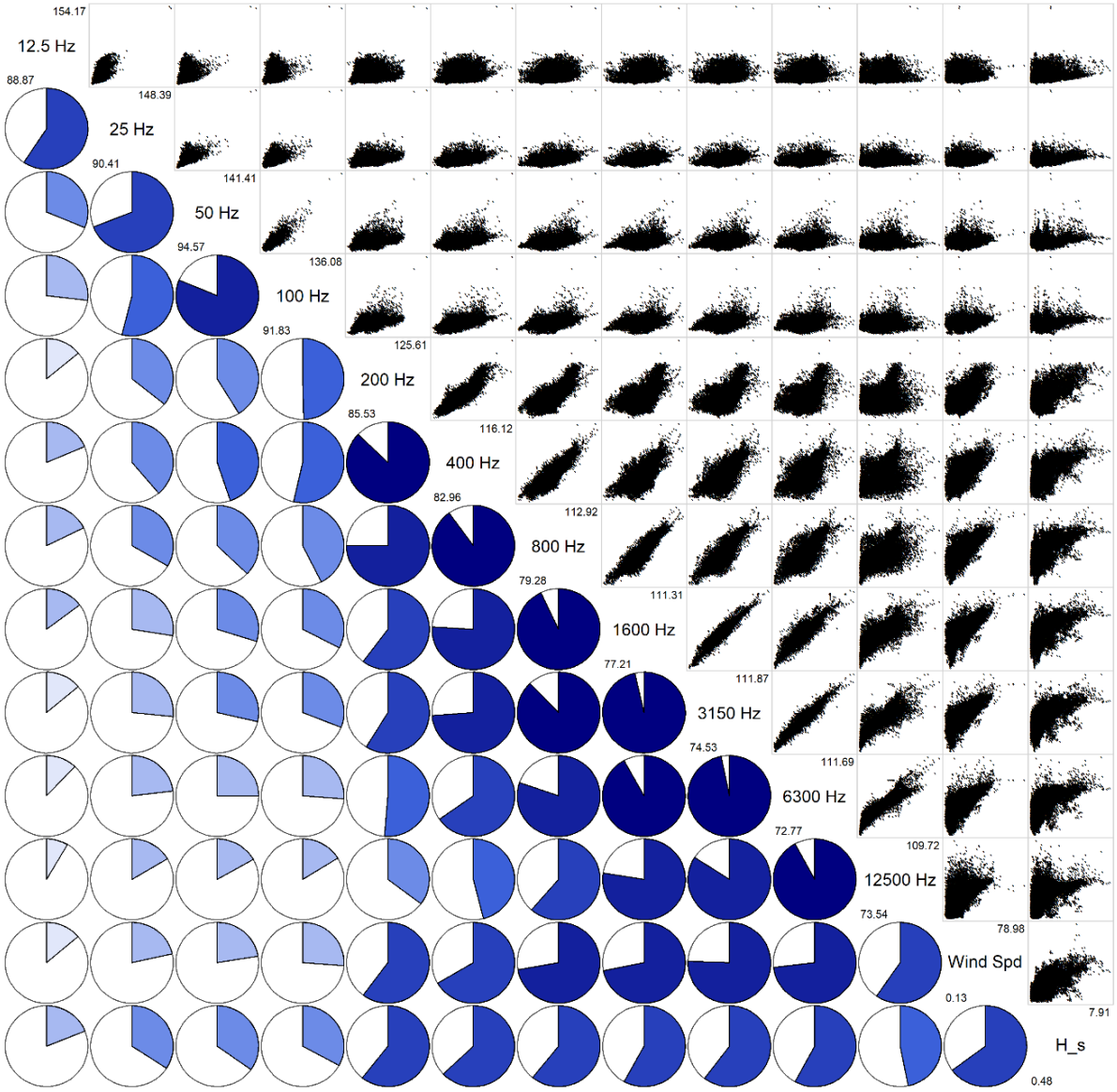

Figure 43. Correlogram for the 20 km location, which depicts the degree of correlation between variables. Two types of variables are shown: one-minute sound pressure levels in 11 octave frequency bands and two environmental variables (wind speed and significant wave height). The diagonal of the figure identifies the variables. The top-right triangles are scatterplots of pairs of variables. The lower left triangles are disks representing the degree of correlation between variables. Blue represents a positive correlation, red is negative correlation. The amount of the pie that is filled and the shading represent the degree of correlation from +1 (full blue) to −1 (full dark red). No negative correlations were found in the data.

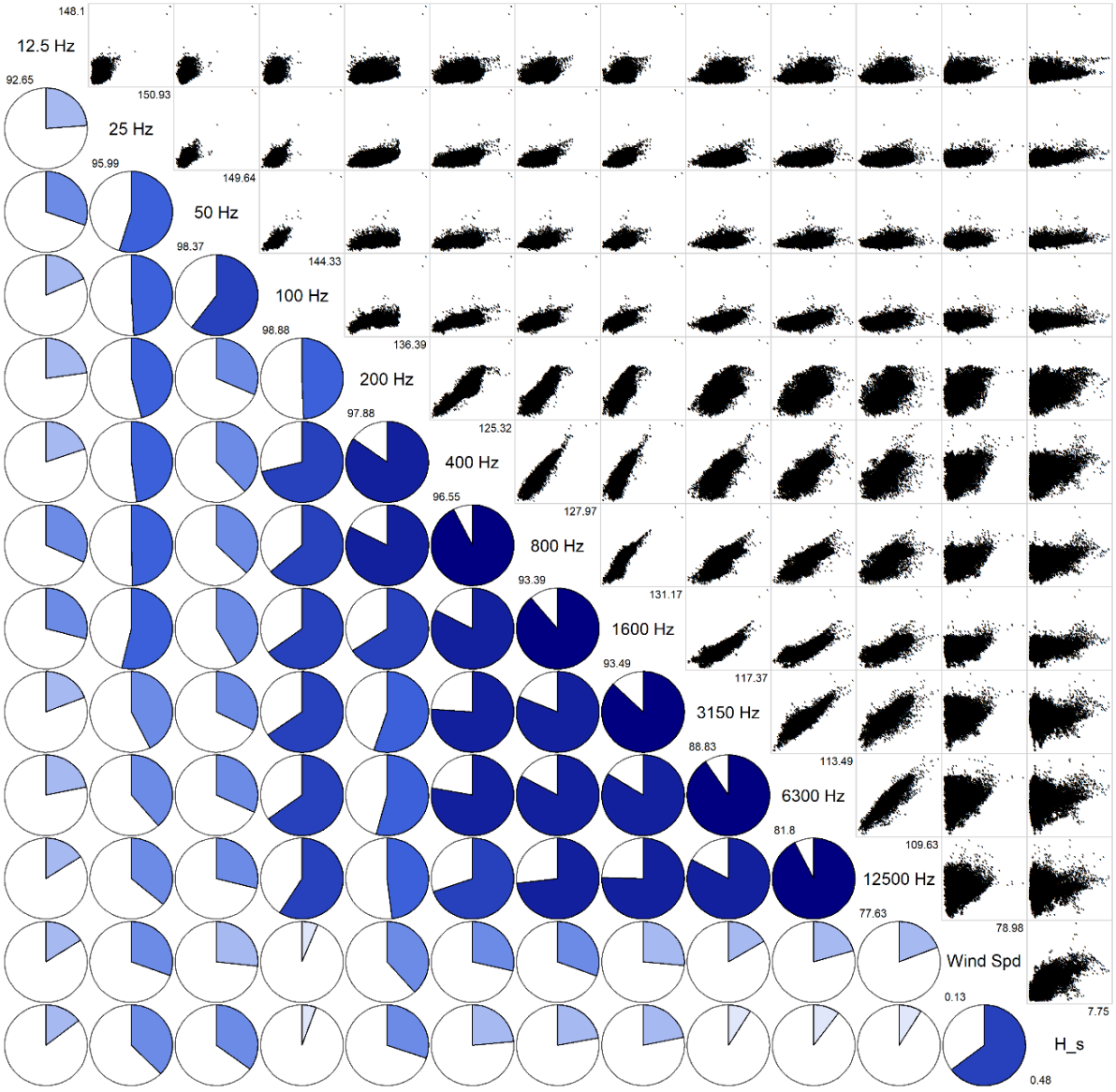

Figure 44. Correlogram for the 2 km location, which depicts the degree of correlation between variables. Two types of variables are shown: one minute sound pressure levels in 11 octave frequency bands and two environmental variables (wind speed and significant wave height). The diagonal of the figure identifies the variables. The top-right triangles are scatterplots of pairs of variables. The lower left triangles are disks representing the degree of correlation between variables. Blue represents a positive correlation, red is negative correlation. The amount of the pie that is filled and the shading represent the degree of correlation from +1 (full blue) to −1 (full dark red). No negative correlations were found in the data.

4.1.2. Effects of MODU West Aquarius on the Soundscape

JASCO previously collected two years of near-continuous acoustic data at a site (Stn 4 in Figure 4) located 45 km NNW from the BP MODU drill site (Delarue et al. 2018). From February to July 2016, Stn 4 was 13 km from Shell Canada's drilling at the Cheshire well. The 2017 data from Stn 4 were analyzed to characterize baseline underwater sound levels, while the 2016 data, which includes the Cheshire well drilling, were expected to be similar to the 20 km data from the BP MODU. The analysis was performed for broadband sound levels and the decade bands from 10–100 Hz, 100–1000 Hz, and 1000–10000 Hz (Figure 45). For all measurements, the period of April to July was used so that seasonal effects were

excluded. A similar comparison between using the Gully recorder which was 30 km from Exxon's operations was not performed due to flow noise in the lower frequency bands.

Statistically, the mean ranks of sound pressure levels were significantly different across stations for each band level (Kruskal-Wallis test, χ^2 values greater than 110, df = 1 or 3, $P < 0.001$) with the mean ranks of sound pressure levels higher at the 2 km station than all other stations and levels at the 20 km station higher than the baseline data at Stn 4 from 2017. Comparing the interquartile ranges (Figure 45), the broadband and 100–1000 Hz band sound pressure levels at 2 km were consistently higher than those at 20 km and Stn 4 in both years, and there was also a significant difference between 20 km and Stn 4 in 2017 for those bands. This suggests that the presence of the MODU significantly increased the ambient soundscape at 2 km and 20 km. Stn 4 in 2016 during the Shell drill program with the Stena IceMAX and data 20 km from the West Aquarius were not significantly different for broadband and 10–100 Hz. Above 100 Hz the 2016 and 2017 data from Stn 4 were similar. The 20 km data were higher than both the 2016 and 2017 at Stn 4.

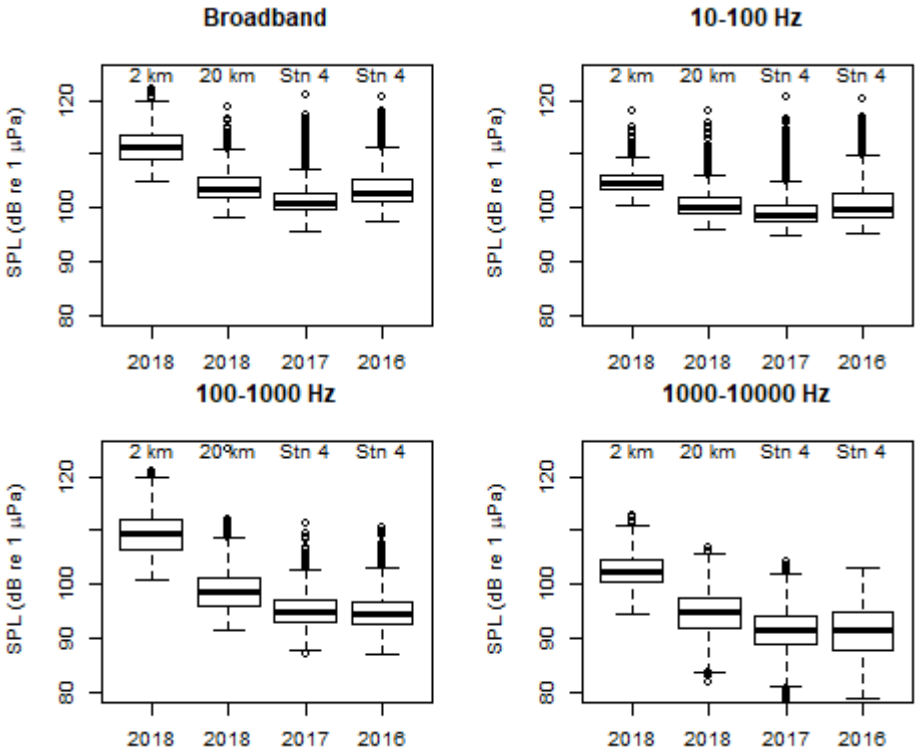

Figure 45. 1-minute average SPL broadband and band levels for 2 km, 20 km, and Stn 4. The 2016 Stn 4 data include the sound from Shell's drilling program with the Stena IceMAX. The Stn 4 2017 data represent the natural soundscape in the project area.

4.1.3. West Aquarius Radiated Sound Level

The measurements at the 2 km location allowed us to estimate the West Aquarius radiated sound levels. The analysis consisted of the following steps:

1. Use the ESRF Stn 4 data to determine the distribution of received 1/3-octave-band sound pressure levels for the same time of year, without the drill activity present (i.e., 2017).
2. Determine the 95th percentile of the 1/3-octave-band SPL at Stn 4. This is considered representative of the maximum ambient levels for the project area.
3. Extract all sample of the received 1/3-octave-band SPL at the 2 km location that exceed the 95th percentile of the data from Stn 4. Discard any 1/3-octave-bands that did not have at least 5 days of

data that exceed the Stn 4 thresholds (i.e., to account for the 5% of expected days above the 95th percentile).

4. Add the propagation loss to the 2 km data to obtain the radiated sound levels. For radiated sound levels, the propagation loss is 20log10(slant range) + absorption*(slant range) where the absorption parameter increases with frequency and was computed using the equations in François and Garrison (1982).

The results are shown in Figure 46. The curve formed by the lowest levels in the received SPL figure (top box plot of Figure 46) are the 95th percentile of SPL measured at ESRF Stn 4. The peak of the West Aquarius radiated sound is in the frequency band of 100–300 Hz, with the peak at 190 Hz. The mean radiated sound level of the West Aquarius was 183.0 dB re 1 µPa. The 75th and 90th percentiles of the radiated sound levels were 183.7 and 186.3 dB re 1 µPa respectively (Table 3).

For comparison, the Stena IceMAX drill ship was measured in 2016 during drilling operations for Shell Canada in a similar location, with similar characteristics and similar distance between the activity and recorder (MacDonnell 2017). The broadband radiated sound level of 187.7 dB re 1 µPa was measured with a peak at 100 Hz (Figure 47), which agrees well with the broadband SPL for source spectrum used in the pre-season modeling (Figure 47, Table 3). The West Aquarius radiated sound levels however were 5–8 dB below the values used for pre-operations modeling at frequencies below 160 Hz, up to 6 dB higher than the pre-operations modeling at 190 Hz, and 0–3 dB below pre-season spectrum above 190 Hz except at very high output levels (90th percentile). The West Aquarius is fitted with 8 Azipod CZ 3300 kW gearless thrusters compared to the UUC 355 geared thrusters employed on the Stena IceMAX. The theoretical spectrum used for the pre-operations modeling was based on the UUC 355. Thus, it appears that the Azipod thrusters may be quieter than standard thrusters except at 190 Hz.

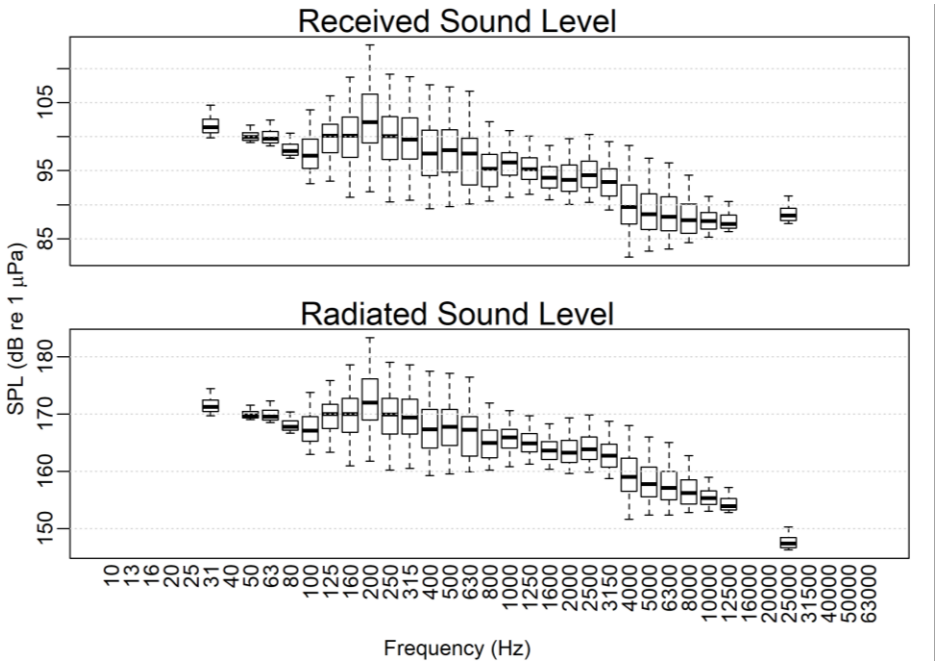

Figure 46. Received sound pressure levels at the 2 km site attributed to the West Aquarius and the computed radiated sound levels.

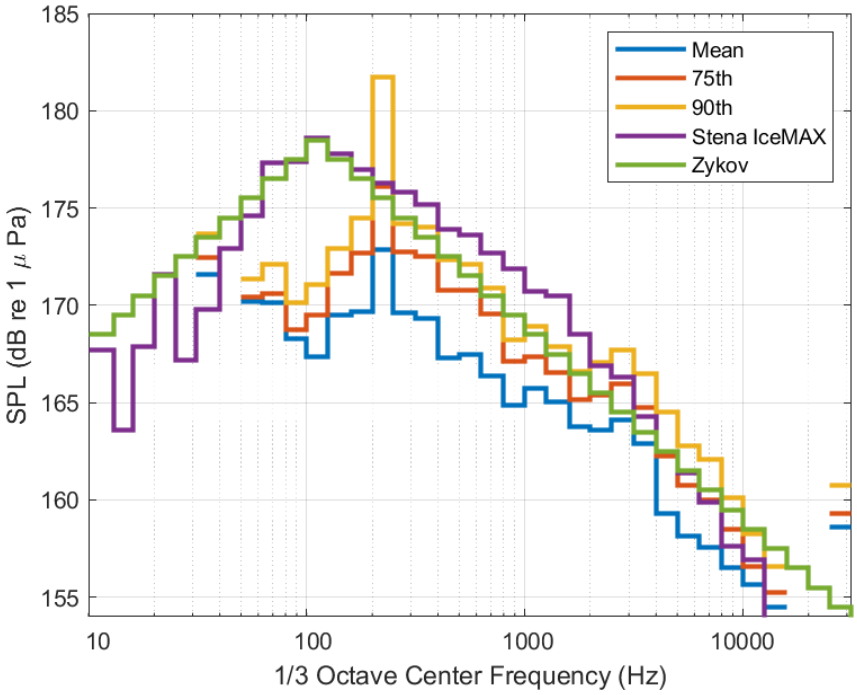

Figure 47. Comparison of the West Aquarius radiated sound levels with the spectrum used for pre-operations modeling (Zykov 2015) and the Stena IceMAX (MacDonnell 2017).

Table 3. West Aquarius MODU radiated sound levels. All values are dB re 1 µPa. Stena IceMAX data can be found in MacDonnell (2017). The modeled values are described in Zykov (2015).

Nominal 1/3-octave-band center frequency (Hz)	Mean radiated sound pressure level	75th percentile radiated sound pressure level	90th percentile radiated sound pressure level	Stena IceMAX radiated sound pressure level	Modeled radiated sound pressure level
10				167.7	168.5
13				163.6	169.5
16				167.9	170.5
20				171.6	171.5
25				167.2	172.5
31	171.6	172.4	173.7	169.8	173.5
40				172.9	174.5
50	170.2	170.4	171.4	174.6	175.5
63	170.1	170.6	172.1	177.3	176.5
80	168.3	168.8	170.2	177.4	177.5
100	167.4	169.5	171.1	178.6	178.5
125	169.5	171.7	172.9	177.8	177.5
160	169.7	172.7	174.5	177	176.5
200	172.8	176.1	181.7	176.3	175.5
250	169.6	172.8	174.2	175.8	174.5
315	169.3	172.5	174.0	175.2	173.5
400	167.3	170.8	172.3	173.9	172.5
500	167.5	170.8	172.1	173.6	171.5
630	166.4	169.5	170.9	172.7	170.5
800	164.9	167.1	168.2	171.9	169.5
1000	165.7	167.3	168.9	170.7	168.5

Nominal 1/3-octave-band center frequency (Hz)	Mean radiated sound pressure level	75th percentile radiated sound pressure level	90th percentile radiated sound pressure level	Stena IceMAX radiated sound pressure level	Modeled radiated sound pressure level
1250	165.0	166.5	167.9	170.5	167.5
1600	163.8	165.2	166.6	168.5	166.5
2000	163.6	165.4	167.1	166.9	165.5
2500	164.1	165.9	167.7	166.3	164.5
3150	162.9	164.7	166.5	164.3	163.5
4000	159.3	162.3	164.5	162.5	162.5
5000	158.1	160.7	162.8	161.4	161.5
6300	157.6	160.0	162.1	159.9	160.5
8000	156.5	158.5	160.1	157.6	159.5
10000	155.7	156.6	158.3	156.9	158.5
12500	154.5	155.2	156.6	150	157.5
16000				146.8	156.5
20000				141.5	155.5
25000	158.6	159.3	160.8	147.1	154.5
31500					153.5
40000					152.5
50000					151.5
63000					150.5
Broadband radiated sound pressure level	181.5	183.7	186.3	187.7	187.6

4.1.4. Expected versus Measured Sound Levels

The West Aquarius MODU radiated signature had a 190 Hz tone that was the strongest spectral peak detected at 2 and 20 km from the MODU. A similar peak was detected at 145 km (the Gully) but with a different spectral shape (Figure 17). Long range propagation was anticipated during winter (Zykov 2015); however, the 190 Hz tone was not expected to be detectable at the Gully in July and August (Figure 15A). This subsection considers whether there is support for the long propagation in summer 2018 and compares the measured to expected sound levels.

During winter, the sound speed profile has a minimum at the surface, which creates conditions that trap sound near the surface, resulting in the long range propagation (Figure 48). In summer, the surface waters warm and the sound speed increases, which creates a subsurface layer that can also trap sound. In both cases, the deep sound channel traps sound at a depth of ~700 m. The effectiveness of low sound speed channels in trapping sound depends on the differences in sound speed between the minimum and maximum values, as well as the height of the channel compared to the wavelength of a sound. Figure 48C shows 20 sound speed profiles generated by the Global Ice-Ocean Prediction System for the drill site for late July and the first half of August 2018. Clearly the subsurface minimum fluctuates in sound speed and height, which significantly effects the sound propagation. Figures 50 to 52 compare the near-surface propagation for the summer, winter, and GIOPS summer profiles with the most favourable conditions for long range propagation, which illustrates the effects of the sound speed profile. Neither the summer and GIOPS summer profiles suggest that sound from the MODU should be detectable at the Gully. We conclude that the 190 Hz signal detected at the Gully was not related to the MODU. It may have been due to sounds from the Exxon platform that was 30 km away, or perhaps a sound generated by the mooring noise that was coincidentally at the same frequency.

The measurements at the 2 km location were made at a radial range of 2000 m and a slant range of 3100 m from the drill rig. In (Zykov 2015) it was predicted that 95% of the received sound pressure levels at 2500 m from drill site would be less than 140 dB re 1 µPa in winter and 133 dB re 1 µPa in summer.

These measurements are maximum over depth, where the maximum values are near the sea surface (Figures 49 and 50). As shown in Figure 49 the sound pressure levels 2 km from the drill site at the seabed in the worst case winter situation were expected to be 115–120 dB re 1 µPa. The summer time levels were similar. The measured 1-minute sound pressure levels at the 2 km location were ~112 dB re 1 µPa on average with a maximum value of ~120 dB re 1 µPa (Figure 45). Thus, the measured values were at or below the expected values.

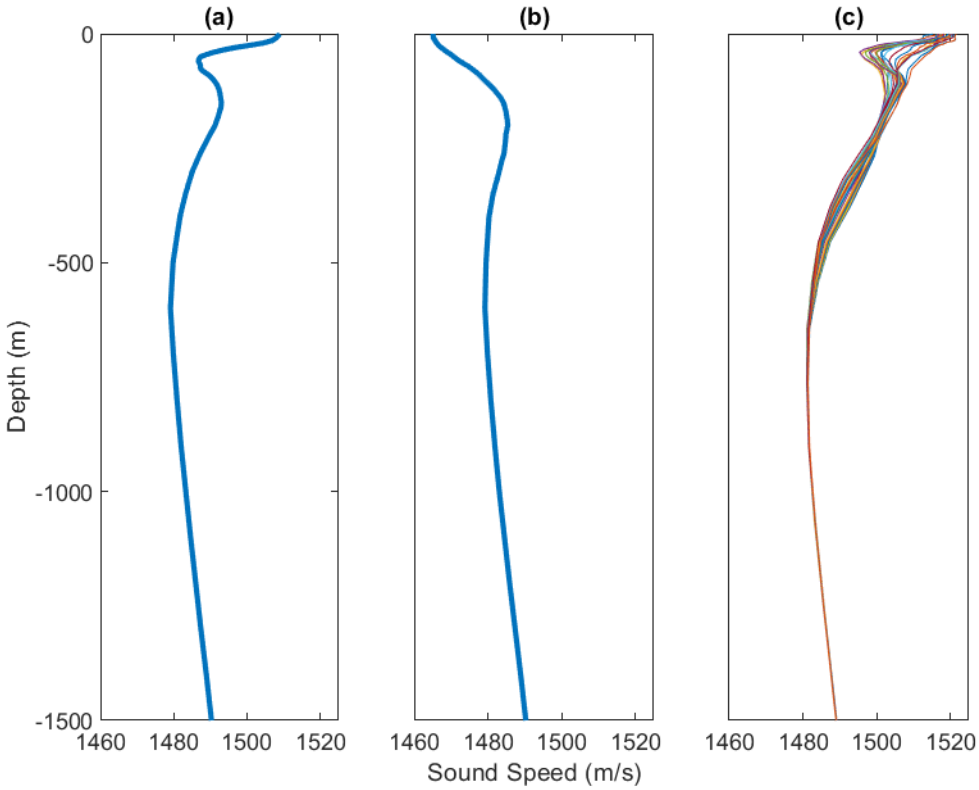

Figure 48. Sound speed profiles for the project site. (a) winter (February) and (b) summer (August) profiles from GDEM that were used in the pre-operations propagation modeling; (c) GIOPS data, which is daily assimilated ocean model outputs from Environment Canada for 25 Jul to 14 Aug 2018.

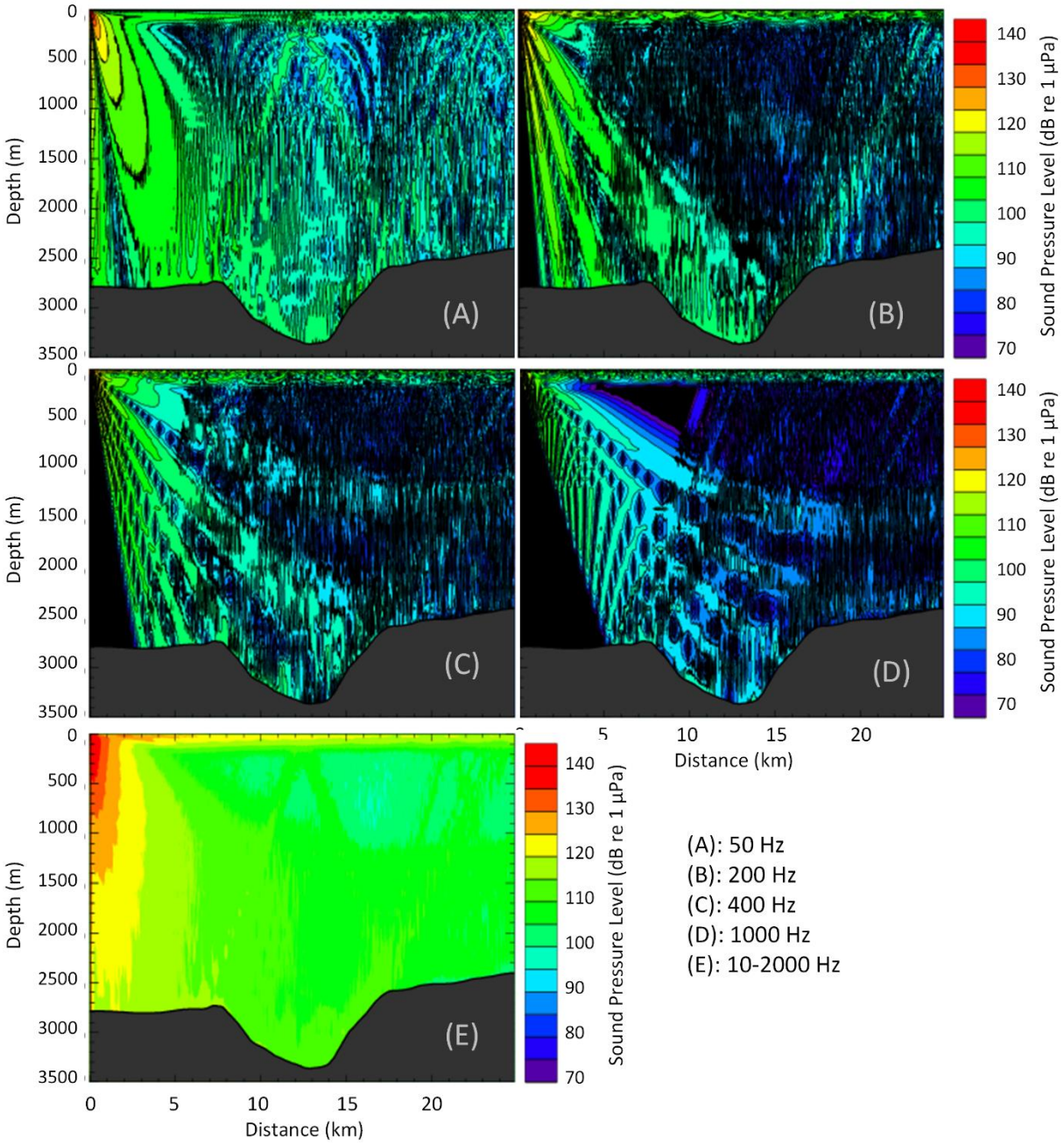

Figure 49. Received sound levels as a function of range, depth, and frequency for a winter sound speed profile (Figure 48a) at the drill site. This data is shown for a range-depth transect from the drill site towards the 2 and 20 km recorders.

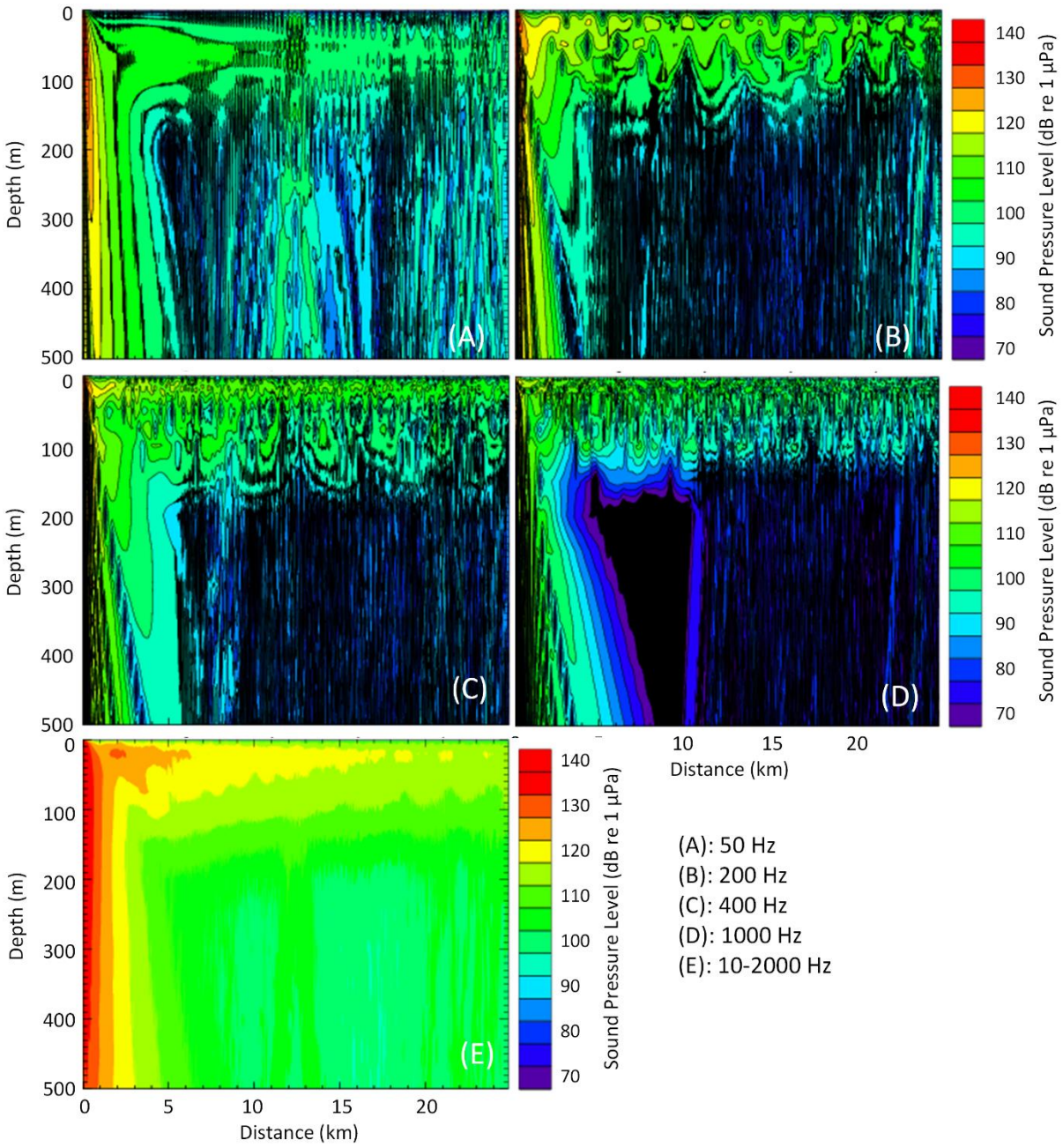

Figure 50. Received sound levels as a function of range, depth, and frequency for the top 500 m of the water column for a winter sound speed profile (Figure 48a) at the drill site. This data is shown for a range-depth transect from the drill site towards the 2 and 20 km recorders.

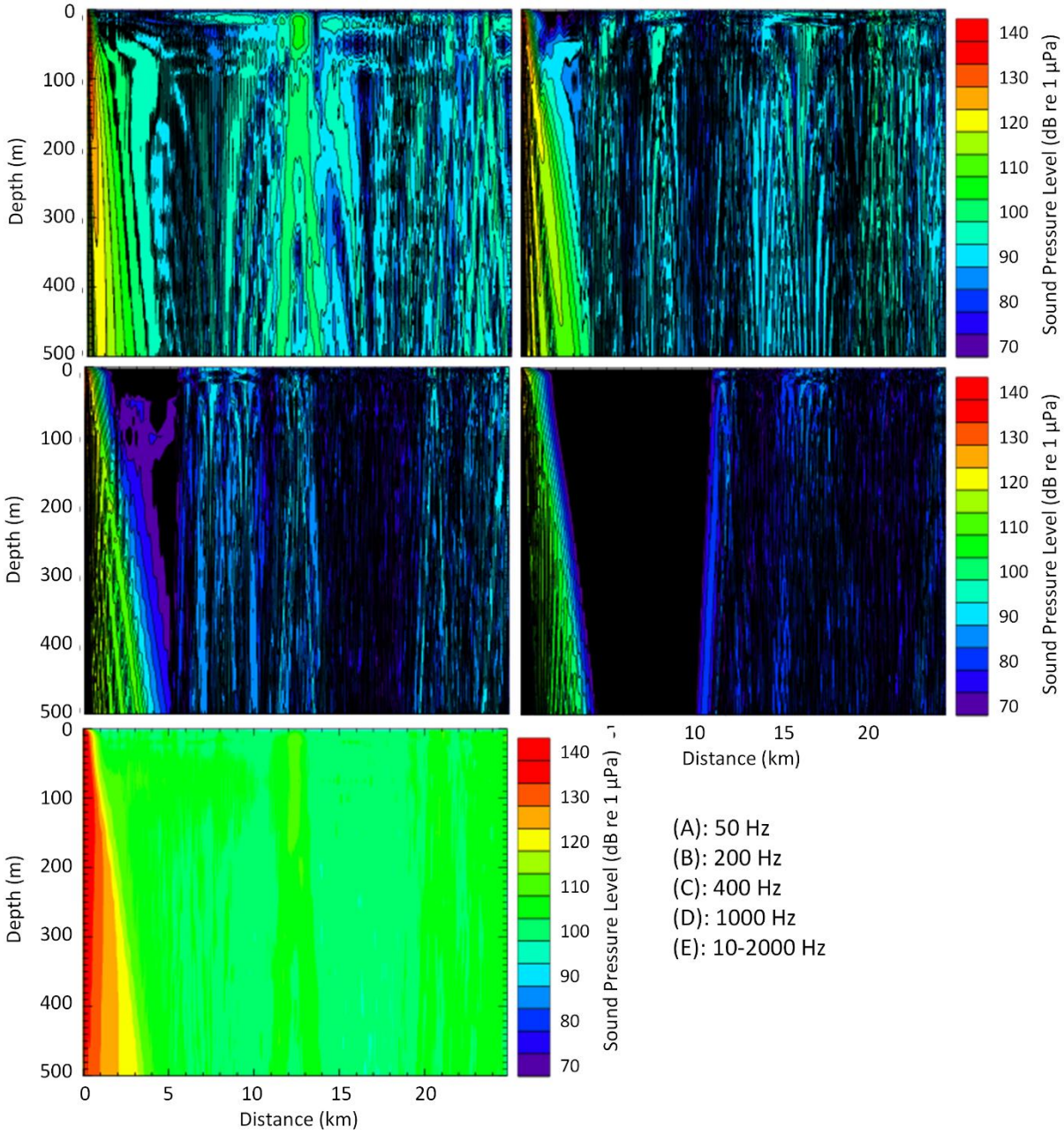

Figure 51. Received sound levels as a function of range, depth, and frequency for the top 500 m of the water column for the summer sound speed profile (Figure 48a) at the drill site. This data is shown for a range-depth transect from the drill site towards the 2 and 20 km recorders

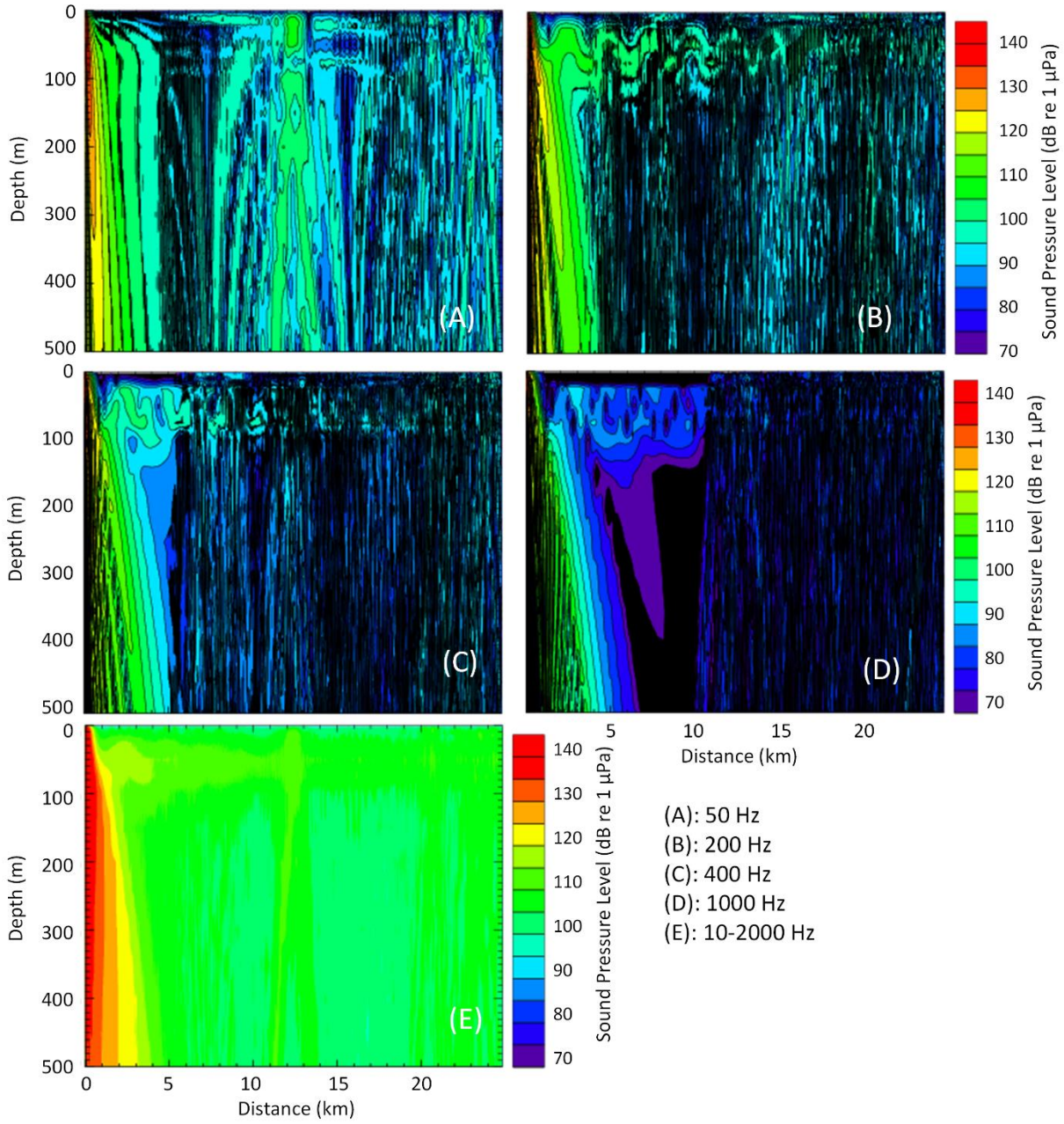

Figure 52. Received sound levels as a function of range, depth, and frequency for the top 500 m of the water column for the GIOPS sound speed profile with the strongest subsurface duct (Figure 48c) at the drill site. This data is shown for a range-depth transect from the drill site towards the 2 and 20 km recorders.

5. Conclusion and Recommendations

Collecting a long-term data set at multiple ranges from a drill site during a 'real-world' industrial operation has produced important new results on dynamic positioning sound variability. At a radial distance of 2 km from the West Aquarius Mobile Offshore Drilling Unit (MODU), only the sounds levels in the 200 Hz octave-band had a correlation coefficient with wind speed that was higher than 0.4. At 20 km, the sounds from the MODU were much more attenuated and all octave-bands between 200 and 12500 Hz had correlation coefficients above 0.6. Thus the soundscape was determined primarily by the wind at 20 km and primarily by the MODU at 2 km. The broadband sound pressure level was ~8 dB higher at 2 km than at 20 km from the MODU.

The measurements identified differences in the sound spectrum produced by different dynamic positioning (DP) thruster systems—geared UUC-355 thrusters versus gearless Azipod CZ-3300 thrusters. The West Aquarius semi-submersible drill rig equipped with the Azipod thrusters that was measured for this study emitted less sound at most frequencies than the Stena IceMAX drill ship measured in 2016 (MacDonnell 2017). However, the West Aquarius emits a strong 190 Hz tone at higher thrust powers that was detectable over long distances. The broadband source level for both platforms was comparable at ~188 dB re 1 µPa, which was 8 dB less than the source level used in pre-operations propagation modeling. As further research, we recommend publishing a short note in the peer-reviewed literature documenting these differences.

The purpose of the Gully recorder was to determine if the MODU was detectable on the shelf break along a direct propagation path between the MODU and Gully Marine Protected Area. These detections were expected to be possible during winter propagation conditions, which typically last until June. For the period recorded by the Gully recorder (late July to August), the MODU was not detected. Given that the measured source level (at its 90th percentile) was 8 dB lower than what was used in the pre-operations modeling it is unlikely that the MODU would have been detectable in winter conditions, except perhaps at 190 Hz.

Glossary

1/3-octave
One third of an octave. Note: A one-third octave is approximately equal to one decidecade (1/3 oct ≈ 1.003 ddec) (ISO 2017).

1/3-octave-band
Frequency band whose bandwidth is one one-third octave. Note: The bandwidth of a one-third octave-band increases with increasing centre frequency.

90%-energy time window
The time interval over which the cumulative energy rises from 5 to 95% of the total pulse energy. This interval contains 90% of the total pulse energy. Symbol: T_{90}.

90% sound pressure level (90% SPL)
The root-mean-square sound pressure levels calculated over the 90%-energy time window of a pulse. Used only for pulsed sounds.

absorption
The reduction of acoustic pressure amplitude due to acoustic particle motion energy converting to heat in the propagation medium.

acoustic impedance
The ratio of the sound pressure in a medium to the rate of alternating flow of the medium through a specified surface due to the sound wave.

ambient noise
All-encompassing sound at a given place, usually a composite of sound from many sources near and far (ANSI S1.1-1994 R2004), e.g., shipping vessels, seismic activity, precipitation, sea ice movement, wave action, and biological activity.

attenuation
The gradual loss of acoustic energy from absorption and scattering as sound propagates through a medium.

Auditory frequency weighting (auditory weighting function, frequency-weighting function)
The process of band-pass filtering sounds to reduce the importance of inaudible or less-audible frequencies for individual species or groups of species of aquatic mammals (ISO 2017). One example is M-weighting introduced by Southall et al. (2007) to describe “Generalized frequency weightings for various functional hearing groups of marine mammals, allowing for their functional bandwidths and appropriate in characterizing auditory effects of strong sounds”.

background noise
Total of all sources of interference in a system used for the production, detection, measurement, or recording of a signal, independent of the presence of the signal (ANSI S1.1-1994 R2004). Ambient noise detected, measured, or recorded with a signal is part of the background noise.

bandwidth
The range of frequencies over which a sound occurs. Broadband refers to a source that produces sound over a broad range of frequencies (e.g., seismic airguns, vessels) whereas narrowband sources produce sounds over a narrow frequency range (e.g., sonar) (ANSI/ASA S1.13-2005 R2010).

bar
Unit of pressure equal to 100 kPa, which is approximately equal to the atmospheric pressure on Earth at sea level. 1 bar is equal to 10^6 Pa or 10^{11} µPa.

box-and-whisker plot
A plot that illustrates the centre, spread, and overall range of data from a visual 5-number summary. The ends of the box are the upper and lower quartiles (25th and 75th percentiles). The horizontal line inside the box is the median (50th percentile). The whiskers and points extend outside the box to the highest and lowest observations, where the points correspond to outlier observations (i.e., observations that fall more than 1.5 × IQR beyond the upper and lower quartiles, where IQR is the interquartile range).

broadband sound level
The total sound pressure level measured over a specified frequency range. If the frequency range is unspecified, it refers to the entire measured frequency range.

cavitation
A rapid formation and collapse of vapor cavities (i.e., bubbles or voids) in water, most often caused by a rapid change in pressure. Vessel propellers typically cause cavitation, which generates significant levels of broadband noise.

cetacean
Any animal in the order Cetacea. These are aquatic, mostly marine mammals and include whales, dolphins, and porpoises.

compressional wave
A mechanical vibration wave in which the direction of particle motion is parallel to the direction of propagation. Also called primary wave or P-wave.

continuous sound
A sound whose sound pressure level remains above ambient sound during the observation period (ANSI/ASA S1.13-2005 R2010). A sound that gradually varies in intensity with time, for example, sound from a marine vessel.

CTD (conductivity-temperature-depth)
Measurement data of the ocean's conductivity, temperature, and depth; used to compute sound speed and salinity.

decade
Logarithmic frequency interval whose upper bound is ten times larger than its lower bound (ISO 2006).

decidecade
One tenth of a decade (ISO 2017). Note: An alternative name for decidecade (symbol ddec) is "one-tenth decade". A decidecade is approximately equal to one third of an octave (1 ddec ≈ 0.3322 oct) and for this reason is sometimes referred to as a "one-third octave".

decidecade band
Frequency band whose bandwidth is one decidecade. Note: The bandwidth of a decidecade band increases with increasing centre frequency.

decibel (dB)
One-tenth of a bel. Unit of level when the base of the logarithm is the tenth root of ten, and the quantities concerned are proportional to power (ANSI S1.1-1994 R2004).

duty cycle
The time when sound is periodically recorded by an acoustic recording system.

far-field
The zone where, to an observer, sound originating from an array of sources (or a spatially-distributed source) appears t o radiate from a single point. The distance to the acoustic far-field increases with frequency.

fast-average sound pressure level
The time-averaged sound pressure levels calculated over the duration of a pulse (e.g., 90%-energy time window), using the leaky time integrator from Plomp and Bouman (1959) and a time constant of 125 ms. Typically used only for pulsed sounds.

fast Fourier transform (FFT)
A computationally efficiently algorithm for computing the discrete Fourier transform.

frequency
The rate of oscillation of a periodic function measured in cycles-per-unit-time. The reciprocal of the period. Unit: hertz (Hz). Symbol: *f*. 1 Hz is equal to 1 cycle per second.

hearing group
Groups of marine mammal species with similar hearing ranges. Commonly defined functional hearing groups include low-, mid-, and high-frequency cetaceans, pinnipeds in water, and pinnipeds in air.

hearing threshold
The sound pressure level for any frequency of the hearing group that is barely audible for a given individual in the absence of significant background noise during a specific percentage of experimental trials.

hertz (Hz)
A unit of frequency defined as one cycle per second.

high-frequency (HF) cetacean
The functional cetacean hearing group that represents those odontocetes (toothed whales) specialized for hearing high frequencies.

hydrophone
An underwater sound pressure transducer. A passive electronic device for recording or listening to underwater sound.

low-frequency (LF) cetacean
The functional cetacean hearing group that represents mysticetes (baleen whales) specialized for hearing low frequencies.

masking
Obscuring of sounds of interest by sounds at similar frequencies.

mean-square sound pressure spectral density
Distribution as a function of frequency of the mean-square sound pressure per unit bandwidth (usually 1 Hz) of a sound having a continuous spectrum (ANSI S1.1-1994 R2004). Unit: $\mu Pa^2/Hz$.

median
The 50th percentile of a statistical distribution.

mid-frequency (MF) cetacean
The functional cetacean hearing group that represents those odontocetes (toothed whales) specialized for mid-frequency hearing.

mysticete
Mysticeti, a suborder of cetaceans, use their baleen plates, rather than teeth, to filter food from water. They are not known to echolocate, but they use sound for communication. Members of this group include rorquals (Balaenopteridae), right whales (Balaenidae), and grey whales (*Eschrichtius robustus*).

octave
The interval between a sound and another sound with double or half the frequency. For example, one octave above 200 Hz is 400 Hz, and one octave below 200 Hz is 100 Hz.

odontocete
The presence of teeth, rather than baleen, characterizes these whales. Members of the Odontoceti are a suborder of cetaceans, a group comprised of whales, dolphins, and porpoises. The skulls of toothed whales are mostly asymmetric, an adaptation for their echolocation. This group includes sperm whales, killer whales, belugas, narwhals, dolphins, and porpoises.

otariid
A common term used to describe members of the Otariidae, eared seals, commonly called sea lions and fur seals. Otariids are adapted to a semi-aquatic life; they use their large fore flippers for propulsion. Their ears distinguish them from phocids. Otariids are one of the three main groups in the superfamily Pinnipedia; the other two groups are phocids and walrus.

otariid pinnipeds in water (OPW)
The functional pinniped hearing group that represents eared seals under water.

peak pressure level (PK)
The maximum instantaneous sound pressure level, in a stated frequency band, within a stated period. Also called zero-to-peak pressure level. Unit: decibel (dB).

peak-to-peak pressure level (PK-PK)
The difference between the maximum and minimum instantaneous pressure levels. Unit: decibel (dB).

percentile level, exceedance
The sound level exceeded *n* % of the time during a measurement.

permanent threshold shift (PTS)
A permanent loss of hearing sensitivity caused by exposure to high sound levels. PTS is considered auditory injury.

phocid
A common term used to describe all members of the family Phocidae. These true/earless seals are more adapted to in-water life than are otariids, which have more terrestrial adaptations. Phocids use their hind flippers to propel themselves. Phocids are one of the three main groups in the superfamily Pinnipedia; the other two groups are otariids and walrus.

phocid pinnipeds in water (PPW)
The functional pinniped hearing group that represents true/earless seals under water.

pinniped
A common term used to describe all three groups that form the superfamily Pinnipedia: phocids (true seals or earless seals), otariids (eared seals or fur seals and sea lions), and walrus.

power spectrum density
Generic term, formally defined as power in W/Hz, but sometimes loosely used to refer to the spectral density of other parameters such as square pressure or time-integrated square pressure.

pressure, acoustic
The deviation from the ambient hydrostatic pressure caused by a sound wave. Also called overpressure. Unit: pascal (Pa). Symbol: *p*.

pressure, hydrostatic
The pressure at any given depth in a static liquid that is the result of the weight of the liquid acting on a unit area at that depth, plus any pressure acting on the surface of the liquid. Unit: pascal (Pa).

rms
root-mean-square.

signature
Pressure signal generated by a source.

sound
A time-varying pressure disturbance generated by mechanical vibration waves travelling through a fluid medium such as air or water.

sound exposure
Time integral of squared, instantaneous frequency-weighted sound pressure over a stated time interval or event. Unit: pascal-squared second ($Pa^2 \cdot s$) (ANSI S1.1-1994 R2004).

sound exposure level (SEL)
A cumulative measure related to the sound energy in one or more pulses. Unit: dB re 1 $\mu Pa^2 \cdot s$. SEL is expressed over the summation period (e.g., per-pulse SEL [for airguns], single-strike SEL [for pile drivers], 24-hour SEL).

sound exposure spectral density
Distribution as a function of frequency of the time-integrated squared sound pressure per unit bandwidth of a sound having a continuous spectrum (ANSI S1.1-1994 R2004). Unit: $\mu Pa^2 \cdot s/Hz$.

sound intensity
Sound energy flowing through a unit area perpendicular to the direction of propagation per unit time.

sound pressure level (SPL)
The decibel ratio of the time-mean-square sound pressure, in a stated frequency band, to the square of the reference sound pressure (ANSI S1.1-1994 R2004).

For sound in water, the reference sound pressure is one micropascal (p_0 = 1 µPa) and the unit for SPL is dB re 1 μPa^2:

$$L_p = 10 \log_{10}(p^2/p_0^2) = 20 \log_{10}(p/p_0)$$

Unless otherwise stated, SPL refers to the root-mean-square (rms) pressure level. See also 90% sound pressure level and fast-average sound pressure level. Non-rectangular time window functions may be applied during calculation of the rms value, in which case the SPL unit should identify the window type.

sound speed profile
The speed of sound in the water column as a function of depth below the water surface.

source level (SL)
The sound level measured in the far-field and scaled back to a standard reference distance of 1 metre from the acoustic centre of the source. Unit: dB re 1 µPa·m (pressure level) or dB re 1 $\mu Pa^2 \cdot s \cdot m$ (exposure level).

spectral density level
The decibel level ($10 \cdot \log_{10}$) of the spectral density of a given parameter such as SPL or SEL, for which the units are dB re 1 μPa^2/Hz and dB re 1 $\mu Pa^2 \cdot s$/Hz, respectively.

spectrogram
A visual representation of acoustic amplitude compared with time and frequency.

spectrum
An acoustic signal represented in terms of its power, energy, mean-square sound pressure, or sound exposure distribution with frequency.

surface duct
The upper portion of a water column within which the sound speed profile gradient causes sound to refract upward and therefore reflect off the surface resulting in relatively long-range sound propagation with little loss.

temporary threshold shift (TTS)
Temporary loss of hearing sensitivity caused by exposure to high sound levels. TTS occurs before PTS for all animal groups.

transmission loss (TL)
The decibel reduction in sound level between two stated points that results from sound spreading away from an acoustic source subject to the influence of the surrounding environment. Also referred to as propagation loss.

wavelength
Distance over which a wave completes one cycle of oscillation. Unit: metre (m). Symbol: λ.

Literature Cited

[ISO] International Organization for Standardization. 2006. *ISO 80000-3:2006. Quantities and Units – Part 3: Space and time*. https://www.iso.org/standard/31888.html.

[ISO] International Organization for Standardization. 2017. *ISO/DIS 18405.2:2017. Underwater acoustics—Terminology*. Geneva. https://www.iso.org/standard/62406.html.

[NMFS] National Marine Fisheries Service. 2018. *2018 Revision to: Technical Guidance for Assessing the Effects of Anthropogenic Sound on Marine Mammal Hearing (Version 2.0): Underwater Thresholds for Onset of Permanent and Temporary Threshold Shifts*. U.S. Department of Commerce, NOAA. NOAA Technical Memorandum NMFS-OPR-59. 167 pp. https://www.fisheries.noaa.gov/webdam/download/75962998.

[NRC] National Research Council. 2003. *Ocean Noise and Marine Mammals*. National Research Council (U.S.), Ocean Studies Board, Committee on Potential Impacts of Ambient Noise in the Ocean on Marine Mammals. The National Academies Press, Washington, DC. http://www.nap.edu/openbook.php?record_id=10564.

ANSI S1.1-1994. R2004. *American National Standard Acoustical Terminology*. American National Standards Institute, New York.

ANSI/ASA S1.13-2005. R2010. *American National Standard Measurement of Sound Pressure Levels in Air*. American National Standards Institute and Acoustical Society of America, New York.

Arveson, P.T. and D.J. Vendittis. 2000. Radiated noise characteristics of a modern cargo ship. *Journal of the Acoustical Society of America* 107(1): 118-129. https://doi.org/10.1121/1.428344.

Au, W.W., R.A. Kastelein, T. Rippe, and N.M. Schooneman. 1999. Transmission beam pattern and echolocation signals of a harbor porpoise (*Phocoena phocoena*). *Journal of the Acoustical Society of America* 106(6): 3699-3705.

Baumann-Pickering, S., M.A. McDonald, A.E. Simonis, A.S. Berga, K.P. Merkens, E.M. Oleson, M.A. Roch, S.M. Wiggins, S. Rankin, et al. 2013. Species-specific beaked whale echolocation signals. *The Journal of the Acoustical Society of America* 134(3): 2293-2301.

Baumgartner, M.F., S.M. Van Parijs, F.W. Wenzel, C.J. Tremblay, H.C. Esch, and A.M. Warde. 2008. Low frequency vocalizations attributed to sei whales (*Balaenoptera borealis*). *Journal of the Acoustical Society of America* 124(2): 1339-1349. https://doi.org/10.1121/1.2945155.

Berchok, C.L., D.L. Bradley, and T.B. Gabrielson. 2006. St. Lawrence blue whale vocalizations revisited: Characterization of calls detected from 1998 to 2001. *Journal of the Acoustical Society of America* 120(4): 2340-2354. https://doi.org/10.1121/1.2335676.

Carnes, M.R. 2009. *Description and Evaluation of GDEM-V 3.0*. U.S. Naval Research Laboratory, Stennis Space Center, MS. NRL Memorandum Report 7330-09-9165. 21 pp. https://apps.dtic.mil/dtic/tr/fulltext/u2/a494306.pdf.

Clark, C.W. 1990. Acoustic behaviour of mysticete whales. *In* Thomas, J. and R.A. Kastelein (eds.). *Sensory Abilities of Cetaceans*. Plenum Press, New York. pp 571-583.

Coppens, A.B. 1981. Simple equations for the speed of sound in Neptunian waters. *Journal of the Acoustical Society of America* 69(3): 862-863. https://doi.org/10.1121/1.382038.

Deane, G.B. 2000. Long time-base observations of surf noise. *Journal of the Acoustical Society of America* 107(2): 758-770. https://doi.org/10.1121/1.428259.

DeAngelis, A.I., J.E. Stanistreet, S. Baumann-Pickering, and D.M. Cholewiak. 2018. A description of echolocation clicks recorded in the presence of True's beaked whale (Mesoplodon mirus). *The Journal of the Acoustical Society of America* 144(5): 2691-2700.

Delarue, J., K.A. Kowarski, E.E. Maxner, J.T. MacDonnell, and S.B. Martin. 2018. *Acoustic Monitoring Along Canada's East Coast: August 2015 to July 2017*. Document Number 01279, Environmental Studies Research Funds Report Number 215, Version 1.0. Technical report by JASCO Applied Sciences for Environmental Studies Research Fund, Dartmouth, NS, Canada. 120 pp + appendices.

Edds-Walton, P.L. 1997. Acoustic communication signals of mysticetes whales. *Bioacoustics* 8(1-2): 47-60. https://doi.org/10.1080/09524622.2008.9753759.

François, R.E. and G.R. Garrison. 1982. Sound absorption based on ocean measurements: Part II: Boric acid contribution and equation for total absorption. *Journal of the Acoustical Society of America* 72(6): 1879-1890. https://doi.org/10.1121/1.388673.

Gillespie, D., C. Dunn, J. Gordon, D. Claridge, C. Embling, and I. Boyd. 2009. Field recordings of Gervais' beaked whales *Mesoplodon europaeus* from the Bahamas. *Journal of the Acoustical Society of America* 125(5): 3428-3433. https://doi.org/10.1121/1.3110832.

Hildebrand, J.A. 2009. Anthropogenic and natural sources of ambient noise in the ocean. *Marine Ecology Progress Series* 395: 5-20. https://doi.org/10.3354/meps08353.

Johnson, M., P.T. Madsen, W. Zimmer, N.A. De Soto, and P. Tyack. 2006. Foraging Blainville's beaked whales (Mesoplodon densirostris) produce distinct click types matched to different phases of echolocation. *Journal of Experimental Biology* 209(24): 5038-5050.

Kowarski, K.A., C. Evers, H. Moors-Murphy, and B. Martin. 2015. Year-round monitoring of humpback whale (*Megaptera novaeangliae*) calls in the Gully MPA and adjacent areas. *Canadian Acoustics* 43(3). https://jcaa.caa-aca.ca/index.php/jcaa/article/view/2756.

MacDonnell, J.T. 2017. *Shelburne Basin Venture Exploration Drilling Project: Sound Source Characterization, 2016 Field Measurements of the Stena IceMAX*. Document Number 01296. Version 3.0. Technical report by JASCO Applied Sciences for Shell Canada Limited. https://www.cnsopb.ns.ca/sites/default/files/pdfs/shelburne_ceaa_3.12.3_sound_source_characterization_final_april202017.pdf.

Martin, B. 2013. Computing cumulative sound exposure levels from anthropogenic sources in large data sets. *Proceedings of Meetings on Acoustics* 19(1): 9. http://dx.doi.org/10.1121/1.4800967.

Merchant, N.D., T.R. Barton, P.M. Thompson, E. Pirotta, D.T. Dakin, and J. Dorocicz. 2013. Spectral probability density as a tool for ambient noise analysis. *Journal of the Acoustical Society of America* 133(4): EL262-EL267. https://doi.org/10.1121/1.4794934.

Mohl, B., M. Wahlberg, P.T. Madsen, L.A. Miller, and A. Surlykke. 2000. Sperm whale clicks: Directionality and source level revisited. *Journal of the Acoustical Society of America* 107(1): 638-648.

Nieukirk, S.L., K.M. Stafford, D.K. Mellinger, R.P. Dziak, and C.G. Fox. 2004. Low-frequency whale and seismic airgun sounds recorded in the mid-Atlantic Ocean. *Journal of the Acoustical Society of America* 115(4): 1832-1843. https://doi.org/10.1121/1.1675816.

Plomp, R. and M.A. Bouman. 1959. Relation between hearing threshold and duration for tone pulses. *Journal of the Acoustical Society of America* 31(6): 749-758. http://dx.doi.org/10.1121/1.1907781.

Rendell, L.E., J.N. Matthews, A. Gill, J.C.D. Gordon, and D.W. Macdonald. 1999. Quantitative analysis of tonal calls from five odontocete species, examining interspecific and intraspecific variation. *Journal of Zoology* 249: 403-410.

Riesch, R. and V.B. Deecke. 2011. Whistle communication in mammal-eating killer whales (*Orcinus orca*): Further evidence for acoustic divergence between ecotypes. *Behavioral Ecology and Sociobiology* 65(7): 1377-1387. https://doi.org/10.1007/s00265-011-1148-8.

Risch, D., C.W. Clark, P.J. Corkeron, A. Elepfandt, K.M. Kovacs, C. Lydersen, I. Stirling, and S.M. Van Parijs. 2007. Vocalizations of male bearded seals, Erignathus barbatus: classification and geographical variation. *Animal Behaviour* 73: 747-762. <Go to ISI>://000246908300002.

Ross, D. 1976. *Mechanics of Underwater Noise*. Pergamon Press, New York.

Simon, M., K.M. Stafford, K. Beedholm, C.M. Lee, and P.T. Madsen. 2010. Singing behavior of fin whales in the Davis Strait with implications for mating, migration and foraging. *The Journal of the Acoustical Society of America* 128(5): 3200-3210.

Southall, B.L., A.E. Bowles, W.T. Ellison, J.J. Finneran, R.L. Gentry, C.R. Greene, Jr., D. Kastak, D.R. Ketten, J.H. Miller, et al. 2007. Marine Mammal Noise Exposure Criteria: Initial Scientific Recommendations. *Aquatic Mammals* 33(4): 411-521. https://doi.org/10.1080/09524622.2008.9753846.

Steiner, W.W. 1981a. Species-specific differences in pure tonal whistle vocalizations of five western North Atlantic dolphin species. *Behavioral Ecology and Sociobiology* 9(4): 241-246. https://doi.org/10.1007/BF00299878.

Steiner, W.W. 1981b. Species-specific differences in pure tonal whistle vocalizations of five western North Atlantic dolphin species. *Behavioral Ecology and Sociobiology* 9: 241-246.

Teague, W.J., M.J. Carron, and P.J. Hogan. 1990. A comparison between the Generalized Digital Environmental Model and Levitus climatologies. *Journal of Geophysical Research* 95(C5): 7167-7183. https://doi.org/10.1029/JC095iC05p07167.

Tyack, P.L. and C.W. Clark. 2000. Communication and acoustic behavior of dolphins and whales. *In Hearing by whales and dolphins*. Springer, New York. pp 156-224.

Watkins, W.A. 1981. Activities and underwater sounds of fin whales. *Scientific Reports of the Whales Research Institute* 33: 83-117.

Wenz, G.M. 1962. Acoustic Ambient Noise in the Ocean: Spectra and Sources. *Journal of the Acoustical Society of America* 34(12): 1936-1956. https://doi.org/10.1121/1.1909155.

Whitehead, H. 2013. Trends in cetacean abundance in the Gully submarine canyon, 1988–2011, highlight a 21% per year increase in Sowerby's beaked whales (*Mesoplodon bidens*). *Canadian Journal of Zoology* 91(3): 141-148. https://doi.org/10.1139/cjz-2012-0293.

Zimmer, W.M.X., M.P. Johnson, P.T. Madsen, and P.L. Tyack. 2005. Echolocation clicks of free-ranging Cuvier's beaked whales (*Ziphius cavirostris*). *Journal of the Acoustical Society of America* 117(6): 3919-3927. https://doi.org/10.1121/1.1910225.

Zykov, M.M. 2015. *Modelling Underwater Sound Associated with Scotian Basin Exploration Drilling Project: Acoustic Modelling Report*. Document Number 01112. Version 1.0. Technical report by JASCO Applied Sciences for Stantec Consulting Ltd.

Appendix A. Calibration and Mooring Designs

A.1. Recorder Calibrations

Each AMAR was calibrated before deployment and upon retrieval (battery life permitting) with a pistonphone type 42AC precision sound source (G.R.A.S. Sound & Vibration A/S; Figure A-1). The pistonphone calibrator produces a constant tone at 250 Hz at a fixed distance from the hydrophone sensor in an airtight space with known volume. The recorded level of the reference tone on the AMAR yields the system gain for the AMAR and hydrophone. To determine absolute sound pressure levels, this gain was applied during data analysis. Typical calibration variance using this method is less than 0.7 dB absolute pressure.

Figure A-1. Split view of a G.R.A.S. 42AC pistonphone calibrator with an M36 hydrophone.

A.2. Mooring Designs

Suspended mooring designs 197 (Figure A-2) and 151 (Figure A-3) were deployed and recovered using an acoustic release.

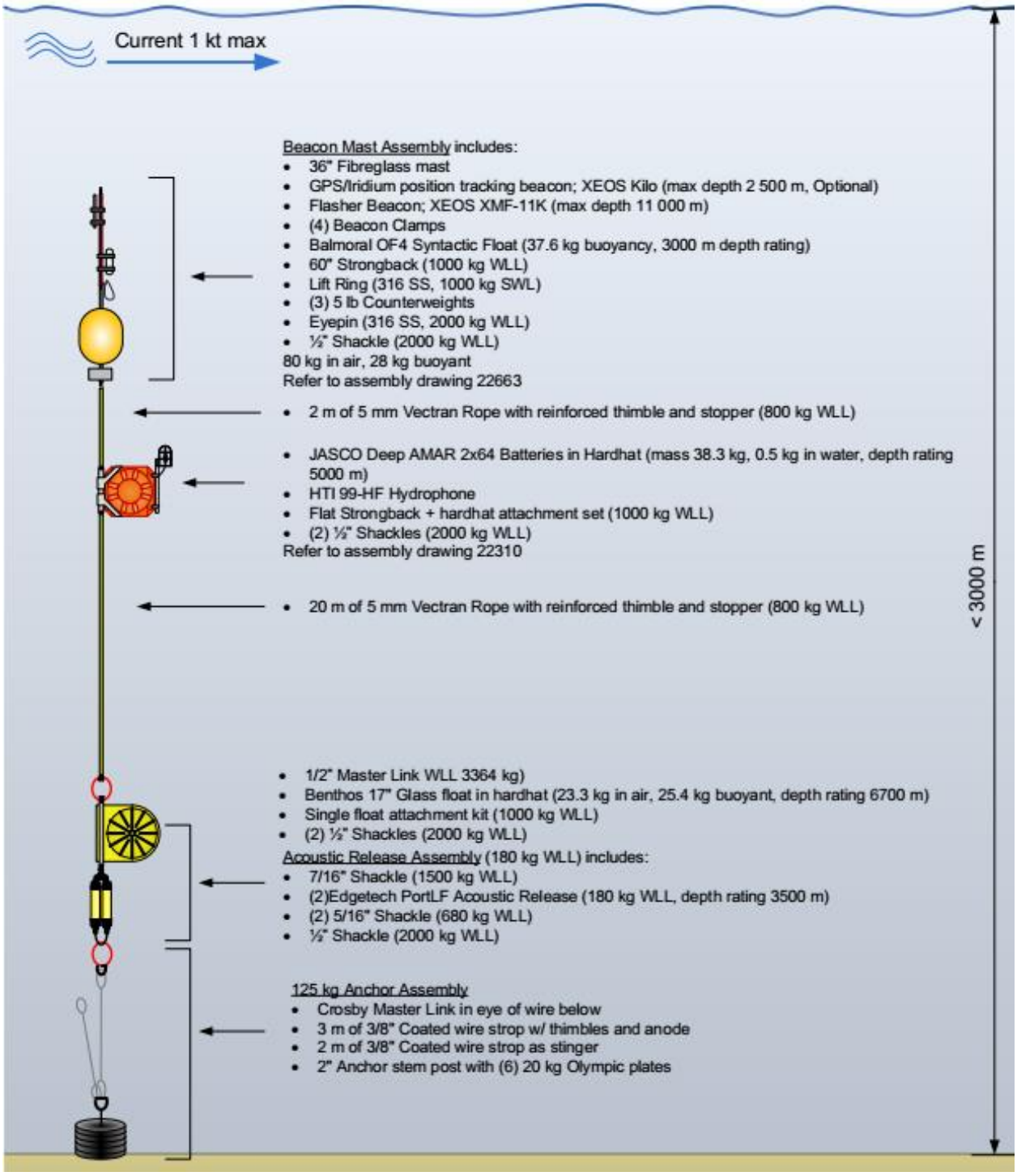

Figure A-2. JASCO mooring design 197 used at the 2 km and 20 km locations.

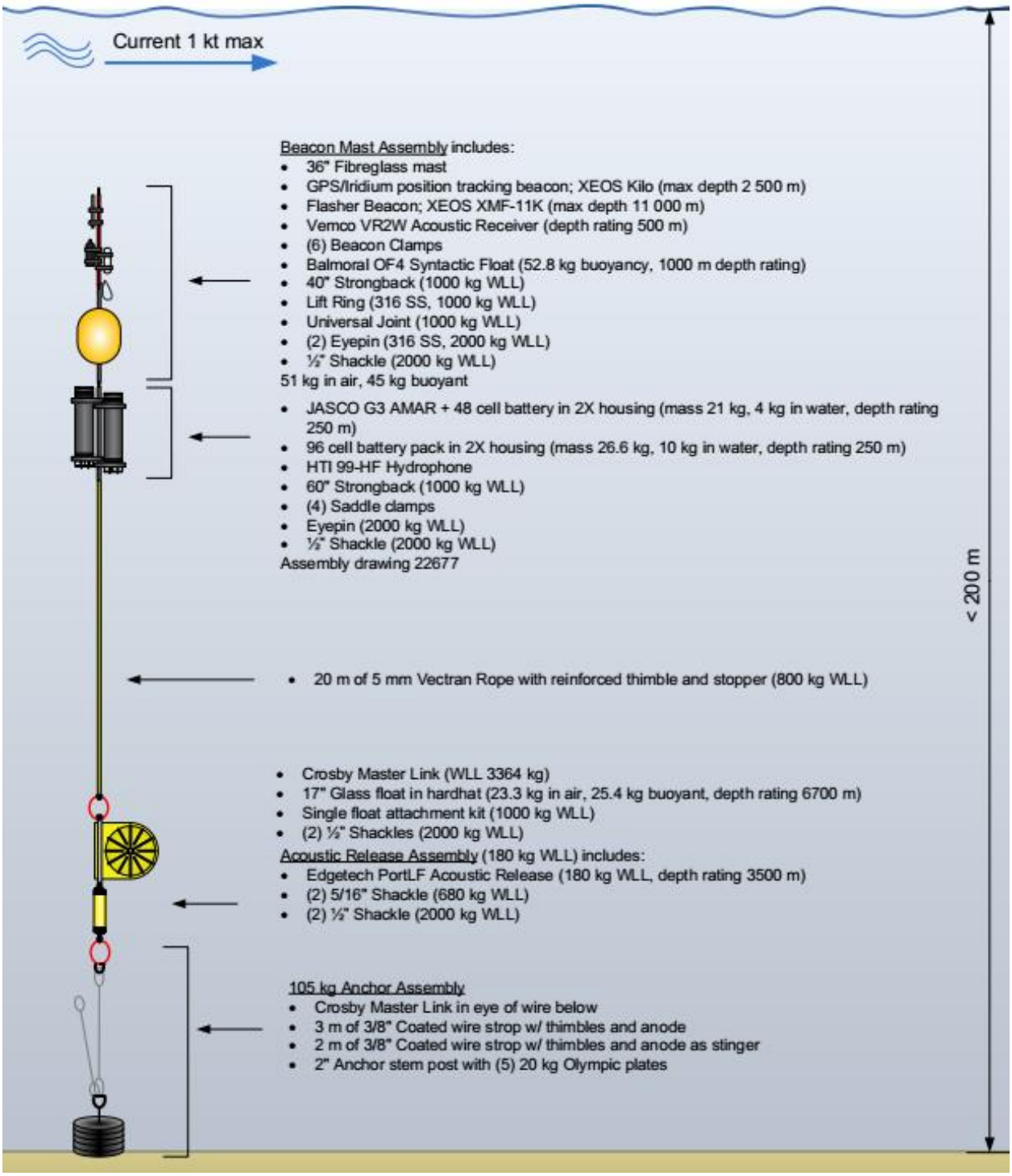

Figure A-3. JASCO mooring design 151 used at the Gully location.

Appendix B. CTD Results

The sound speed profile was measured with a CTD to about 100 m depth at all three stations in mid-April (Figures B-1, B-2, and B-3). The sound speed profile for the remaining depths at the deeper stations (2 km and 20 km) were later estimated based on the monthly historical average temperature and salinity profiles from the U.S. Naval Oceanographic Office's *Generalized Digital Environmental Model V 3.0* (GDEM; Teague et al. 1990, Carnes 2009).

GDEM provides an ocean climatology of temperature and salinity for the world's oceans on a latitude-longitude grid with 0.25° resolution, with a temporal resolution of one month, based on global historical observations from the U.S. Navy's Master Oceanographic Observational Data Set (MOODS). The climatology profiles include 78 fixed depth points to a maximum depth of 6800 m (where the ocean is that deep). The GDEM temperature-salinity profiles were converted to sound speed profiles according to Coppens (1981). The GDEM sound speed profiles for the 2 km and 20 km sites provide an estimate of the sound speed at the deepest point in the CTD data that is 18.8 and 19 m/s lower, respectively, than the CTD-based sound speed. Transmission loss of sound in water is mainly affected by the sound speed gradient, not the absolute sound speed at depth. The GDEM sound speed profile values for these two sites were therefore uniformly increased by 18.8 and 19 m/s, respectively, to smoothly fit the CTD sound speed values.

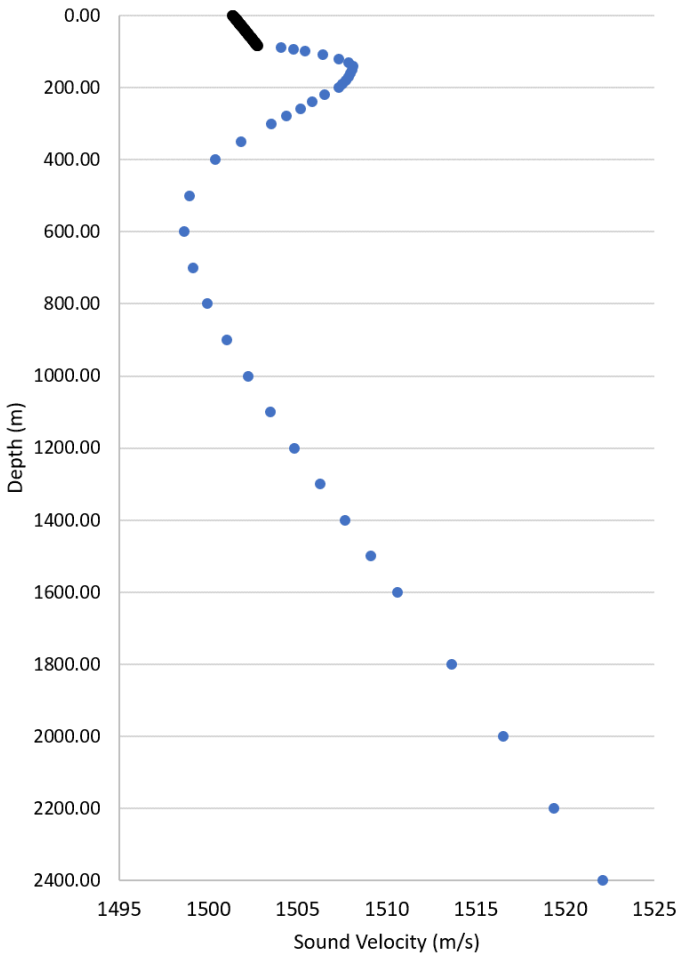

Figure B-1. 2 km: Sound velocity versus depth measured on 14 Apr 2018 (black) and estimated (blue).

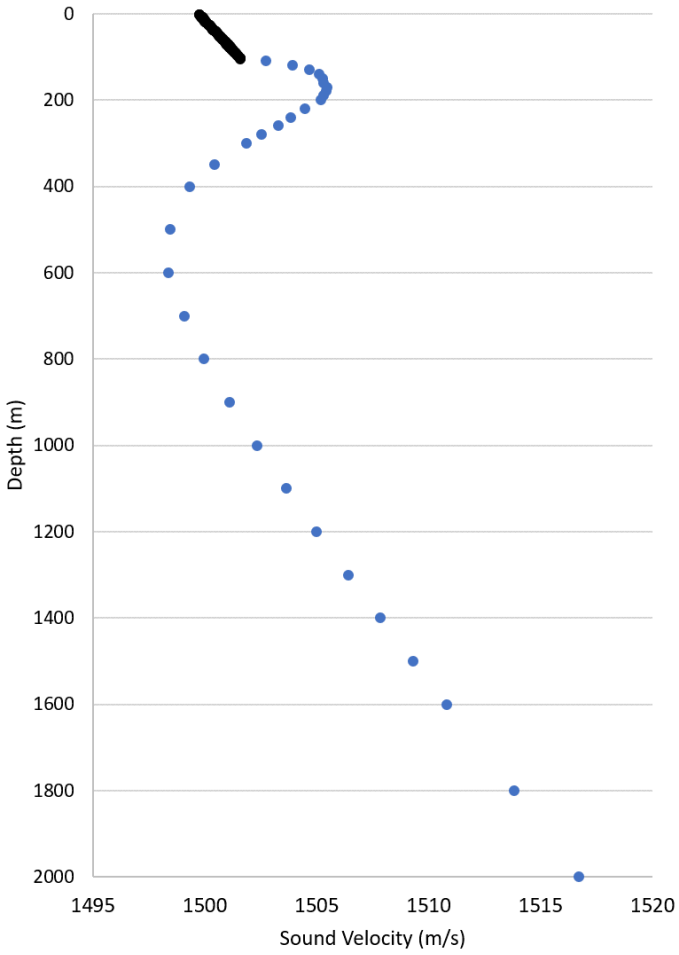

Figure B-2. 20 km: Sound velocity versus depth measured on 15 Apr 2018 (black) and estimated (blue).

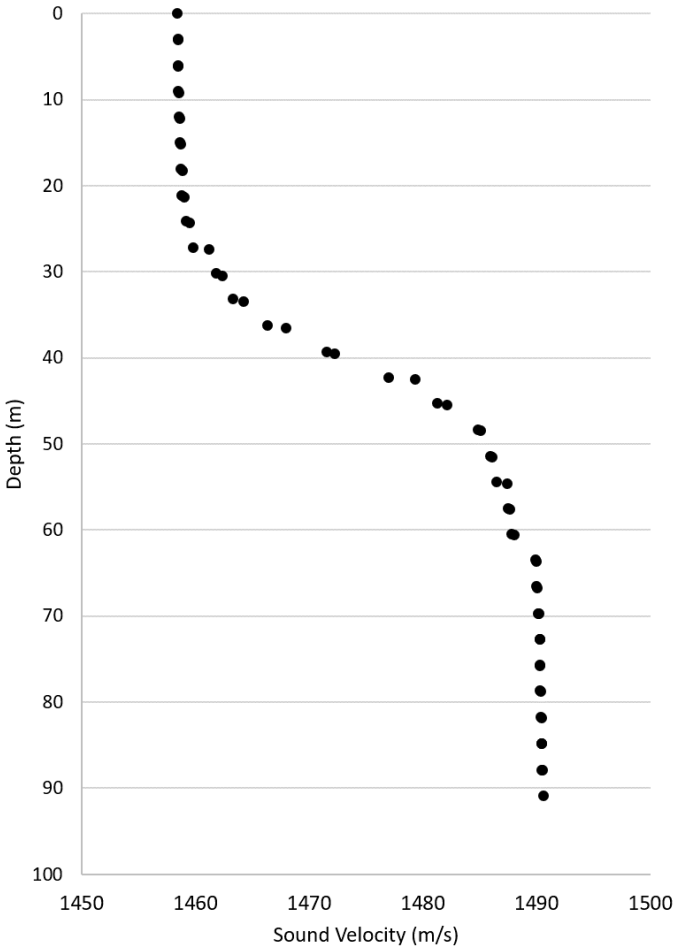

Figure B-3. The Gully: Sound velocity versus depth measured on 16 Apr 2018.

Appendix C. Acoustic Data Analysis Methods

The data sampled at 16 kHz was processed for ambient sound analysis, vessel detection, and detection of all marine mammal calls except clicks. Click and whistle detections were performed on the data sampled at 375 kHz. This section describes the ambient, vessel, and marine mammal detection algorithms employed (Figure C-1).

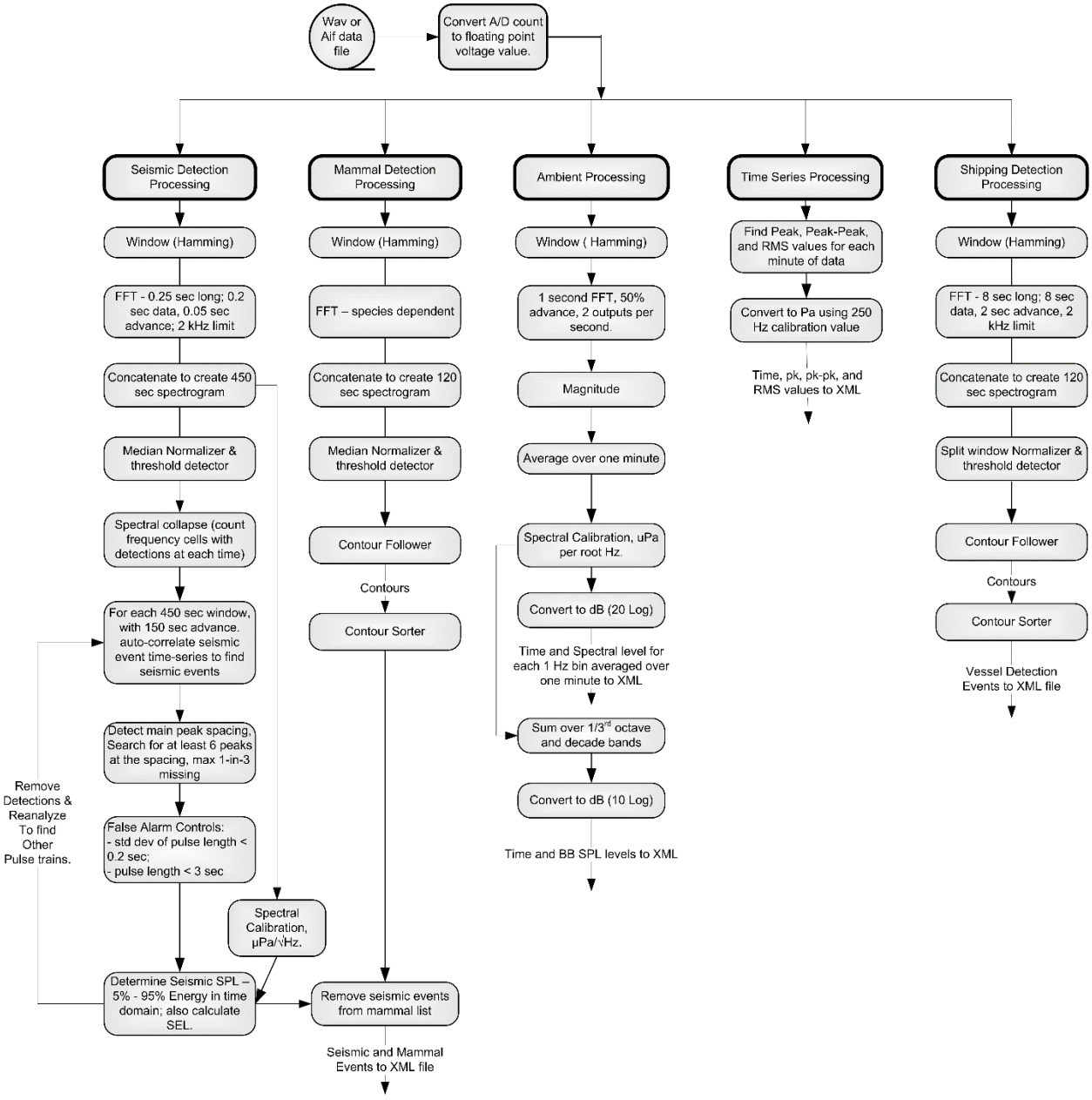

Figure C-1. Major stages of the automated acoustic analysis process performed with JASCO's custom software suite.

C.1. Total Ambient Sound Levels

Underwater sound pressure amplitude is measured in decibels (dB) relative to a fixed reference pressure of p_0 = 1 µPa. Because the perceived loudness of sound, especially impulsive sound such as from seismic airguns, pile driving, and sonar, is not generally proportional to the instantaneous acoustic pressure, several sound level metrics are commonly used to evaluate sound levels and its effects on marine life. We provide specific definitions of relevant metrics used in the accompanying report. Where possible we follow the ANSI and ISO standard definitions and symbols for sound metrics, but these standards are not always consistent.

The zero-to-peak pressure level, or peak pressure level (PK; dB re 1 µPa), is the maximum instantaneous sound pressure level in a stated frequency band attained by an acoustic pressure signal, $p(t)$:

$$PK = 10\log_{10}\left[\frac{\max\left(\left|p^2(t)\right|\right)}{p_0^2}\right] \tag{1}$$

$L_{p,pk}$ is often included as criterion for assessing whether a sound is potentially injurious; however, because it does not account for the duration of an acoustic event, it is generally a poor indicator of perceived loudness.

The sound pressure level (SPL or L_p; dB re 1 µPa) is the root-mean-square (rms) pressure level in a stated frequency band over a specified time window (T, s) containing the acoustic event of interest. It is important to note that SPL always refers to an rms pressure level and therefore not instantaneous pressure:

$$SPL = 10\log_{10}\left(\frac{1}{T}\int_T p^2(t)dt \Big/ p_0^2\right) \tag{2}$$

The SPL represents a nominal effective continuous sound over the duration of an acoustic event, such as the emission of one acoustic pulse, a marine mammal vocalization, the passage of a vessel, or over a fixed duration. Because the window length, T, is the divisor, events with similar sound exposure level (SEL), but more spread out in time, have a lower SPL.

The sound exposure level (SEL, dB re 1 µPa²·s) is a measure related to the acoustic energy contained in one or more acoustic events (N). The SEL for a single event is computed from the time-integral of the squared pressure over the full event duration (T):

$$SEL = 10\log_{10}\left(\int_T p^2(t)dt \Big/ T_0 p_0^2\right) \tag{3}$$

where T_0 is a reference time interval of 1 s. The SEL continues to increase with time when non-zero pressure signals are present. It therefore can be construed as a dose-type measurement, so the integration time used must be carefully considered in terms of relevance for impact to the exposed recipients.

SEL can be calculated over periods with multiple events or over a fixed duration. For a fixed duration, the square pressure is integrated over the duration of interest. For multiple events, the SEL can be computed by summing (in linear units) the SEL of the N individual events:

$$L_{E,N} = 10\log_{10}\left(\sum_{i=1}^{N} 10^{\frac{L_{E,i}}{10}}\right). \tag{4}$$

To compute the SPL(T_{90}) and SEL of acoustic events in the presence of high levels of background noise, equations Equation 5 and 6 are modified to subtract the background noise contribution:

$$L_{p90} = 10\log_{10}\left(\frac{1}{T_{90}}\int_{T_{90}}(p^2(t)-\overline{n^2})dt \Big/ p_0^2\right) \tag{5}$$

$$L_E = 10\log_{10}\left(\int_{T}(p^2(t)-\overline{n^2})dt \Big/ T_0 p_0^2\right) \tag{6}$$

where $\overline{n^2}$ is the mean square pressure of the background noise, generally computed by averaging the squared pressure of a temporally-proximal segment of the acoustic recording during which acoustic events are absent (e.g., between pulses).

Because the SPL(T_{90}) and SEL are both computed from the integral of square pressure, these metrics are related by the following expression, which depends only on the duration of the time window T:

$$L_p = L_E - 10\log_{10}(T) \tag{7}$$

$$L_{p90} = L_E - 10\log_{10}(T_{90}) - 0.458 \tag{8}$$

where the 0.458 dB factor accounts for the 10% of SEL missing from the SPL(T_{90}) integration time window.

Energy equivalent SPL (dB re 1 µPa) denotes the SPL of a stationary (constant amplitude) sound that generates the same SEL as the signal being examined, $p(t)$, over the same time period, T:

$$L_{eq} = 10\log_{10}\left(\frac{1}{T}\int_{T} p^2(t)dt \Big/ p_0^2\right). \tag{9}$$

The equations for SPL and the energy-equivalent SPL are numerically identical; conceptually, the difference between the two metrics is that the former is typically computed over short periods (typically of one second or less) and tracks the fluctuations of a non-steady acoustic signal, whereas the latter reflects the average SPL of an acoustic signal over times typically of one minute to several hours.

C.2. One-Third-Octave-Band Analysis

The distribution of a sound's power with frequency is described by the sound's spectrum. The sound spectrum can be split into a series of adjacent frequency bands. Splitting a spectrum into 1 Hz wide bands, called passbands, yields the power spectral density of the sound. These values directly compare to the Wenz curves, which represent typical deep ocean sound levels (Figure 1) (Wenz 1962). This splitting of the spectrum into passbands of a constant width of 1 Hz, however, does not represent how animals perceive sound.

Because animals perceive exponential increases in frequency rather than linear increases, analyzing a sound spectrum with bands that increase exponentially in size better approximates real-world scenarios. In underwater acoustics, a spectrum is commonly split into 1/3-octave-bands, which are one-third of an octave wide; each octave represents a doubling in sound frequency. A very similar measure is to logarithmically divide each frequency decade into 10 passbands, which are commonly misnamed the 1/3-octave-bands (base 10) rather than deci-decades; we use this naming in the report. The centre frequency of the ith 1/3-octave-band, $f_c(i)$, is defined as:

$$f_c(i) = 10^{i/10}, \tag{10}$$

and the low (f_{lo}) and high (f_{hi}) frequency limits of the ith 1/3-octave-band are defined as:

$$f_{lo} = 10^{-1/20} f_c(i) \quad \text{and} \quad f_{hi} = 10^{1/20} f_c(i). \tag{11}$$

The 1/3-octave-bands become wider with increasing frequency, and on a logarithmic scale the bands appear equally spaced (Figure C-2).

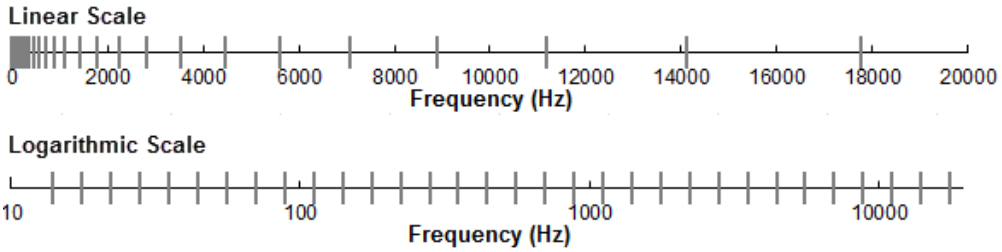

Figure C-2. One-third-octave-bands shown on a linear frequency scale and on a logarithmic scale.

The sound pressure level in the ith 1/3-octave-band $(L_b^{(i)})$ is computed from the power spectrum $S(f)$ between f_{lo} and f_{hi}:

$$L_b^{(i)} = 10 \log_{10} \left(\int_{f_{lo}}^{f_{hi}} S(f) df \right) \tag{12}$$

Summing the sound pressure level of all the 1/3-octave-bands yields the broadband sound pressure level:

$$\text{Broadband SPL} = 10 \log_{10} \sum_i 10^{L_b^{(i)}/10} \tag{13}$$

Figure C-3 shows an example of how the 1/3-octave-band sound pressure levels compare to the power spectrum of the same signal. Because the 1/3-octave-bands are wider with increasing frequency, the 1/3-octave-band SPL is higher than the power spectrum, especially at higher frequencies.
1/3-octave-band analysis is applied to both continuous and impulsive sound sources. For impulsive sources, the 1/3-octave-band SEL is typically reported.

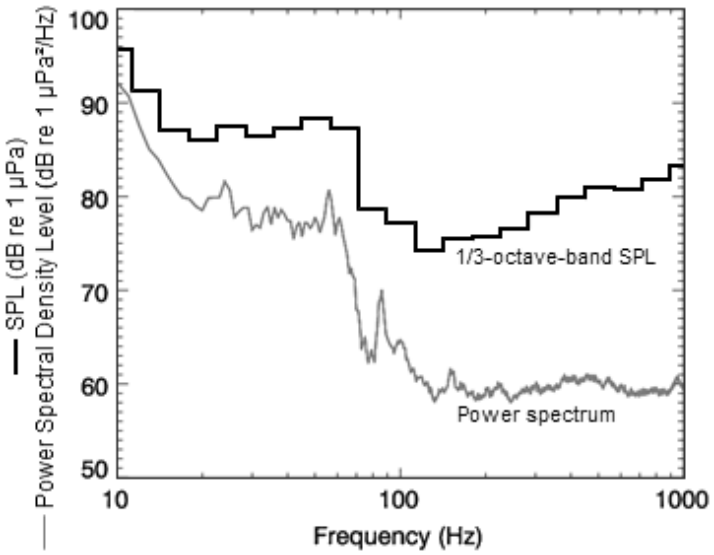

Figure C-3. A power spectrum and the corresponding 1/3-octave-band sound pressure levels of example ambient noise shown on a logarithmic frequency scale. Because the 1/3-octave-bands are wider with increasing frequency, the 1/3-octave-band SPL is higher than the power spectrum.

Table C-1. Third-octave-band frequencies (Hz).

Band	Lower frequency	Nominal centre frequency	Upper frequency
1	8.9	10	11.2
2	11.6	13	14.6
3	14.3	16	17.9
4	17.8	20	22.4
5	22.3	25	28.0
6	28.5	32	35.9
7	35.6	40	44.9
8	45.0	51	57.2
9	57.0	64	71.8
10	72.0	81	90.9
11	90.9	102	114.4
12	114.1	128	143.7
13	143.4	161	180.7
14	180.8	203	227.9
15	228.0	256	287.4
16	287.7	323	362.6
17	362.7	406	455.7
18	456.1	512	574.7
19	574.6	645	723.9
20	724.2	813	912.6
21	912.3	1024	1149
22	1,150	1,290	1,447
23	1,448	1,625	1,824
24	1,824	2,048	2,297
25	2,298	2,580	2,896
26	2,896	3,251	3,649
27	3,649	4,096	4,597
28	4,598	5,161	5,793
29	5,793	6,502	7,298
30	7,298	8,192	9,195
31	9,195	10,321	11,585
32	11,585	13,004	14,597

Table C-2. Decade-band frequencies (Hz).

Decade band	Lower frequency	Nominal centre frequency	Upper frequency
2	10	50	100
3	100	500	1,000
4	1,000	5,000	10,000

C.3. Marine Mammal Detections

JASCO applied automated analysis techniques to the acoustic data. Automated detectors were employed to detect (if present) impulsive clicks of odontocetes including porpoise, sperm whales, delphinids, and beaked whales, tonal whistles of delphinids, and tonal moans of mysticetes including fin, blue, sei, right, and humpback whales.

C.3.1. Automated click detectors

Odontocete clicks were detected by the following steps (Figure C-4):

1. The raw data was high-pass filtered to remove all energy below 8 kHz. This removed most energy from other sources such as shrimp, vessels, wind, and cetacean tonal calls, while allowing the energy from all marine mammal click types to pass.
2. The filtered samples were summed to create a 0.5 ms rms time series. Most marine mammal clicks have a 0.1–1 ms duration.
3. Possible click events were identified with a Teager-Kaiser energy detector.
4. The maximum peak signal within 1 ms of the detected peak was found in the high-pass filtered data.
5. The high-pass filtered data was searched backwards and forwards to find the time span where the local data maxima were within 12 dB of the maximum peak. The algorithm allowed two zero-crossings to occur where the local peak was not within 12 dB of the maximum before stopping the search. This defined the time window of the detected click.
6. The classification parameters were extracted. The number of zero crossings within the click, the median time separation between zero crossings, and the slope of the change in time separation between zero crossings were computed. The slope parameter helps to identify beaked whale clicks, as beaked whale clicks increase in frequency (upsweep).
7. The Mahalanobis distance between the extracted classification parameters and the templates of known click types was computed. The covariance matrices for the known click types, computed from thousands of manually identified clicks for each species, were stored in an external file. Each click was classified as a type with the minimum Mahalanobis distance, unless none of them were less than the specified distance threshold.

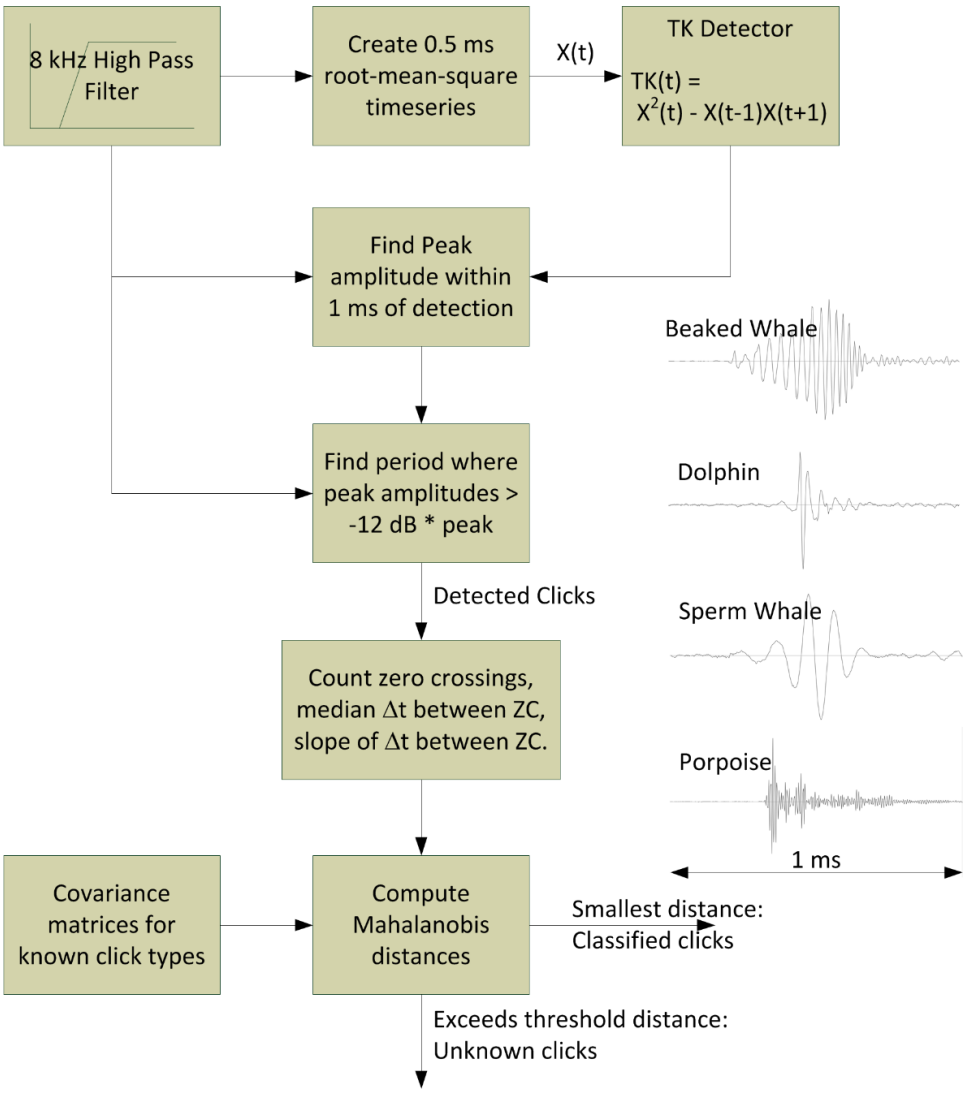

Figure C-4. The click detector/classifier and a 1-ms time-series of four click types.

C.3.2. Cetacean tonal call detection

Marine mammal tonal acoustic signals are detected by the following steps:

1. Spectrograms of the appropriate resolution for each mammal vocalization type that were normalized by the median value in each frequency bin for each detection window (Table C-3) were created.
2. Adjacent bins were joined, and contours were created via a contour-following algorithm (Figure C-5).
3. A sorting algorithm determined if the contours match the definition of a marine mammal vocalization (Table C-4).

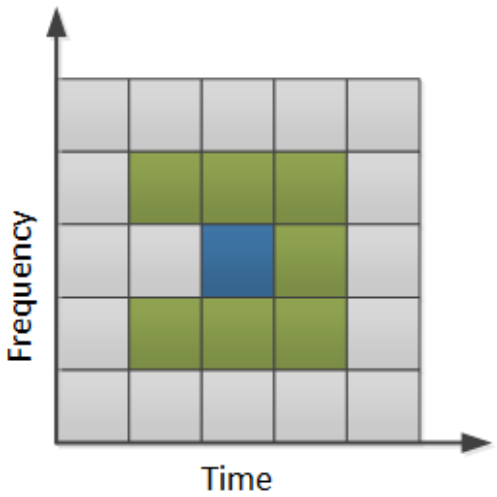

Figure C-5. Illustration of the search area used to connect spectrogram bins. The blue square represents a bin of the binary spectrogram equalling 1 and the green squares represent the potential bins it could be connected to. The algorithm advances from left to right so grey cells left of the test cell need not be checked.

Table C-3. Fast Fourier Transform (FFT) and detection window settings used to detect tonal vocalizations of marine mammal species expected in the data. Values are based on JASCO's experience and empirical evaluation on a variety of data sets.

Possible species	Vocalization	FFT			Detection window (s)	Detection threshold
		Resolution (Hz)	Frame length (s)	Timestep (s)		
Pilot whales	Whistle	16	0.03	0.015	5	3
Dolphins	Whistle	64	0.015	0.005	5	3
Humpback whales	Moan	4	0.2	0.05	5	3
Blue whales	Infrasonic moan	0.125	2	0.5	120	4
Fin whales	20-Hz note	1	0.2	0.05	5	4
Sei whales	Downsweep	3.25	0.2	0.035	5	3.5

Table C-4. A sample of vocalization sorter definitions for the tonal vocalizations of cetacean species expected in the area.

Possible species	Vocalization	Frequency (Hz)	Duration (s)	Bandwidth (Hz)	Other detection parameters
Pilot whales	Whistle	1,000–10,000	0.5–5	>300	Minimum frequency <5,000 Hz
Dolphin	Whistle	4,000–20,000	0.3–3	>700	Maximum instantaneous bandwidth = 5,000 Hz
Humpback whales	Moan	100–700	0.5–5	>50	Maximum instantaneous bandwidth = 200 Hz
Blue whales	Infrasonic moan	15–22	8–30	1–5	Minimum frequency <18 Hz
Fin whales	20 Hz downsweep	8–40	0.3–3	>6	Minimum frequency <17 Hz Sweep rate = −100 to 0 Hz/s
Sei whales	Downsweep	20–150	0.5–1.7	19–120	Maximum instantaneous bandwidth = 100 Hz Sweep rate = −100 to −6 Hz/s

C.3.3. Validation of automated detectors

C.3.3.1. Selecting Data for Manual Validation

To standardize the file selection process, we developed an algorithm that automatically selects a sample of files for review. The sample size *N* is set based on the amount of time allocated to the review effort. *N* = 1% of acoustic data was applied in the present report. The algorithm selects files to manually review based on the following criteria:

1. All species targeted by a detector whose performance needs to be assessed must be represented within a minimum of 10 files (unless fewer than 10 files have detections).
2. The sample should not include more than one file per day unless *N* is greater than the number of recording days or the "minimum 10 files per species" rule dictates that more than one file per day be reviewed.
3. Select files containing low, medium, and high numbers of detected species. Files with no detected species are excluded from the pool of eligible files. Files are selected such that the proportion of each species count bin within the sample matches the per-file species count distribution in the whole data set.
4. Select files with low, medium, and high numbers of detections per file for each species. The number of detections per file is split into low (but at least one), medium, and high bins, which corresponded to the lower, middle, and upper third percentile of the range, respectively. Files with no detection for each species will appear among those with detections of other species, allowing us to evaluate false negatives. We choose to slightly oversample the high detection counts (40% of files compared with 30% from the medium and low bins) to avoid biasing the threshold high. The three files with the highest detection counts are automatically included in those selected from the high bins for the same reason.

We score the goodness of fit of a sample of files according to how well it conforms to the "preferred" distribution of detections, as determined by the initial distribution and the preferred final sampling. A lower score implies a better fit. To score the goodness of fit, we perform the following step for a selected sample of files:

1. Determine the diversity (species count per file) proportions (Pc) of the selected sample of files, and calculate a diversity score based on how much the current proportions differ from the original diversity proportions (Po).

   DiversityScore = average(abs(Pc[i]–Po[i]))

2. For each species, determine the proportion of files (C) that have detection counts in the low/medium/high original species count distributions. Files with no detections are not included in the calculation for each species (0-detection files for a species will unavoidably be included in files selected for other species).

   $PerSpeciesScore[i] = abs(C_{low}–0.3) + abs(C_{medium}–0.3) + abs(C_{high}–0.4)$

   DetectionScore = average(PerSpeciesScore[1..n]), where n is the number of species

   FitScore = (DiversityScore + DetectionScore)/2

C.3.3.2. Detector Performance Calculation and Optimization

All files selected for manual validation were reviewed by one of two experienced analysts using JASCO's PAMlab software to determine the presence or absence of every species, regardless of whether a species was automatically detected in the file. Although the detectors classify specific signals, we validated the presence/absence of species at the file level, not the detection level. Acoustic signals were only assigned to a species if the analyst was confident in their assessment. When unsure, analysts would consult one another, peer reviewed literature, and other experts in the field. If certainty could not be reached, the file of concern would be classified as possibly containing the species in question, or containing an unknown acoustic signal. Next, the validated results were compared to the raw detector results in three phases to refine the results and ensure they accurately represent the occurrence of each species in the study area.

In phase 1, the validated versus detector results were plotted as time series and critically reviewed to determine when and where automated detections should be excluded. Questionable detections that overlap with the detection period of other species were scrutinized. By restricting detections spatially and/or temporally where appropriate, we can maximize the reliability of the results. The following restrictions were applied to our detector results:

1. If a species was automatically detected at a station, but was never manually validated, all automated detections at that station were considered false and the station was not included in the results as the species was considered absent.
2. If a species was automatically detected over a specific timeframe, but manual validation revealed all detections to be falsely triggered by another sound source or species, all automated detections during that time at that station were excluded.

In phase 2, the performance of the detectors was calculated based on the phase 1 restrictions and optimized for each species using a threshold, defined as the number of detections per file at and above which detections of species were considered valid. This was completed for each station as automated detectors perform differently depending on factors, such as the species diversity of the area or human activity, which vary in space and time.

To determine the performance of each detector and any necessary thresholds, the automated and validated results (excluding files where an analyst indicated uncertainty in species occurrence) were fed to a maximum likelihood estimation algorithm that maximizes the probability of detection and minimizes the number of false alarms using the MCC:

$$MCC = \frac{TPxTN - FPxFN}{\sqrt{(\mathrm{TP}+\mathrm{FP})(\mathrm{TP}+\mathrm{FN})(\mathrm{TN}+\mathrm{FP})(\mathrm{TN}+\mathrm{FN})}}$$

$$P = \frac{TP}{TP+FP}; R = \frac{TP}{TP+FN}$$

where *TP* (true positive) is the number of correctly detected files, *FP* (false positive) is the number of files that are false detections, and *FN* (false negatives) is the number of files with missed detections.

P is the classifier's precision, representing the proportion of files with detections that are true positives. A *P* value of 0.9 means that 90% of the files with detections truly contain that species, but says nothing about whether all files containing acoustic signals from the species were identified. *R* is the classifier's recall, representing the proportion of files containing the species of interest that are identified by the detector. An *R* value of 0.8 means that 80% of all files containing acoustic signals from the species of interest also contained automated detections, but says nothing about how many files with detections were incorrect. Thus, a perfect detector would have *P* and *R* values equal to 1. The algorithm determines a detector threshold for each species, at every station, for both years, that maximizes the F-score. The resulting thresholds, *P*s, and *R*s are presented in Section 3.2.

Where the number of validated files was too low, and/or the overlap between manual and automated detections was too limited for the calculation of *P* and *R*, automated detections were ignored, and only validated results were used to describe the acoustic occurrence of a species.

In phase 3, the detections were further restricted to include only those where *P* was greater than or equal to 0.75. When *P* less than 0.75, only the validated results were used to describe the acoustic occurrence of a species.

The occurrence of each species (both validated and automated, or validated only where appropriate) was plotted using JASCO's Ark software as time series showing presence/absence by hour over each day.